TAMPEREEN TEKNILLINEN YLIOPISTO
TAMPERE UNIVERSITY OF TECHNOLOGY

RIINA MAKSIMAINEN

PREPARATION AND CHARACTERIZATION OF COMPOSITE SURFACES FOR ADHESIVE JOINING

Master of Science Thesis

Examiner: Prof. Jyrki Vuorinen and Dr. Tech. Essi Sarlin
Examiner and topic approved by the Faculty Council of the Faculty of Engineering Sciences
on 9h December 2015

ABSTRACT

RIINA MAKSIMAINEN: Preparation and characterization of composite surfaces for adhesive joining
Tampere University of Technology
Master of Science Thesis, 47 pages, 44 Appendix pages
January 2016
Master's Degree Programme in Materials Science
Major: Technical polymer materials
Examiner: Professor Jyrki Vuorinen, Dr. Tech. Essi Sarlin

Keywords: adhesive joining, air-inhibited layer, glass fiber laminate, surface pre-treatment

Composites are widely used in large industrial tanks and vessels due to their excellent mechanical and chemical durability. Large tanks and vessels are typically assembled from multiple parts, thus joints are unavoidable. The goal of this thesis is to determine the optimal surface treatments for adhesive joining, and an on-site inspection method to verify the surface characteristics.

This thesis is divided in theoretical and experimental parts. The theoretical part concentrates on design, pretreatments, manufacture and inspection of adhesive composite joints. The effect of moisture, sulphuric acid and temperature on joint durability is discussed as well. The experimental part is divided into two parts. In the first part the formation and removal of air-inhibited layer is studied. Four different vinyl-ester epoxy resins were cured and the surfaces were measured with Fourier transform infrared spectroscopy (FT-IR) before and after abrading. The second part consists of different characterization methods of six mechanically pretreated filament wound laminates. The aim is to determine the best surface for adhesive joining, and determine an on-site inspection method for the pretreated surface. The surface energy of the laminates is measured with contact angle measurement, and the surface roughness is measured with a stylus system and optical 3D profilometer. The surfaces are also analyzed with FT-IR and scanning electron microscope (SEM). Lastly, mechanical pull-off adhesion tests are performed. The test series was carried out as blind test; the pretreating methods were revealed after the characterization and analysis was done.

It was discovered that the thickness of the air-inhibited layer is less than 3 mm, and even light mechanical pretreatments removed the layer, thus its formation is not concerning. In the surface treatment methods sandblasting stood out. However, it is important to choose the sandblasting parameters right; negligent sandblasting or too fine sand do no result in adequate surface for adhesive joining. To verify the roughness of a sandblasted surface on-site, a stylus system can be used when the limit values are outlined. To verify these results, more mechanical testing (e.g. single lap shear tests) should be carried out.

TIIVISTELMÄ

RIINA MAKSIMAINEN: Komposiittien liitospintojen esikäsittely ja karakterisointi adhesiivisiin liitoksiin
Tampereen teknillinen yliopisto
Diplomityö, 47 sivua, 44 liitesivua
Tammikuu 2016
Materiaalitekniikan diplomi-insinöörin tutkinto-ohjelma
Pääaine: Tekniset polymeerimateriaalit
Tarkastaja: professori Jyrki Vuorinen, TkT Essi Sarlin

Avainsanat: adhesiivinen liitos, ilman inhibitoima pintakerros, lasikuitulaminaatti, pinnan esikäsittely,

Komposiitteja käytetään teollisuudessa laajasti suurissa tankeissa ja säiliöissä niiden erinomaisen mekaanisen ja kemiallisen keston takia. Säiliöt joudutaan usein kasaamaan useista osista niiden suuren koon vuoksi, eikä liitoksilta voida välttyä. Tämän työn tarkoituksena on selvittää paras pintakäsittelymenetelmä adhesiiviselle liitokselle, ja löytää kenttäkelpoinen pinnan ominaisuuksien tarkastusmenetelmä.

Työn teoria käsittelee liitoksen suunnittelua, esikäsittelyjä, valmistusta ja tarkastusta. Myös lämpötilan, kosteuden ja hapon vaikutusta liitoksen kestävyyteen käsitellään. Kokeellinen osuus on kaksiosainen; ensimmäisessä osassa tutkitaan hartsin pintaan muodostuvaa hapen kanssa vaikutuksessa olevaa kerrosta. Neljän erilaisen vinyylisteriepoksin pintaa tutkitaan Fourier-muunnosinfrapunaspektroskopialla (FT-IR) sekä käsittelemättömänä että hiottuna. Toisessa osassa kuutta eri tavoin mekaanisesti esikäsiteltyä lasikuitulaminaattia tutkitaan. Tarkoituksena on selvittää paras esikäsittelymetodi. Laminaateista mitataan pintaenergia kontaktikulmamittauksella, ja pinnankarheus määritellään sekä karheusmittarilla että optisella 3D-profilometrillä. Pinnat analysoidaan myös FT-IR:llä sekä pyyhkäisyelektronimikroskoopilla (SEM). Lopuksi laminaatin ja hartsin välistä adheesiota mitattaan mekaanisella pull-off –testillä. Testisarja toteutettiin sokkotestinä; esikäsittelymenetelmät paljastettiin vasta karakterisoinnin ja tulosten analysoinnin jälkeen.

Ilman inhibitoiman pintakerroksen havaittiin tutkimuksessa olevan alle 3 mm, ja jopa kevyet mekaaniset esikäsittelyt poistivat kerroksen. Tämän vuoksi kerroksen muodostumisesta ei ole haittaa. Esikäsittelymenetelmistä parhaimmaksi erottui hyvä hiekkapuhallus. On kuitenkin tärkeää tehdä puhallus oikein, sillä huolimaton hiekkapuhallus tai puhallus liian hienolla hiekalla ei johda toivottuun pinnanlaatuun. Pinnankarheusmittarilla voidaan todentaa onnistunut hiekkapuhallus myös työmaalla, kunhan raja-arvot on määritelty etukäteen. Tutkimusta voitaisiin vielä jatkaa laajemmilla mekaanisilla testauksilla, joissa tutkitaan liitoksen leikkauslujuutta.

.

PREFACE

This study was carried out between May 2015 and January 2016 in the Department of Material Science at Tampere University of Technology in collaboration with Outotec.

I would like to express my gratitude to Dr. Tech. Essi Sarlin for the guidance, help and support throughout the work. I would like to thank Professor Jyrki Vuorinen, as well as the staff and my colleagues in the Department of Materials Science. I am grateful to Mari Lindgren and Markus Lehtonen for giving me this opportunity and guiding me to the right direction. Also, I would like to express my gratitude to Aki Ahola and Matti Rauva for their help and advice of the practical side of composite manufacturing.

To my friend and family; thank you for the wonderful support, encouragement, and fruitful lunch discussions. Without you this journey would have been rough.

Tampere, January 14th 2016

Riina Maksimainen

TABLE OF CONTENTS

LIST OF SYMBOLS AND ABBREVIATIONS

ASTME	American society of tool and manufacturing engineers
ATR	Attenuated total reflection
ECR-glass	Electrically and chemically resistant special purpose glass
E-glass	Electrically resistant glass
FRP	Fiber reinforced plastic
FT-IR	Fourier transform infrared spectroscopy
γ_{lv}	Total surface energy of a liquid
γ_s	Surface energy of a solid
HDT	Heat deflection temperature
ITR	Infrared thermography
MEKP	Methyl ethyl ketone
Nd:YAG	Neodymium-doped yttrium aluminum garnet
NDT	Non-destructive testing
R_a	Center line average height
RMS	Root mean square value
R_z	10-point height average
SEM	Scanning electron microscopy
T_g	Glass transition temperature
θ	Contact angle

1. INTRODUCTION

Composite structures are widely used in industrial applications due to their excellent mechanical and chemical durability, relatively light weight and versatility. If the application is large or complex, it is typically assembled from multiple parts. A good example of such application is a leaching reactor vessel. Leaching reactors are used in metal industry to leach metals from ores or other raw materials into solution. The reactor vessels are operated at elevated temperatures and the solution inside the reactors is typically acidic. The operating environment is challenging and a high mechanical durability and chemical resistance are required from such vessels.

The joints are typically the weakest part of the structure, and therefore the design and the manufacturing of the joints is very important. Adhesion and surface treatments are just a few elements influencing the durability of the joint. Further, there are many factors that influence the adhesion. For example the thickness of the adhesive layer, curing cycle, air-inhibited layer and surface energy all play their part when making a successful composite joint.

Pretreating the surface of the laminate is known to improve the mechanical strength of the joint [1]. The pretreatments can be divided into mechanical, chemical and physio-chemical treatments. In practice the large size of the vessel components restrict the used methods to mechanical, as chemical treatments require submersion of the part, and physio-chemical treatments require special equipment.

After pretreating the surface should be inspected to verify proper pretreatment. As of now the verification is typically visual, and no test data is obtained. The inspection of the joint after it is made is very difficult due to the heterogeneous nature of composite laminates.

Due to the large size of the vessels, they are assembled on-site, and the conditions are quite challenging. The size and the on-site conditions restrict the pretreatment methods and inspection methods as well. Especially the bottom joints are under a lot of mechanical stress. A failure of such joint would be very dangerous.

In this thesis, the details of adhesion and its influencing factors are discussed in Chapter 2. Chapter 3 concentrates on the different methods of surface preparation. The surface characterization methods are discussed in Chapter 4 and non-destructive inspection of composite joints in Chapter 5. Lastly, the effect of environmental factors of the joint is discussed in Chapter 6. In the Chapters 7 and 8 the experimental part is described.

THEORETICAL PART

2. ADHESION AND ITS INFLUENCING FACTORS

Large composite products are typically made of multiple parts; therefore joints in the structure are unavoidable. Since joints are considered the weakest part of the structure, it is important to design the joints correctly [2]. The structure of composite part is not homogeneous and its mechanical properties depend strongly on the orientation of the reinforcement. Thus the mechanical modelling of such structures is difficult, and the design of such component should not be only based on numerical and computer modelling, but also on test data. [3] .

The joint should be designed so that the joint itself never fails because the adherend fails first [2]. The selection of adhesive material plays an important role as well. Adhesives are typically monomer compositions that have adequate shelf life, viscosity, wetting ability, gel time, cure time and environmental resistance [5].

2.1 Structural design of the joint

The bonding of composite parts is either mechanical or adhesive. The mechanical joints are usually either riveted or bolted, and the objective of this type of bonding is to transfer applied load through a fastener from one part of the joint to another. Mechanical joints require drilling holes to the structure, damaging the reinforcing fibers. The holes also cause stress concentrations to the structure, whereas adhesively bonded joints carry the load evenly. Uneven stress distribution reduces fatigue durability and mechanical strength of the structure [3]. Thus, the area around the holes is more prone to local damage and micro-cracking than the areas that are intact [4]. However, mechanical joints do not require surface preparation and thermal cycling and humidity do not affect adversely in the mechanical behavior of the joint [5].

Adhesive joints have some benefits compared to mechanical joints. As stated, the load carrying capacity is uniform; therefore the joints are more resistant to flexural, fatigue and vibrational stresses [1]. Adhesive joints are generally lighter as there are no screws or bolts adding to the weight. If the joint is properly made, it seals the joint preventing galvanic corrosion between dissimilar adherend materials. Adhesive joints are usually cheaper to make. Adhesives often require heat and/or pressure to cure and this sets some limitations to the size and geometry of the parts. Some adhesives also require a long curing time. Repairing adhesively bonded joints is difficult, since the bonds are permanent and it is not possible to disassemble them without damaging the surface [2]. Additionally it is more difficult to inspect adhesive joints than mechanical joints [5]. Possible

non-destructive testing (NDT) methods for adhesive composite joints are discussed further in Chapter 5.

Adhesive joints have various configurations depending on the application. Some of these configurations are presented in Figure 1. The load-bearing capacity of the joint varies with different configurations, and the configuration should be chosen accordingly [6].

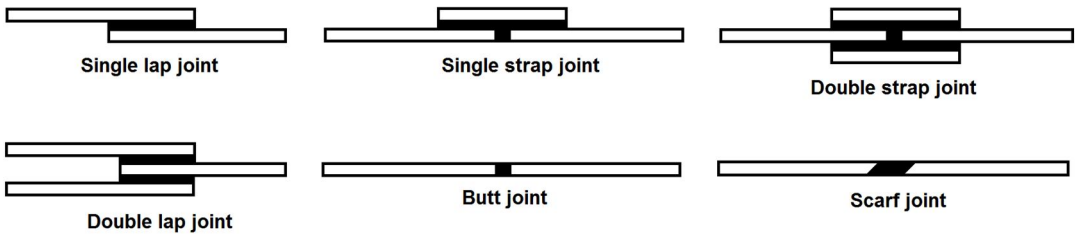

Figure 1. *Different joint configurations for adhesive joints, according to [1]*

2.2 Adhesive layer thickness

The thickness of the adhesive layer has an impact on the mechanical behavior of the joint. Increasing thickness of the adhesive increases the interfacial shear stress significantly especially on the edges of the joint [3]. As presented in Figure 2 the increase in layer thickness decreases the average failure load and corresponding joint displacement [6]. The layer thickness effects on the failure mode of a broken joint. Thin adhesive layer results in a failure where the both interfaces fracture. In thick adhesive layer the fracture propagates only on one interface [6]. In other words the fracture that propagates in a thin layer is brittle and the fracture load is high. The fracture in thick adhesive layer is ductile and requires lower load to propagate.

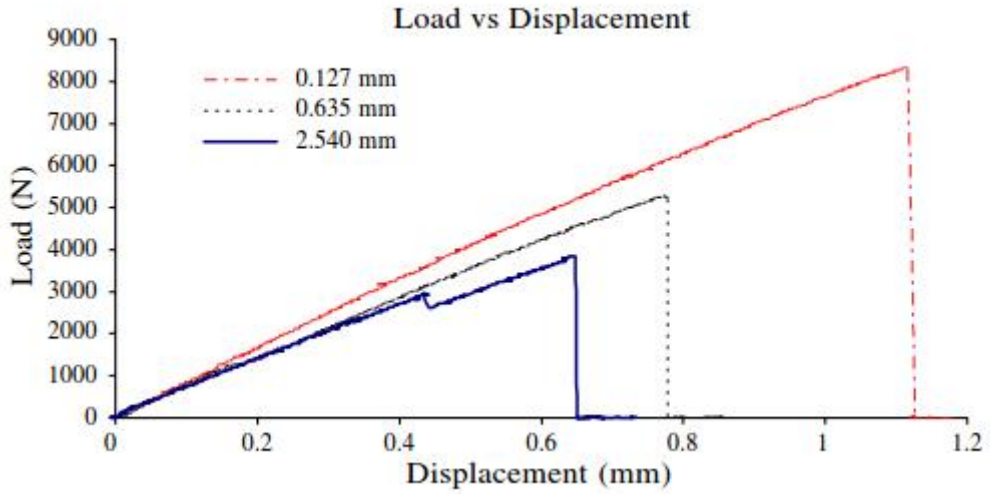

Figure 2. *Load-displacement for various adhesive layer thicknesses for glass-fiber-reinforced vinyl ester composite laminates bonded with epoxy [6]*

2.3 Curing cycle

The main curing method of vinyl ester epoxy is free radical curing. There are three stages of free radical cure of thermosetting resins. The first stage is initiation, where peroxide, usually methyl ethyl ketone (MEKP) decomposes into free radicals. The decomposition leads monomer radical formation. These radicals promote the curing chain reaction, by providing the active positions to sustain the chain propagation. Vinyl ester epoxy contains both styrene monomers and vinyl ester monomers. It is reported that the activation energy required for curing is lower when the styrene content increases [7].

During chain propagation, styrene monomer provides linear chain extension and the crosslinking capacity is provided by vinyl ester monomer. The diffusional limitations in bimolecular termination yield to increasing polymerization rate. When the polymerization reaction accelerates, the resin begins to gel. While the reaction accelerates, it may appear autocatalytic. This auto acceleration is also known as gel effect or Trommsdorff effect, and it is a result of a decrease in the chain termination rate caused by diffusional limitations [8]. As crosslinking continues, the mobility of large molecules decreases, thus decreasing the polymerization rate until it finally terminates [7].

The curing temperature has been shown to impact the curing process. If the curing is executed above the glass transition temperature T_g, the monomers are not completely converted [9; 10]. The strength of a joint is lower if the adhesive is undercured, as the crosslinking has not been carried through. On the other hand, higher curing temperature means faster curing, as both the reaction rate and final conversion rate are greater [7; 11].

2.4 Air-inhibited layer

When resin is cured in normal atmosphere, the surface is affected by oxygen. Oxygen inhibits polymerization, thus there are unreacted double bonds on the surface. The bulk material cures without air-inhibition and there are hardly any unreacted double bonds after curing. Studies show that the partially uncured surface layer is thicker when the resin cured in room air compared to resins cured in argon atmosphere. This suggests that it is oxygen that causes the unreacted surface [12].

The fiber orientation has an effect on the passage of oxygen, thus the thickness of air-inhibited layer depends on the fiber orientation. Oriented fibers favor the air-inhibition as the oxygen is able to diffuse in the uniform structure better than in randomly oriented structure. [13]

There have been many studies on the impact of air-inhibited layer on adhesion and the results are controversial. According to some studies [14; 15] the air-inhibited layer is a precondition for a proper adhesive bond. Other studies [12; 16] suggest that the air-inhibited surface layer decrease the bond strength in adhesive joints. There are also studies [17; 18] claiming that the layer has no effect on bond strength. However these studies are conducted in the field of dentistry, where the applications and materials are very different from large industrial tanks and vessels.

2.5 Surface energy

Surface energy influences greatly to the gained bond strength. Surface energy of the adherend is directly linked to how well the adhesive spreads on the surface of the adherend, i.e. the wettability of the surface. The greater the surface energy, the better its wettability is. [19; 20] The surface energy can be measured by a drop test. Figure 3 shows the basic principle of a contact angle measurement. A drop of liquid is placed on the surface of the adherend, and the contact angle θ is measured from the digital images taken of the drops. If the contact angle is low and the drop spreads on the surface, the surface is considered hydrophilic, thus the adhesive forces are greater. If the contact angle is large, the surface is hydrophobic and the wetting on such surface is poor. [20] However, if the surface is rough the contact angle measurement may give false results. This is presented in Figure 4, where solid line is the real contact angle and dotted line shows different surface energy value depending on the orientation of the drop. [21]

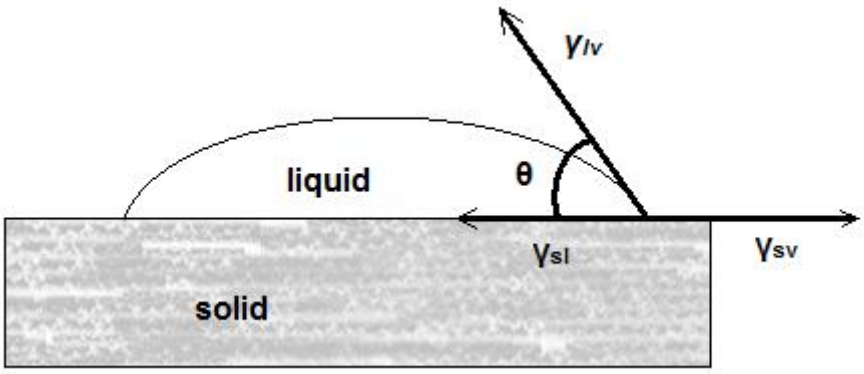

Figure 3. *Principle of contact angle θ measurement.*

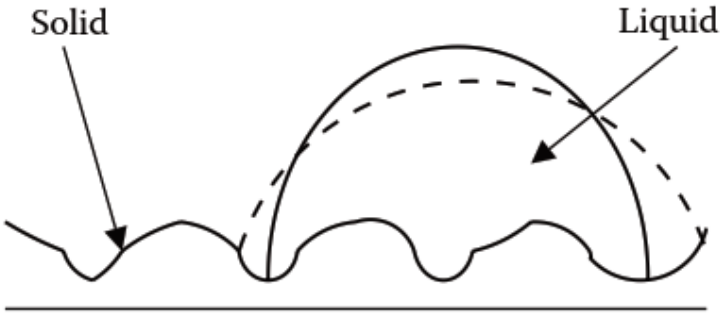

Figure 4. *Contact angle measurement of rough surface. The solid line is the real contact angle and the dotted line is apparent contacts angle that depends on the drop orientation. [21]*

There are several methods to calculate surface energy from the contact angle measurement. The method used in this study is the Wu method. In this method it is assumed that the total surface energy of the substrate can be divided into dispersive adhesion and polar adhesion [19]. The surface energy can be calculated from a series of test liquids on a solid surface with the equation

$$\gamma_{lv}(1+\cos\theta) = 4(\gamma_s^d\gamma_{lv}^d)/(\gamma_s^d+\gamma_{lv}^d) + 4(\gamma_s^p\gamma_{lv}^p)/(\gamma_s^p\gamma_{lv}^p)$$

where γ_{lv} is the total surface energy of the liquid, γ_s is the surface energy of the solid, and θ is the contact angle. The *d* and *p* represent the dispersive and polar surface energies. [22]

Surface energy can be increased by altering the surface chemistry with a suitable pretreatment. Mechanical surface treatment does not increase the surface energy per unit area intrinsically, but it increases the surface area, thus the total surface energy is greater. Different types of surface treatments are discussed further in Chapter 3.

3. SURFACE PREPARATION FOR JOINING

In order to achieve adequate bond strength in adhesively bonded joints, surface preparation is necessary. It is sometimes falsely thought that proper bond strength is achieved by cleaning the surface [2]. Adequate surface preparation not only cleans the surface, but also removes the weak air-inhibited layer that has formed during the cure, and increases the surface area, which increases mechanical interlocking [1]. Proper surface preparation also removes foreign particles, grease, oil and dust from the surface, but should not expose the load-bearing fibers in the matrix [23].

3.1 Mechanical surface preparation

In mechanical surface preparation the surface is roughened by abrasion or cutting. Roughness affects directly to the bond strength, as it increases the contact area between the two substrates, thus increasing the surface area for chemical bonding and improving the mechanical interlocking. However, too rough surface can lead to stress concentrations if the adhesive does not penetrate to the cavities and air is trapped in the joint interface [24]. Mechanical abrading, such as grinding and sandblasting, removes the weak surface layer, but the surface chemistry is not changed. The surface is cleaned by blasting the surface with clean air, nitrogen gas stream or wiping it with a solvent after roughening in order to remove the solid particles. [1; 2]

When the surface is removed mechanically, it should be done in a manner that removes the weak layers, but does not expose load-bearing fibers in the matrix. The surface can be sanded with medium grit emery paper and it is recommended to sand parallel to the surface fiber direction to minimize the damage to fibers [25]. Grinding or abrasive machining is usually done with a tool made of aluminum oxide, silicon carbide or diamond particles. A diamond abrasive cutter is presented in the Figure 5. The tool chips the surface removing the top layer. Resulting roughness depends highly on the grit of the tool. With a coarse cutter the resulting surface is rough, and with a fine grit cutter a smooth surface is achieved. When grinding the surface it must be noted that the faster the cutting is, the more heat the friction causes and thus the surface might require cooling to prevent thermal degradation [26].

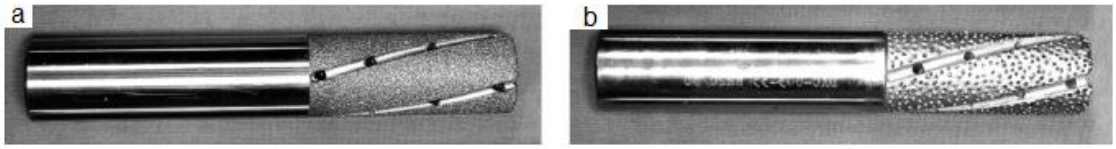

Figure 5. *Example of abrasive cutters. a) A fine 80 grit cutter and b) coarse 30 grit cutter. [26]*

Grit blasting is an effective way to roughen the surface in production. The abrasive must be chosen correctly; the particles should cut the surface, not punch through it. It is recommended to grit blast the surface with aluminum oxide [2]. For the preparation to be successful the grit should be delivered to the surface in a dry inert gas stream such as nitrogen gas. Compressed air is not optimal as it might contain oil, water and other contaminants [2].

Peel ply or tear film treatment is a mechanical surface preparation and it is quite straightforward way to prepare the joint surface for joining. Peel plies are sheets typically made of polyamide or polyester. Peel ply is placed on the joint surface during the manufacturing the component, integrating the ply to the composite. After curing the peel ply can be removed, and the surface is adequately roughened as well as cleaned of dust and other contaminants [27]. Unwanted residue of the peel ply is a major disadvantage. Sometimes peel plies are difficult to remove and it might tear away the first layers of the laminate as well, thus causing damage to the component itself [2].

3.2 Chemical surface preparation

Chemical treatments usually aim to modify the polarity of the surface. Increased polarity leads to better chemical adhesion [27]. When treating the surface with chemicals, the parts are submerged in a solution that contains a detergent at 65°C to 95°C for 10 minutes. Typical detergents are combinations of alkaline salts and surfactants. After immersion the parts are cleaned with deionized water. Chemical treatments modify the surface energy, thus improving adhesion. [1]

Thermoset materials cannot be treated with solvents because they are insoluble, however the mold release agents and other contaminants can be cleaned from the surface with a solvent [25]. Wiping the surface of thermoset composite with acetone only cleans it, and it is not sufficient surface treatment for bonding [2]. Due to the large size of the vessels, chemical surface preparation is not a viable option.

3.3 Physio-chemical surface preparation

Laser treatment is a physio-chemical method to improve adhesion. It removes the surface layer without causing degradation in the matrix or fibers [28]. Other physio-

chemical treatments, such as plasma treatment, can be performed on fiber reinforced (FRP) surfaces, but they have their disadvantages. Plasma treatment requires the use of either special gases or vacuum, which means the size of the treated component is restricted. After the components have been plasma treated, they should be joined immediately since the open time of plasma treatment is only a few hours, after which the advantages in adhesion are lost. The open time in laser treatment is significantly longer in comparison to plasma treatment. [29]

Two types of laser methods are used in surface treatments. Pulsed excimer lasers have been studied and used for 20 years and recent studies show that Nd:YAG (neodymium-doped yttrium aluminum garnet) laser treatments have been successful in increasing adhesion [29]. Excimer lasers are based on the combination of rare gasses such as argon and krypton, and halides such as fluorine and chlorine [30]. However the halides are hazardous gasses and their emission harm the environment. The maintenance costs of excimer laser equipment are high, as the halides also damage the equipment [29]. Nd:YAG laser treatment is less hazardous than excimer laser treatment and it is widely used method in aerospace industry to drill holes [31]. However the size of the vessel restricts the use of laser treatment.

4. CHARACTERIZATION OF COMPOSITE SURFACE

After the surface is prepared for joining, it should be inspected to make sure the preparation is properly done. One way to do this is to visually inspect the surfaces, but there are also measurements that can verify adequate surface properties.

4.1 Surface texture

American society of tool and manufacturing engineers (ASTME) defines roughness as irregularities in the surface texture, which are either repetitive or random deviations from the nominal surface that form the surface pattern [32]. Measuring the surface texture has a number of benefits comparing to profile measuring. The areal measurements give more realistic representation of the surface. [33] The surface roughness can be measured with non-contact, optical method or with a contact method such as stylus system.

There are three different ways to determine roughness values. The most commonly used roughness value is center line average height R_a. The R_a value is a representation of the average height form a mean line of all ordinates of the surface. Center line average height is presented in Figure 6. Also other R-values are used, such as $R_{z,}$ value, which is 10-point height average, where the value is counted from the average height of ten consecutive peaks and values. The 10-point height average is presented in Figure 7. The 10-point height average is always greater than center line average height. [32]

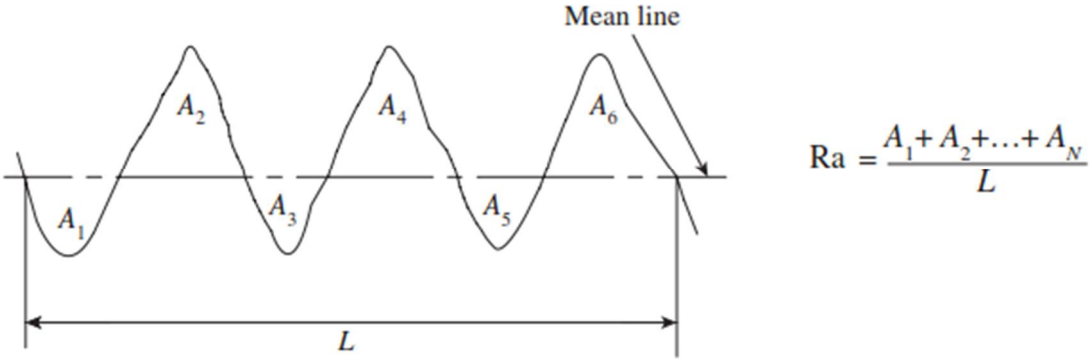

Figure 6. *The basic principle to determine the center line average height R_a [32].*

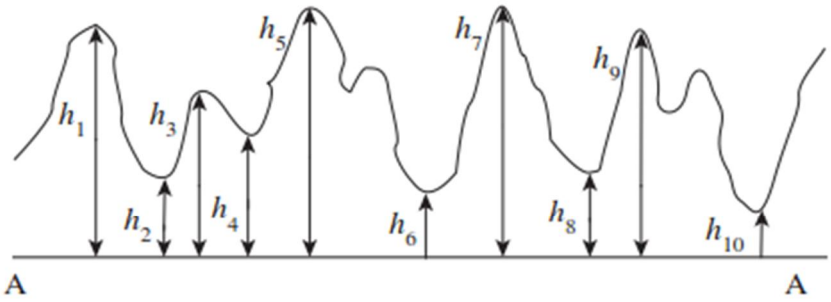

$$Rz = \frac{(h_1 + h_3 + h_5 + h_7 + h_9) - (h_2 + h_4 + h_6 + h_8 + h_{10})}{5}$$

Figure 7. *The basic principle to determine the 10-point height average R_z [32].*

Root mean square value (RMS) used to be a popular choice of quantifying roughness, but has been replaced by center line average height. RMS is the square root of the mean of squares of the ordinates of the surface measured from a mean line. [32] The basic principle of defining RMS value is shown in Figure 8.

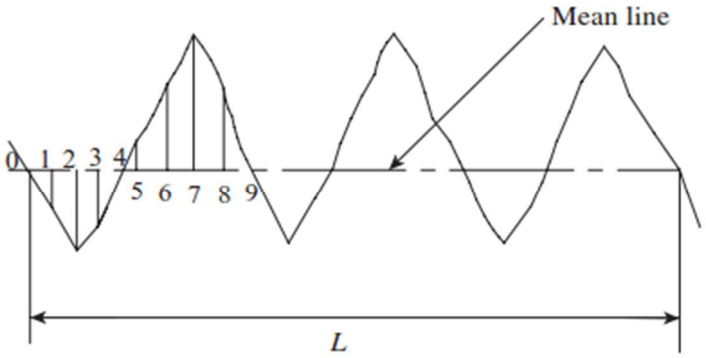

$$h_{RMS} = \frac{\sqrt{(h_1^2 + h_2^2 + \ldots + h_n^2)}}{n}$$

Figure 8. *The basic principle to determine root mean square value [32].*

Surface roughness can be obtained either by comparing the surface to a surface with known roughness, or measured directly from the surface. When measured with comparison the results are more subjective in nature but the measurement is also simpler. In comparative methods the surface texture is obtained from observation or feel of the surface (i.e. microscopic examination, touching). This might be deceptive, as two different surfaces may appear identical. It might be difficult to determine the height of the peaks and valleys. Surface texture can be determined also by touching the surface, but the result depends greatly on the judgment of one person. As stated, these methods are very subjective and therefore not reliable. Comparative methods do not provide numerical values to assess the surface, and therefore direct measuring gives more reliable results. [32]

Basic surface roughness is measured with stylus system. Basically in this method a stylus is drawn on the surface of the specimen and it generates electrical signals that are proportional to the surface topography. The output of the electric signal is then either generated on a hard copy or stored on magnetic strip. [32] A stylus system is presented in Figure 9.

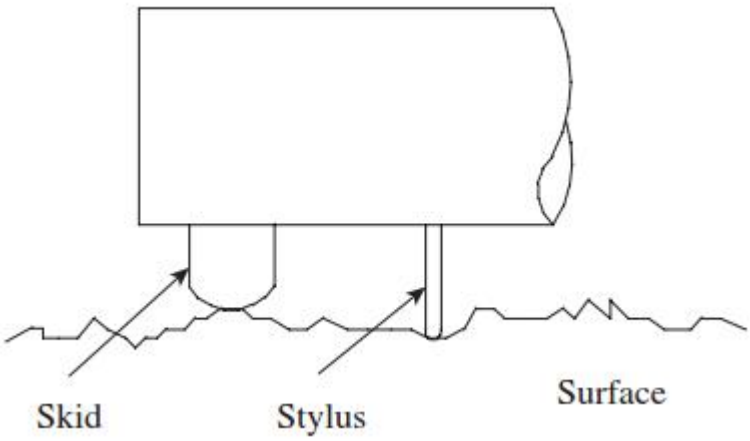

Figure 9. *A stylus system to measure surface roughness [32]*

Interferometers have been widely used in optical characterization of surface topography. These interferometers produce a fringe image of the valleys and peaks, but the analysis of the fringe images requires high speed computing [33]. Optical instruments either scan a beam over the surface (a lot like a stylus system) or measure the area by using the finite field of view of microscope objective. The latter analyzes usually the distribution of scattered light. Optical surface analysis is a non-contact method; therefore it does not damage or alter the surface during measurement. Optical measurement quality depends on the surface. If the surface is very smooth, there might not be wholly destructive interference. On the other hand, if the surface is very rough, full contrast speckles may occur in the image of the surface. [36]

Focus variation is relatively new method of optical surface characterization. It is based on small depth of focus of an optical system combined with vertical scanning [37]. It can provide information about the texture and the form of the measured surface, as it is not limited to coaxial illumination like traditional optical measurements. Focus variation provides a 3D model of the surface, from which various surface features can be measured.

4.2 Surface composition and chemical structure

Infrared spectroscopy is widely used method for characterization of polymers. Fourier transform infrared (FT-IR) with germanium or diamond crystal achieves a spatial resolution that is smaller than the infrared wavelength in air. FT-IR utilizes attenuated total

reflection (ATR) imaging, and it does not require any special sample preparation, which makes it optimal to polymeric materials. Infrared spectroscopy is very universal, as many molecules have strong absorbance in the mid-infrared range. However, there are some materials that cannot be measured with FT-IR. For example, monoatomic materials that are not chemically bonded to anything, do not have anything that could absorb the IR waves. The measurement is relatively easy, fast and inexpensive. The measurement is also very sensitive, and even tiny amount of certain molecule can be detected [34].

With FT-IR it is possible to determine what molecules are in the sample. The infrared wave is absorbed differently in different parts of the molecular structure, and the result is on spectra, that has peaks [35]. The spectrum can be then compared to a spectrum of known sample, and the measured sample can be identified. There are portable, handheld FT-IR devices as well, and they can be easily used on site.

5. NDT CHARACTERIZATION OF COMPOSITE JOINTS

After the assembly of the parts, a non-destructive testing (NDT) should be performed to ensure the bonding is properly done. There should be no delamination or voids in the joint as they form stress concentrations and decrease the overall joint strength. The non-destructive testing of reinforced materials is often more difficult than the nondestructive testing of homogenous materials. In composites the reinforcing fibers or particles form interfaces within the material. These interfaces reflect radiation and waves similarly the possible voids and delamination, and it can be difficult to interpret the results.

5.1 Microwave

In order to find defects with microwave technique, the specimen is irradiated with high frequency electromagnetic energy (200 MHz – 200 GHz). The structure can be determined by measuring the properties of the scattered waves or waves that has transmitted through. A flaw reflects the waves differently than the intact matrix [38]. The location, dimension and geometry of debonded area can be determined with microwaves. [39] Microwaves have the ability to penetrate inside dielectric materials and it is possible to evaluate even thick composite structures. [39; 40] Microwave characterization can be conducted either in in-contact or non-contact matter, and it is possible to use only one side or both sides. While operating on one side, the method is based on reflection. While operating both sides, it is based on transmission. [40] Resolution depends on the wavelength of the microwave but also the geometry of the specimen [40].

Microwave NDT can be quite inexpensive too, when in the field the primary objective is to detect delamination. There is no need for complicated post signal processing. It is very suitable for on-field inspections, as the data is real time and required operating power is relatively low. The microwave devices can be made as hand-held, battery operating systems. It is possible to inspect even large areas with array of sensors [40]

There are many applications in microwave inspection for glass fiber reinforced polymers other than detection of disbonded areas and delamination. These applications include accurate coating thickness measurement, thickness variation measurement, detection of fiber bundle orientation, breakage in fibers and impact damage detection. [40]

5.2 Digital radiography

Radiography is based on material's absorption ability of penetrating radiation. Materials absorb different amounts of radiation depending on the thickness and density. [38; 39] The most common type of radiographic imaging utilizes X-rays, but also gamma rays are used. Radiation penetrates the specimen and the image is captured on radiographic film [39]. Once the film is exposed, the film is processed and analyzed. With digital radiography the image is processed digitally, and it is possible to get real time radiographic image of the specimen [38].

However, radiographic imaging has its disadvantages. It is possible to detect honeycomb-core defects in sandwich structures, but delamination is not detectable, as the density of delaminated and intact areas is the same. It is not possible to detect small flaws or flaws that are non-parallel to the radiation beam. [38] Radiography is very hazardous due to radiation; therefore the safety regulations are strict when using radiography [39]. The equipment for radiographic inspection is quite expensive and also not entirely portable. However the inspection can be automated using real-time radiography and pattern recognition facility. [41]

5.3 Ultrasound

Ultrasound testing utilizes high frequency waves in detecting defects and changes in material properties. When the wave encounters a discontinuity, a part of it echoes back, and the size, location and orientation of the discontinuity can be determined. [39]

Ultrasound is the most widely used NDT method, since it is relatively inexpensive, the data is real-time and the results can be presented in 3D format. Ultrasonic testing is also portable, as shown in Figure 10. Ultrasound has its disadvantages: if there are variations density, porosity and composition of the inspected material, it causes depletion in the ultrasonic beam [38]. The anisotropic nature of the matrices may cause the ultrasonic energy to propagate in a different direction that the wave normal, which leads to difficulties in locating and sizing the flaws. The characteristics of composite material can be very similar to the ultrasonic wavelengths, causing wave dispersion and multiple scattering, distorting the ultrasonic signal [42].

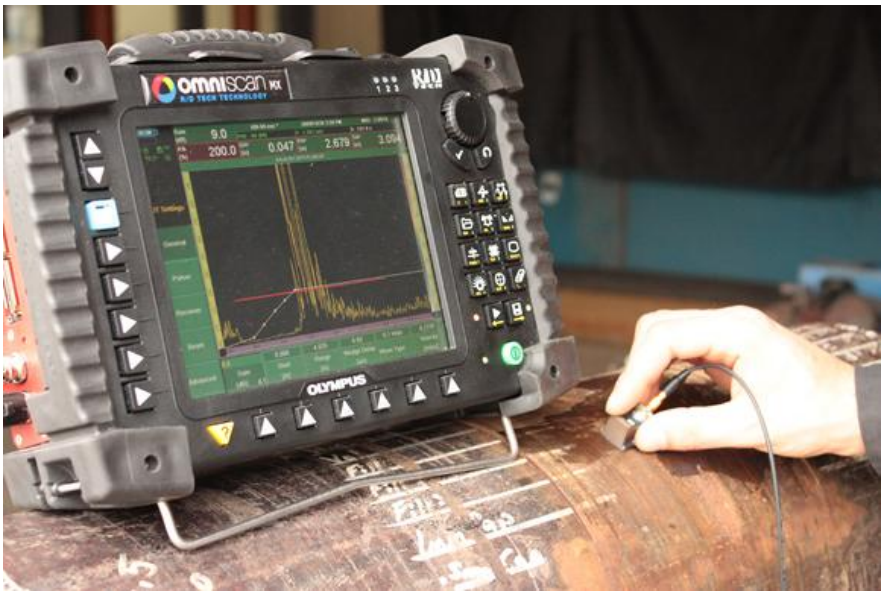

Figure 10. *A portable ultrasonic apparatus [43]*

In order to inspect a material with ultrasonic testing, an interface between specimen and censor is required. The interface can be achieved by adding a couplant such as gel or water. Using water as a couplant, the specimen should be immersed in water, or a steady water flow should be present. This is major disadvantage when the inspected area is large. Using a gel couplant, the inspected area should be cleaned afterwards which can be very time-consuming. [38]

Ultrasonic testing is very prone to human error, and it requires experienced inspector. The process can be automated, but it requires special immersion tanks and multi-axis robotic system which makes large specimen and on-site inspections impossible [38].

5.4 Thermography

Thermographic inspection is based on scanning heat flow from, to or through specimen. Usually the measurement is done with infrared camera. Infrared thermography (ITR) can be divided into active and passive thermography. In active thermography the heat is from external heat source, whereas passive thermography relies on natural heat distribution over the surface of the structure. Passive thermography detects irregularities in the structure and gives qualitative information. [39]

Active IRT requires external heat source that distributes the heat uniformly. The heat conductivity of intact area is more efficient than in the defected areas. Defects, such as cracks, voids and delaminated areas cause interfaces in the structure and they can act as insulators. The defected area has a lower thermal conductivity, and it appears hotter in the infrared image. [39]

Infrared thermography is a portable, real-time, non-contact NDT method that is widely used in examination. Thermal imaging setup is shown in Figure 11. Materials with low thermal conductivity can be evaluated, even though the sensitivity of thermography is highly dependent on the thermal conductivity of the specimen. It is a standard method for on-site inspection in aerospace industry. [38]

(a) (b)

Figure 11. *(a) Set-up using infrared camera to detect irregularities (b) close up view of infrared camera [44]*

6. THE EFFECT OF ENVIRONMENT ON COMPOSITE JOINT DURABILITY

There are many environmental factors that impact on the joint durability, such as moisture and temperature. There are environment impacts on the components in storage before the joining, as well as in use after the joints are made. In the case of leaching reactors, the main environmental factors are oxidation during storing or manufacturing, moisture, high temperature and sulphuric acid.

6.1 Moisture

Moisture penetrates through the free edges of the laminates, where the fiber ends are exposed. As the load is concentrated in the area of the edges of the joint, the moisture has a rather direct effect on the degradation of the adhesive and matrix. The amount of free edges can be minimized by designing the joint properly. [6] Moisture can diffuse through the laminate surface as well, and the diffusion rate increases in higher temperatures [45]. An increase in styrene content increases hydrophobicity, thus decreasing water absorption. However, higher styrene content also increases shrinkage and it may lead to micro-cracking in the matrix. [45]

Exposing dried FRP laminates to moisture prior to bonding decreases the bond strength significantly, but if the laminate is re-dried before joining, the most bond strength is regained. [46; 47] Plasticization is reversible effect, however some of the strength is lost after re-drying, and if the joint is exposed to water and then dried multiple times, the bond strength decreases [47]. The drying should be executed the material properties in mind, but the rule of thumb is to dry the component twice as long as the curing time has been. [48]

It is known that water uptake of resins causes plasticization in short term and hydrolysis in long term. Both hydrolysis and plasticization result in higher molecular mobility, which again decreases glass transition temperature T_g [49].

6.2 Temperature

The effect of temperature on load-bearing, fiber reinforced resin is not as significant as the effect on adhesive. At temperatures below glass transition temperature of the adhesive the elongation of adhesively bonded double lap joint is minimal and failure abrupt. However the increase in temperature increases elongation and the behavior load vs.

elongation is non-linear. The stiffness of the specimen decreases as well [50]. It has been observed that the mechanical behavior of the adhesive changes around the glass transition temperature [50]. The failure mechanism at high temperatures is adhesive. It seems that the adherend-adhesive interface is more affected by the high temperature than the adhesive.

When the glass fiber – vinyl-ester laminate joint is exposed to high temperatures and moisture at the same time, water diffusion causes degradation in the matrix. Long exposure will also propagate micro-cracking and contributing to diffusion of water to the matrix [45]. Poor bonding, delamination and voids in the structure also accelerate water diffusion.

If the environment is hot and dry, it has been observed in glass-vinyl-ester laminate joints that the mechanical properties start to decrease, but after certain amount of time the mechanical properties are better than the mechanical properties of virgin, unexposed components. This can be explained with post-curing. The mechanical properties decrease during post-cure, and when the post-cure is fully achieved, the mechanical properties increase, providing high strength to the application. [45]

At elevated temperatures the natural degradation process is accelerated, but at higher temperature such degradations mechanisms would occur that would not in normal operating temperatures [47].

6.3 Sulphuric acid

Studies have shown that exposure to relatively weak (~5 %) sulphuric acid (H_2SO_4) has little to no effect on the mechanical behavior of vinyl ester resins [51]. The heat deflection temperature HDT is not affected by weak acidic environment. Vinyl ester resin has a lightly lower modulus when exposed to sulphuric acid and it shows sensitivity to high temperatures as well. These changes however are not detrimental. Sulphuric acid has been detected to penetrate cracks or voids in the vinyl ester matrix, and this may cause the joint to weaken.

More concentrate sulphuric acid solutions (25 %) has been observed to change the color of resin to brown and slightly lighten the fibers. The Barcol hardness decreases after 9 months of exposure. The strength decreases during the first six months of sulphuric acid immersion. In the study only strength has significant decrease after 9 months of immersion, the changes in stiffness were only minor [52].

EXPERIMENTAL PART

7. MATERIALS

The materials used in the vessels are made of vinyl ester epoxy and glass fibers. The walls are manufactured by filament winding and the bottom is made of chopped strand mat by vacuum infusion.

7.1 Resins

Vinyl esters are thermosetting resins that consist of an epoxy backbone and unsaturated vinyl and ester groups. The chemical structure of vinyl ester epoxy is presented in Figure 12. Vinyl ester epoxy resins are manufactured by addition reaction of an epoxy resin with acrylic monomer such as methacrylic or acrylic acid. [53] Vinyl esters are cured with free radical mechanism, which is further discussed in Chapter 2.3. The crosslinking monomer in vinyl ester epoxy resins is typically styrene, of which vinyl ester epoxies contain 30-50 weight% [7; 54]. The chemical structure of styrene is presented in Figure 13. Vinyl ester resins usually require promoters and catalyst in order to cure. Metal compounds such as cobalt naphthalene are used as promoters, and ketone peroxides as catalysts. [54]

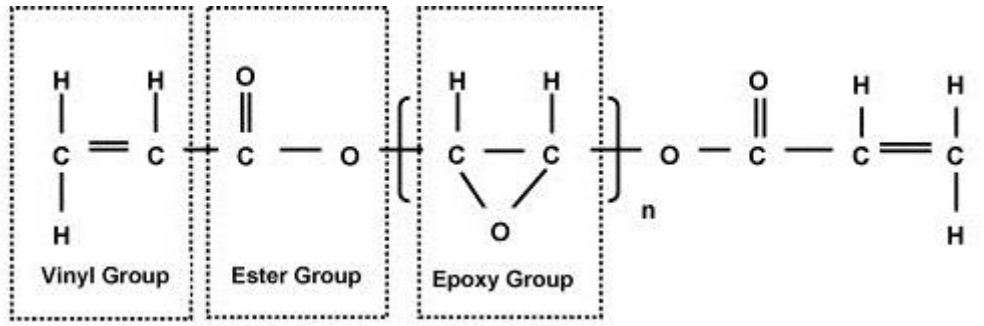

Figure 12. *Chemical structure of vinyl ester epoxy resin, adapted from [53]*

Vinyl esters have advantages compared to unsaturated polyester resins. The molecular weight of vinyl ester epoxy is relatively small compared to traditional polyester resins, and the structure is more regular than the polyester one [55]. This contributes to their chemical resistivity, which is superior to polyesters. In vinyl esters the chemically weak ester bonds are present only at the end of the molecule structure, and this minimizes the number of those bonds that can be chemically attacked. On the other hand the unsaturated vinyl groups in the end of the molecule provide good reactivity, and rapid free radical curing is possible with the presence of the vinyl groups and monomers such as styrene. [53]

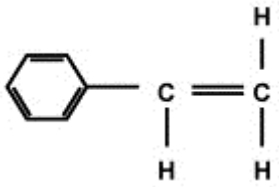

Figure 13. *Chemical structure of styrene, adapted from [53]*

Four different types of vinyl-ester epoxies were used in this study to compare the properties to each other. The mixing ratios of resin, promoter and catalyst are presented in Table 1.

Table 1. *Mixing rations of resin, promoter and catalyst (parts per hundred (pht) resin moulding compound).*

Resin	**promoter** [phr]	**catalyst** [phr]
1	0.30	1.50
2	0.30	2.50
3	0.55	1.25
4	0.20	1.25

7.2 Fibers

The reactor vessels are reinforced with glass fibers. Glass fibers can be divided into general-purpose and special-purpose glass fibers. Most common general-purpose glass fiber is E-glass and its variants. ECR-glass is a special-purpose glass fiber [56], which is electrically and chemically resistant. It is used in reactor vessels due its good chemical resistivity.

E-glass is calcium alumino-borosilicate glass containing typically 5-6 weight% of boron oxide and less than 1 weight% of alkali oxide [56; 57]. However, the boron emissions are harmful to environment, and an environmental friendly option of boron-free E glass exists. Boron free E-glass has a better corrosion resistance than boron-containing glass, almost as high as that of ECR-glass. ECR-glass is chemically resistant special purpose E-glass, and it has long term acid resistance and short term alkali resistance. The corrosion resistance of glass fibers depends on their chemical structure. [56] The typical physical and mechanical properties of glass fibers are presented in Table 2.

Table 2. *Physical and mechanical properties of glass fibers, adapted from [56].*

	Bulk density [g/cm^3]	**Weight loss in 24 h in 10 % H_2SO_4 [%]**	**Young's modulus [GPa]**	**Filament elongation at break [%]**
Boron-containing E-glass	2.54-2.55	~41	76-78	4.5-4.9
Boron-free E-glass	2.62	~6	80-81	4.6
ECR-glass	2.66-2.68	5	80-81	4.5-4.9

ASTM standards [58] distinguish commercial E-glass variants by their end use. Glass containing 0-10 % are certified for general applications Aerospace applications and circuit boards are made of composition containing 5-10 % boron. Both of these compositions can contain 0-2 % alkali oxide and 0-1 % of fluoride.

Glass fibers come in various forms. The glass is molten and wound into rovings. The rovings can be used as such, or woven into a fabric. Chopped strand mat non-woven fabric in which the glass fiber rovings are chopped into 20-50 mm long strands. The chopped strands are then compacted in a random orientation and bounds together with either fused polymer powder binder or aqueous polymer emulsion [57]. The reactor vessel parts are manufactured by filament winding. The impregnated glass fiber rovings are wound around a mould, and a chopped strand mat is laminated on the surface.

8. METHODS

The experimental part of this thesis focuses on two parts: identifying the air-inhibited layer and characterizing surfaces after various mechanical preparations. Resins without fibers were used to characterize the air-inhibited layer. Seven samples of each resin were prepared. They were first cured in room temperature for 24 hours, and then post-cured in 80 °C for 4 hours (resin 4) or 8 hours (resins 1, 2 and 3), according to instructions.

The surface preparations were characterized from six filament wound laminates, each the size of approximately 30 cm * 21 cm. The thickness of the laminates was approximately 1 cm, and they were slightly curved as they were cut off from the real sized vessel. Two of the laminates are presented in Figure 14. The laminates were mechanically prepared on both sides. Each laminate had a different method of preparation. The methods are described in Table 3. The characterizations of the laminates were conducted as a blind test; the preparation methods were revealed after the characterization and analysis was done. This way the results were not compromised by preconceptions. The outer side of the laminates is indicated with a number 1 and the mould side is indicated with a number 2.

Table 3. *The mechanical preparation methods of each laminate.*

Laminate	
A	Well abraded
B	Abraded with a worn wheel
C	Well sandblasted
D	Negligently sandblasted
E	Sandblasted with too fine sand
F	Abraded with wire brush

Figure 14. *Surface treated laminates F (abraded with a wire brush) and C (well sandblasted.*

8.1 Fourier transform infrared spectroscopy

Fourier transform infrared spectroscopy FT-IR was used to detect the air-inhibited layer in the resin. The measuring set-up of FT-IR is presented in Figure 15. After preparing the samples, both mould surface and outer surface of the sample were measured with FT-IR to determine the formation of air-inhibited layer. Both surfaces were measured to see if the mould would hinder the formation of the air-inhibited layer. The measurements were done in function of time as presented in Table 4. Measurements no. 7-11, a 3 mm layer was sanded off from both sides of a comparison sample, and the sample was measured to determine the thickness of the air-inhibited layer. For every measurement a 3 mm layer of a new sample was abraded off. One of the samples was split in half (Figure 16) to obtain the FT-IR spectrum of the bulk resin without air-inhibited layer.

Figure 15. *FT-IR measurement of resin sample.*

Figure 16. *A resin sample split in half.*

A test series of partially cured samples were carried out, as presented in Table 4. Resin samples were measured after 8 hours curing, abraded, and measured again. The process was repeated after 24 hours. No post-curing was performed. The spectra of these measurements were compared to the spectra of post-cured resin samples.

Table 4. *The measuring schedule for determining air-inhibited layer. In measurements 7-11 a surface layer of 3 mm of comparison sample was sanded off. A sample without post-curing was measured after 8 hours and 24 hours of cure.*

Measurement	Time	Original post-cured sample	Abraded post-cured sample	Sample without post-curing
1	0	x		
2	0.5 h	x		
3	1 h	x		
4	5 h	x		
5	8h			x
6	12 h	x		
7	24 h	x	x	x
8	72 h	x	x	
9	7 d	x	x	
10	14 d	x	x	
11	28 d	x	x	

The surfaces of the laminates were measured with FT-IR as well. The spectra were then compared to the spectra of sanded resin samples in order to determine if the air inhibited layer was removed during the preparation.

8.2 Contact angle

The surface energy of the samples was measured with a drop test. In this method, drops of liquid are placed on the surface, and the contact angle θ is measured. The set-up is shown in Figure 17. The image of the drop is recorded with a camera, and the contact angle is calculated from the image. The measurement was conducted with two liquids, water and ethylene glycol, as shown in Figure 18.

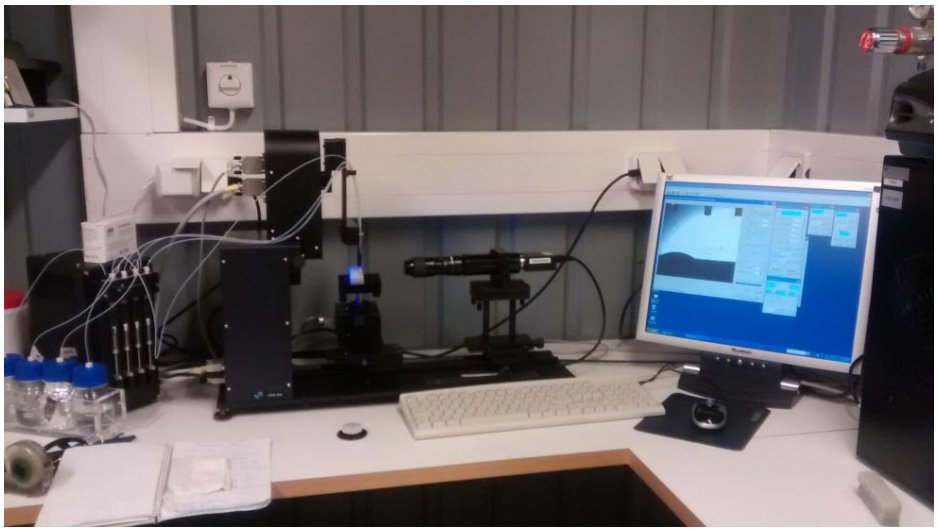

Figure 17. *The set-up of contact angle measurement.*

The surface energy of each resin (1, 2, 3 and 4) was measured after post-curing and after wiping the surfaces with acetone. Five drops of each liquid were placed on the samples and the surface energy was calculated with Wu method. The surface energy of the laminates was measured placing ten drops of each liquid. The measurement was repeated to the other side of the laminate. The surface energy was calculated with the Wu method, which is introduced in Chapter 2.5.

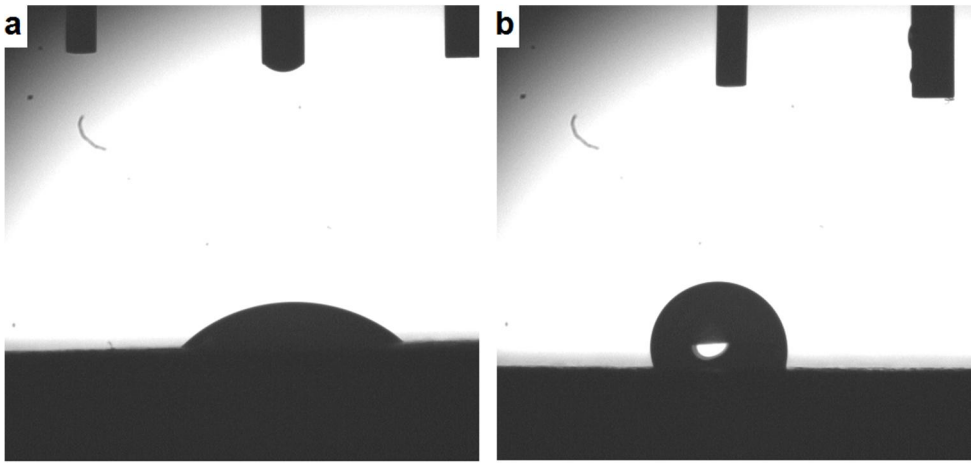

Figure 18. *Drop test to calculate the surface energy of the laminate F2 with a) ethylene glycol and b) water.*

8.3 Surface roughness

Conventional surface roughness measurement with a stylus system was conducted on both sides of the laminate. The basic principle of measuring the R_a value is presented in Chapter 4.1. Ten measurements were made of each side of the laminates, five of which perpendicular to the other five. The surface roughness was measured with Mitutoyo Surftest SJ-301.

The surface was also scanned with an optical profilometer Alicona InfiniteFocus G5 (in Figure 19). The profilometer is based on focus-variation, which is discussed in Chapter 4.1. An area of ca. 2.5 cm * 2.5 cm was scanned and a high resolution digital 3D image of the surface was formed. The R_a values were determined from the 3D image. These R_a values were then compared to the R_a values obtained from the basic surface roughness measurement. An area of 400 mm^2 from the 3D image was analyzed and the true area with all the peaks and valleys was calculated with the profilometer's software Infinite Focus.

.

Figure 19. *Alicona InfiniteFocus G5 profilometer [59]*

8.4 Scanning electron microscope

Both sides of each laminate were investigated with scanning electron microscope (SEM). Zeiss ULTRAplus scanning electron microscope is in Figure 20. Small laminate samples were cut off, coated with thin gold layer to ensure electrical conductivity and studied with SEM. The obtained SEM images were compared to each other.

Figure 20. *Scanning electron microscope Zeiss ULTRAplus [60]*

8.5 Pull-off tests

Adhesion between resin and laminate surface was measured with a pull-off tester. The adhesion tests were performed with Elcometer 110 Pneumatic Adhesion Tester, which is presented in Figure 21. A screw is adhered to the surface and the screw is then pulled off with compressed air. The adhesive used in these tests was resin 2, which is the same resin used in the manufacturing of the laminates.

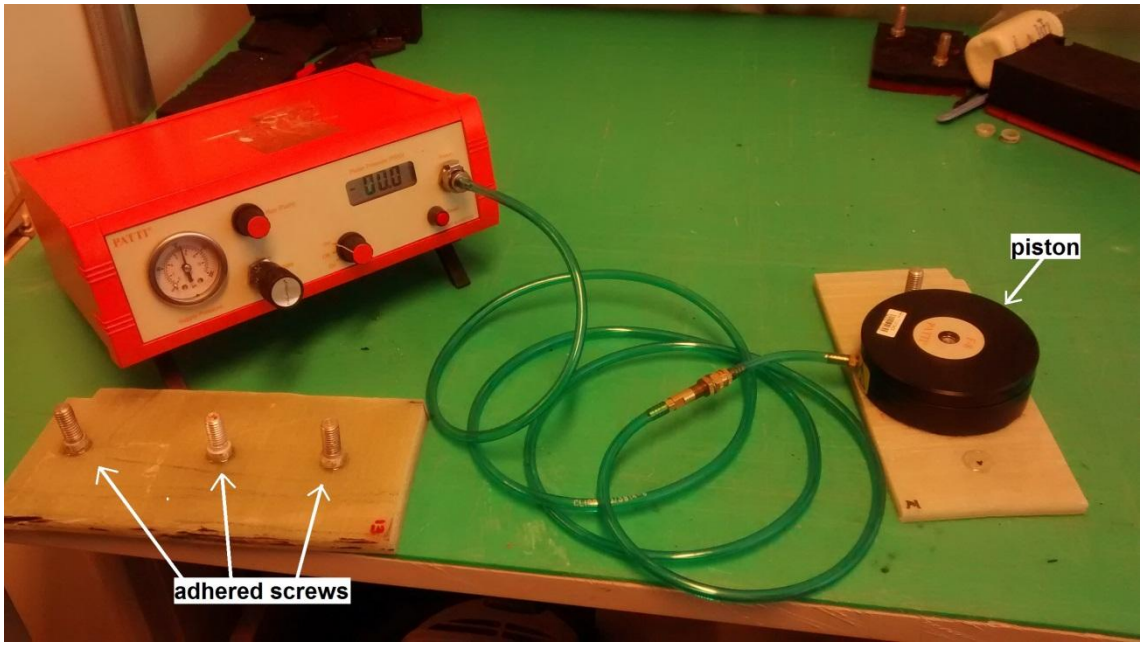

Figure 21. *The set-up of Elcometer 110 pneumatic adhesion tester and test laminates with adhered screws.*

Figure 22 presents the cross section of the piston that is used to pull the screw off. The pressure lifts the gaskets, when the reaction plate attached to the screw is lifted, pulling off the screw. The pressure needed to pull of the screw is then recorded and converted with conversion table to MPa.

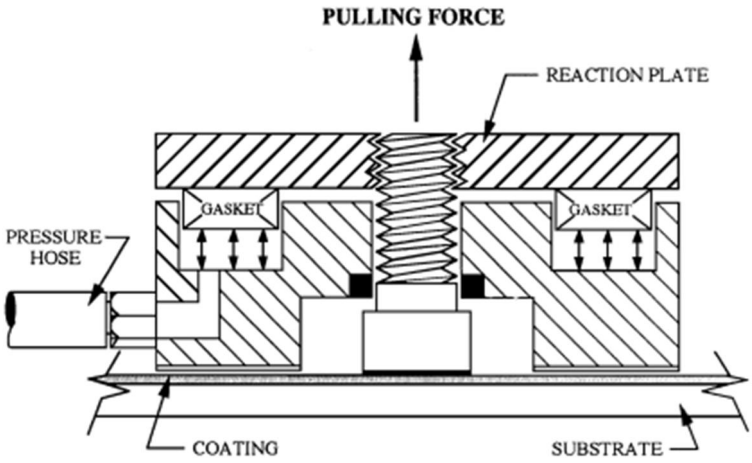

Figure 22. *Cross section of the piston of the adhesion tester. [61]*

For the blind test laminates three screws were adhered to each surface. After 24 hours of curing in room temperature the screws were pulled off and the results were recorded and converted.

8.6 Photography

Photographing the laminates to determine the sufficient pretreatment was also considered. Well roughened areas reflect light differently and appear lighter in the photos, and it should be possible to determine the uniformity of the roughened area based on the contrasting areas. However, the vinyl ester epoxy resins are translucent and the fibers are visible through the matrix, as presented in Figure 23. Thus determining the sufficiency of the surface treatment from photographs is not possible.

Figure 23. *A photograph of the test laminate F1. The fibers can be seen through the matrix.*

9. RESULTS AND DISCUSSION

The results of the characterization methods presented in Chapter 8 are presented and discussed in this chapter. All the FT-IR curves and SEM images are presented in Appendix A and Appendix B, respectively.

9.1 Fourier transformation infrared spectroscopy

FT-IR was used to detect the air-inhibited layer from the resin samples. The spectra of resin 2 right after post curing, 24 hours after post curing and 72 hours after post curing are presented in Figure 24. The spectra are identical, which indicates that the air inhibited layer forms already during the post curing. A comparison between a spectrum of post-cured but untreated and a spectrum of abraded resin sample is shown in Figure 25. The beginning of the spectrum of the abraded sample is almost straight and the peaks at 2925 cm^{-1} and 3430 cm^{-1} are missing. This indicates that the surface of the cured resin is indeed different in structure compared to the rest of the resin. This was confirmed by splitting a post-cured sample in half and measuring the split surface. The spectrum of the spilt surface in presented in Figure 26. The same peaks are missing from the split sample spectrum as from the abraded sample spectrum.

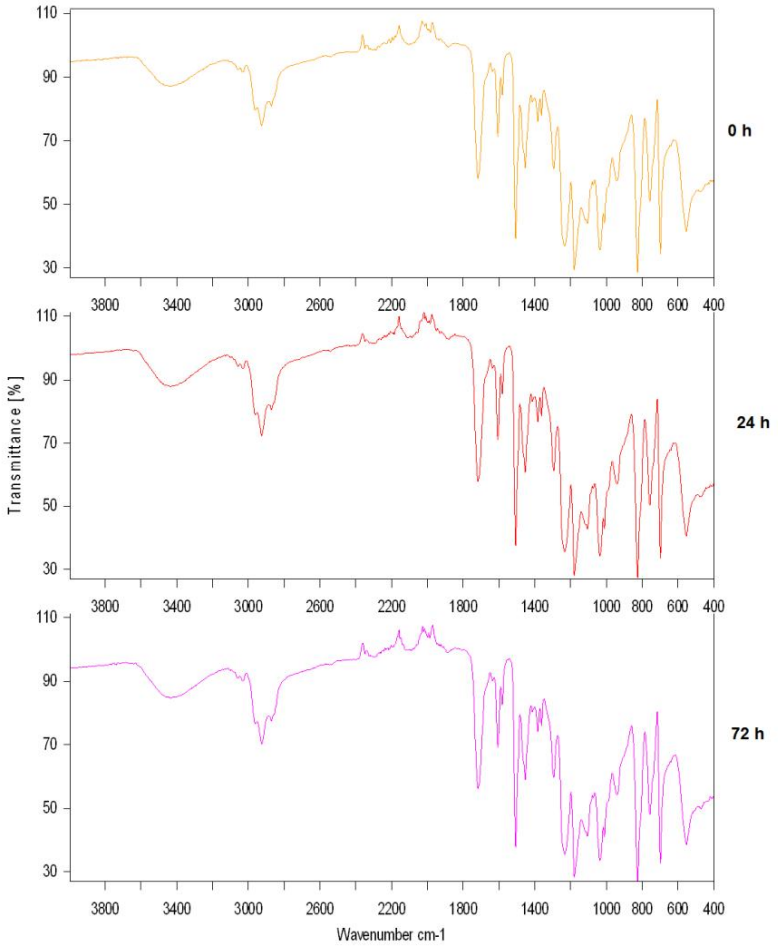

Figure 24. *The FT-IR spectra of resin 2 right after post curing (0 h), 24 h after post curing and 72 h after post curing.*

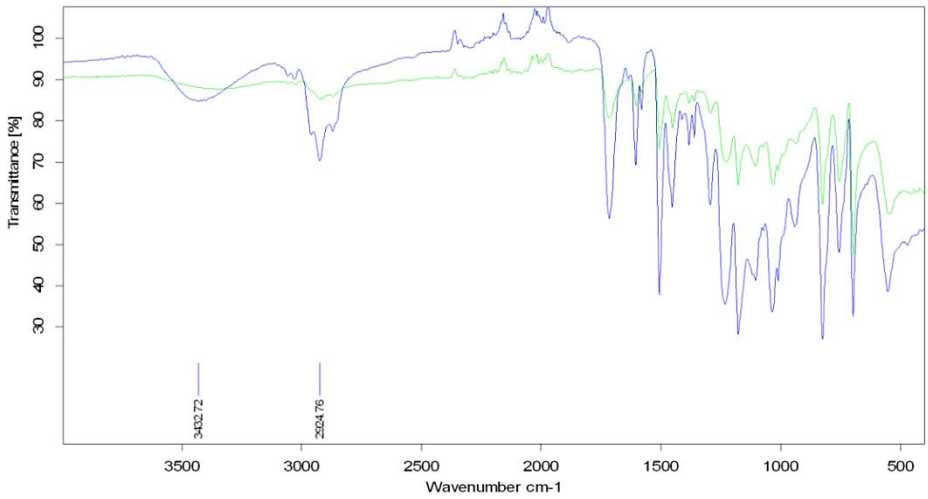

Figure 25. *The FT-IR spectra of resin 2. The blue curve is from untreated resin sample measured after 72 hours after post curing. The green curve is the comparison sample of which a 3 mm layer was grinded off.*

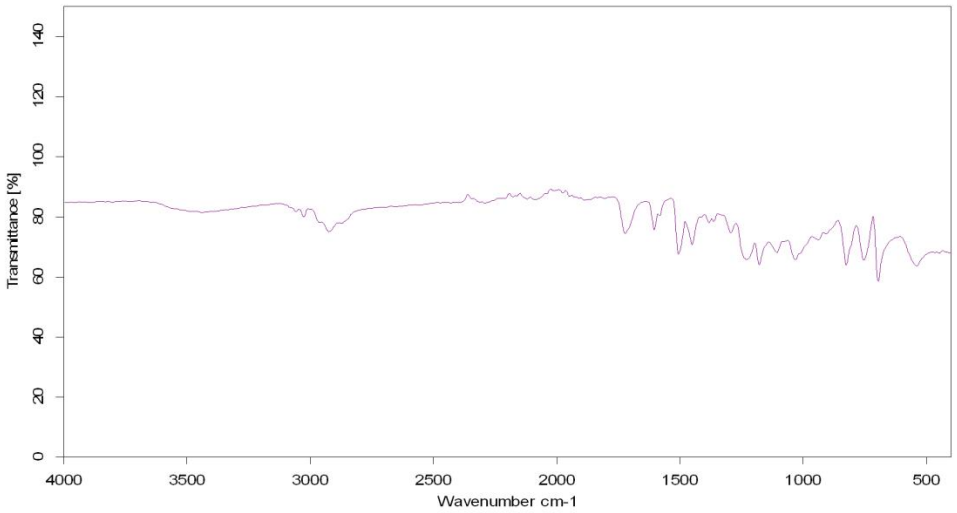

Figure 26. *The FT-IR spectrum of a resin 2 sample split in half.*

The FT-IR measurements were also made from samples after 8 hours curing at room temperature. The measurements were repeated after 24 hours of cure. The spectra of 24 hours of cure and abraded comparison sample are shown in Figure 27. The spectra are very similar to the non-abraded spectra of the post cured samples, and this indicates that the surface does not change during curing, but the change happens in the composition of the rest of the resin. As the air inhibits the polymerization, the surface remains similar to the uncured resin. Therefore the layer cannot reform once the layer is removed. It is probable that if the joint is made soon after the component starts curing, the surface is still active and there is no need to remove the layer. However it is unclear when the layer becomes inactive.

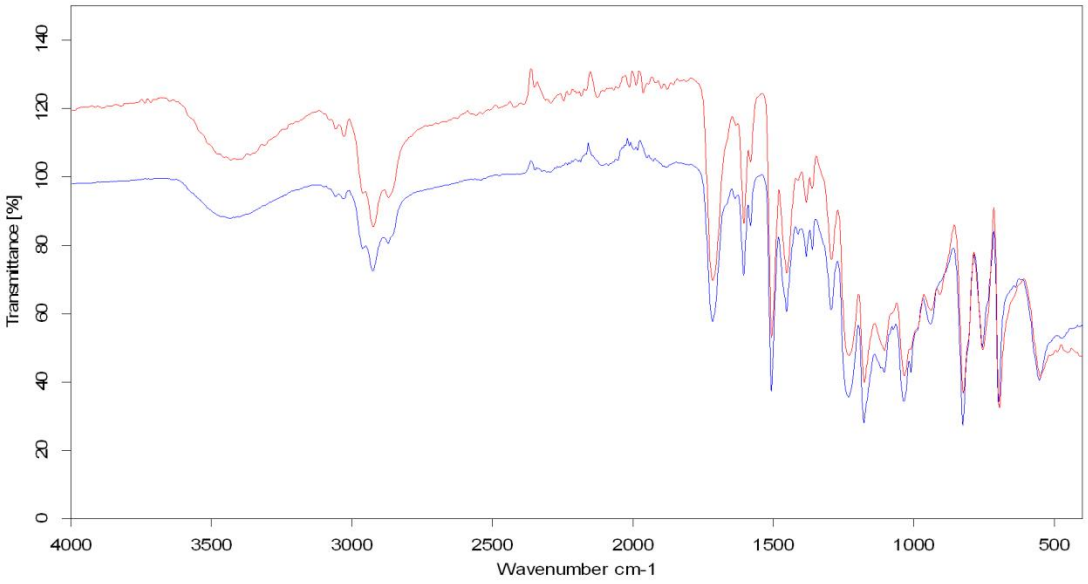

Figure 27. *The FT-IR spectra of resin 2 post-cured sample after 24 hours (blue) and a sample without post-curing after 24 hours.*

All the pretreated laminate surfaces were measured as well. Figure 28 shows the spectrum of the well abraded laminate A. All the laminates had similar curves, which mean that the air-inhibited layer was removed in all of the pretreatments. Even though some of the laminates were clearly poorly pretreated, this indicates that the air-inhibited layer is easily removed at least from the peaks on the surface.

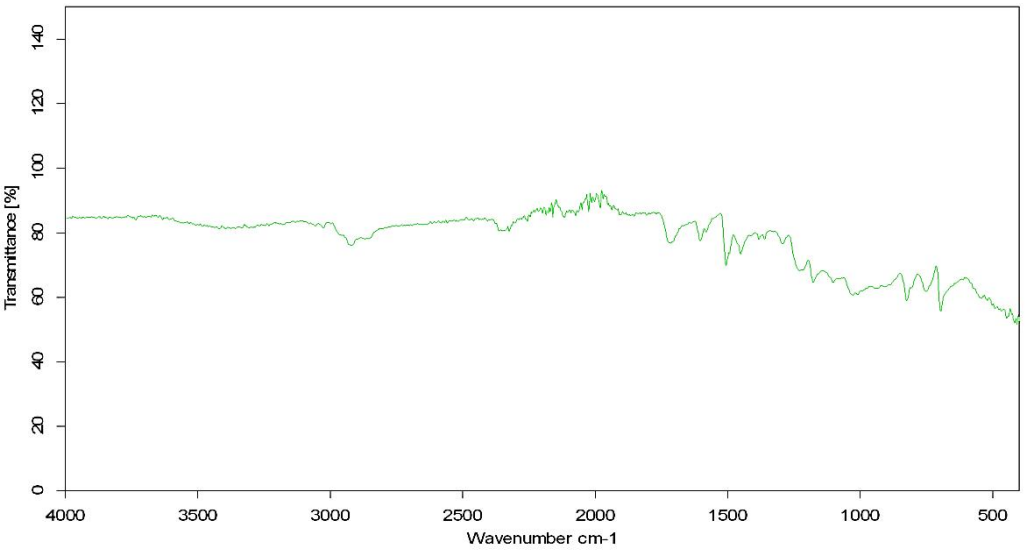

Figure 28. *The FT-IR spectrum of the well abraded laminate A1.*

9.2 Surface energy

The mould surfaces of resin samples were wiped with acetone to determine if it increases the surface energy. The increase in surface energy increases adhesion. The results are

shown in Figure 29. There is a slight growth in surface energy after acetone wiping, but is not significant considering the deviation and the fact that the acetone used was laboratory grade. Acetone used in the field might contain grease and other impurities, which contaminate the surfaces and decreases adhesion in the joint. Therefore wiping the surfaces with acetone should be avoided.

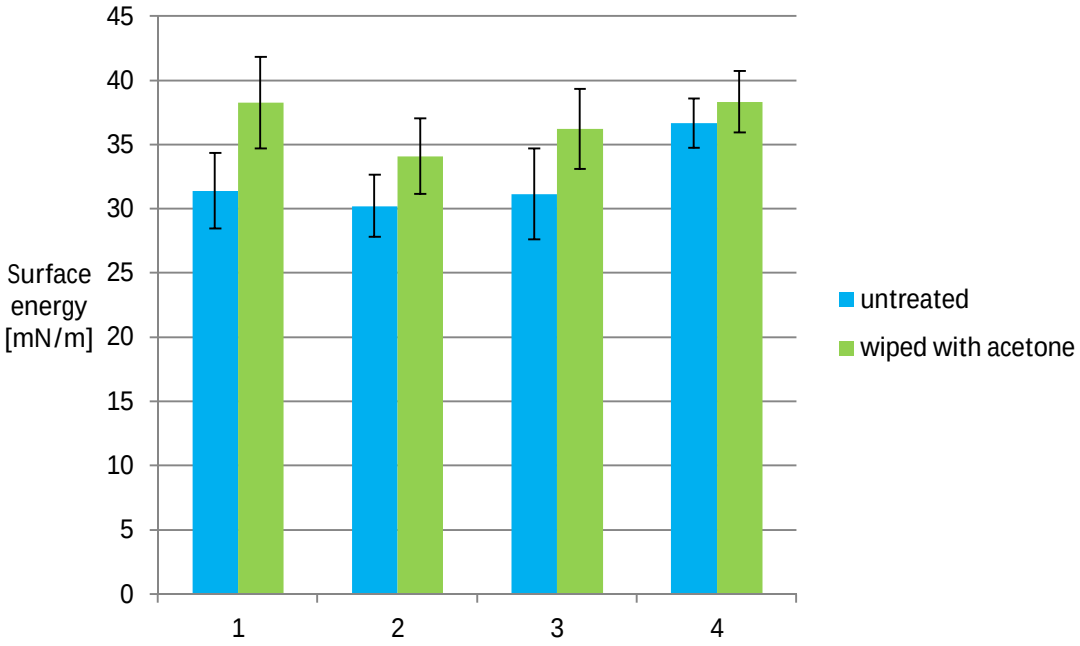

Figure 29. *The effect of wiping the surfaces with acetone on surface energy. The measurements were made from the mould surface of the resin samples 1, 2, 3 and 4.*

The surface energy of the pre-treated laminates was also calculated and the results are presented in Figure 30. The results of C1 (well sandblasted) and D2 (negligently sandblasted) are left out as the results were distinctly false due to the effect described in Figure 4 in Chapter 2.5. The sandblasted surface C2 stands out with a high surface energy, as does well abraded surface A1 and the surface ground with wire brush (F2). The latter surface was very unevenly roughened, and the measured area was most likely from the rougher end of the roughness spectrum. There are hardly any difference between negligently abraded laminates (B) and negligently sandblasted laminates (D) in terms of surface energy,

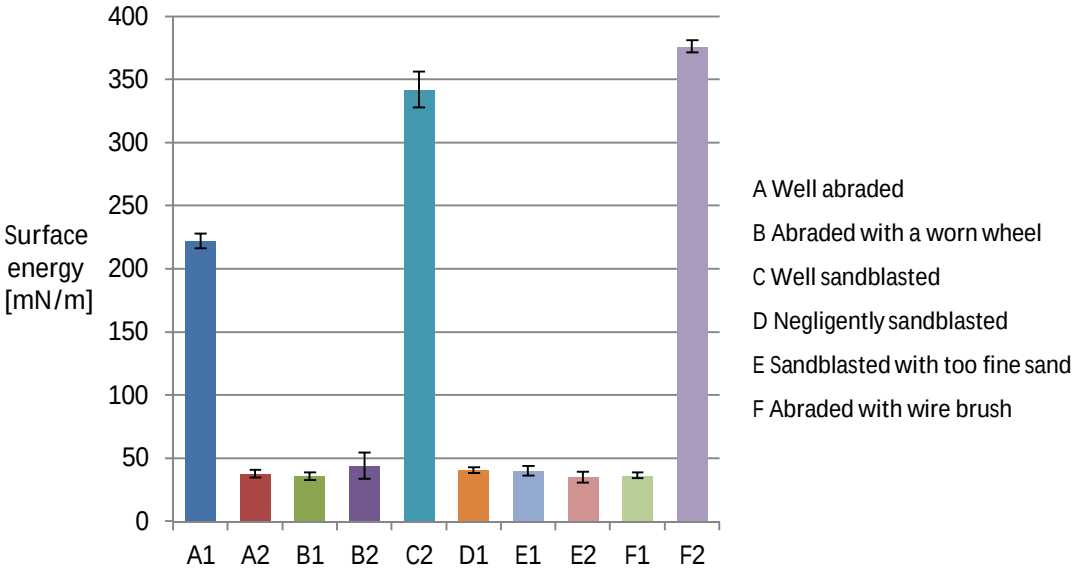

Figure 30. *Surface energy of the test laminates.*

9.3 Surface roughness

The R_a values measured with both stylus system and profilometer are presented in Figure 31. Roughness measurements made with the optical profilometer are generally more accurate than the measurements made with stylus system. However the measured area is smaller as high resolution 3D imaging is very slow. The well sandblasted surface C is can be distinguished from the other laminates with both measuring methods as it is distinctly rougher. The laminate F abraded with a wire brush seems to have a high roughness value, but the deviation is notable. This indicates that the surface is uneven in terms of roughness and there are areas that are much smoother than the average suggests. It is hard to distinguish well abraded surface A from the negligently abraded surface B in terms of roughness values. The negligently sandblasted surface D and the too finely sandblasted surface E are in the same roughness range with the abraded laminates A and B. Therefore the roughness measurement on field is adequate only to verify the roughness of the sandblasted surface.

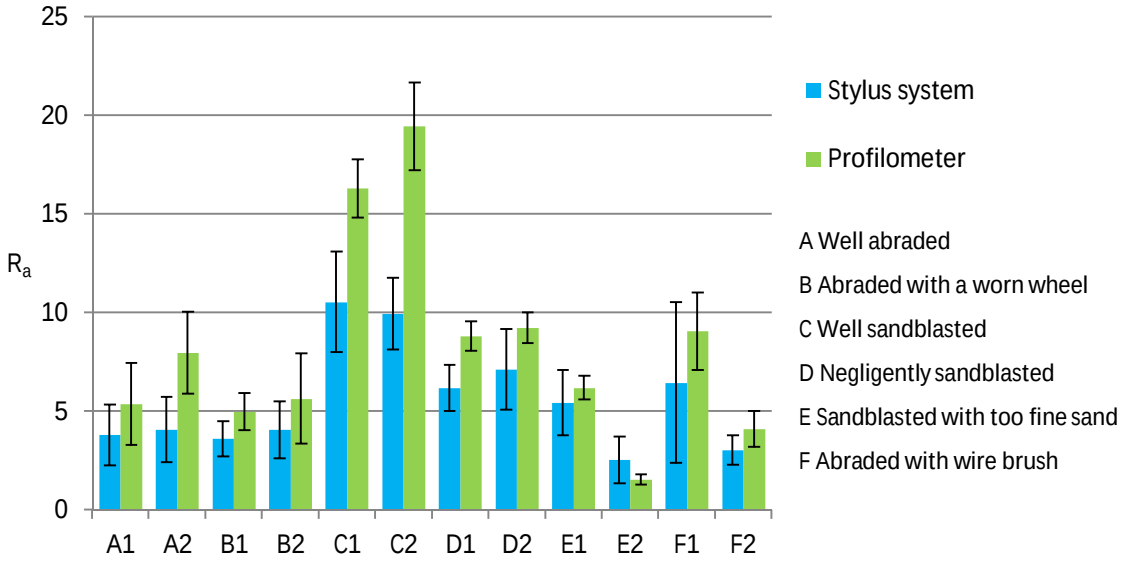

Figure 31. *Surface roughness of the laminates measured with stylus system (blue) and profilometer (green).*

The surface area was analyzed from the 3D image with Infinite Focus. An example of a 3D image is shown in Figure 32. An area of 400 mm^2 was projected from the image, and the actual area including all the peaks and valleys was calculated. If the surface was totally smooth, the true area would also be 400 mm^2. The relative true areas are presented in Figure 33. It seems that the best way to increase the surface area is sandblasting. Both well sandblasted laminate C and negligently sandblasted laminate D have larger true area than others. Interestingly the difference in the true surface area of well abraded A and poorly abraded B laminates is rather insignificant. The large true area of laminate B2 is most likely due to the fact that the measured area was small, and the sample area was from the rougher area of the laminate. The surface preparation did not substantially increase the true surface area of too finely sandblasted laminate E and the laminate F abraded with a wire brush.

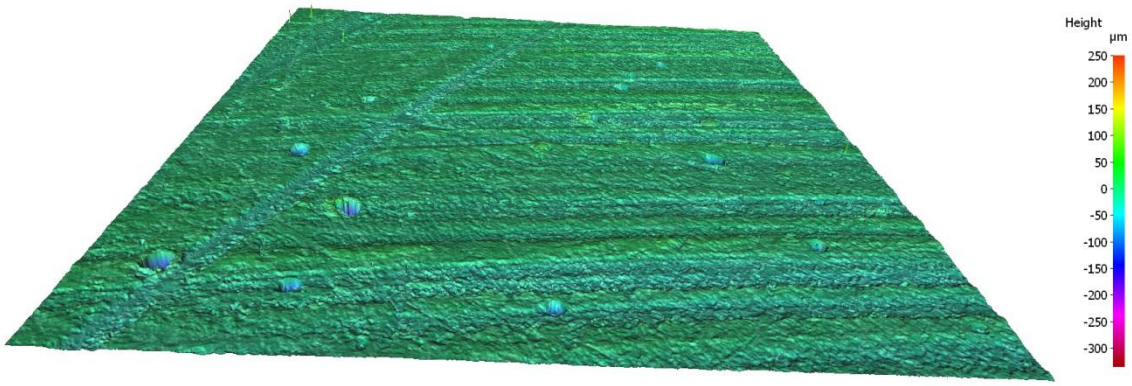

Figure 32. *A 3D image of poorly abraded mould surface B2.*

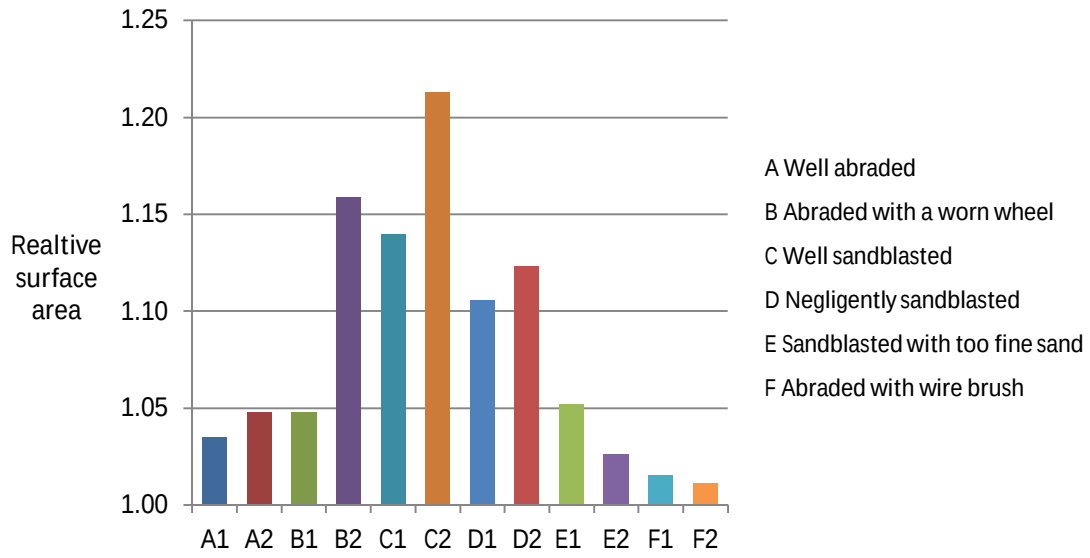

Figure 33. *The relative surface area measured from a 400 mm^2 projected area.*

9.4 Scanning electron microscope

The outer surface and the mould surface of the well abraded laminate A are presented in Figure 34 and Figure 35, respectively. Deep and wide grooves intersecting each other can be seen on the surface. Broken glass fibers can be detected on the outer surface but not on the mould surface, as there is a chopped strand mat over the filament wound structure. The pores seen in the images have formed during the filament winding,

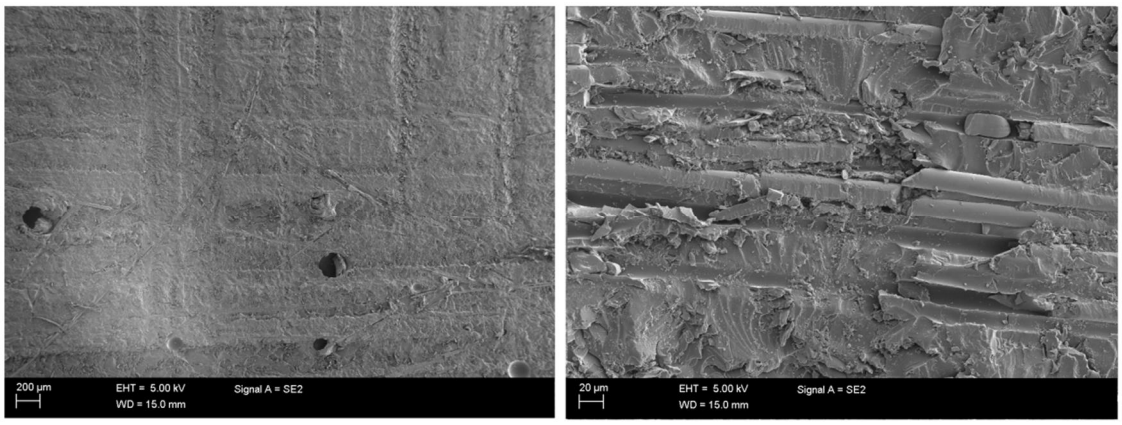

Figure 34. *Scanning electron microscope pictures of laminate A1 (well abraded outer surface).*

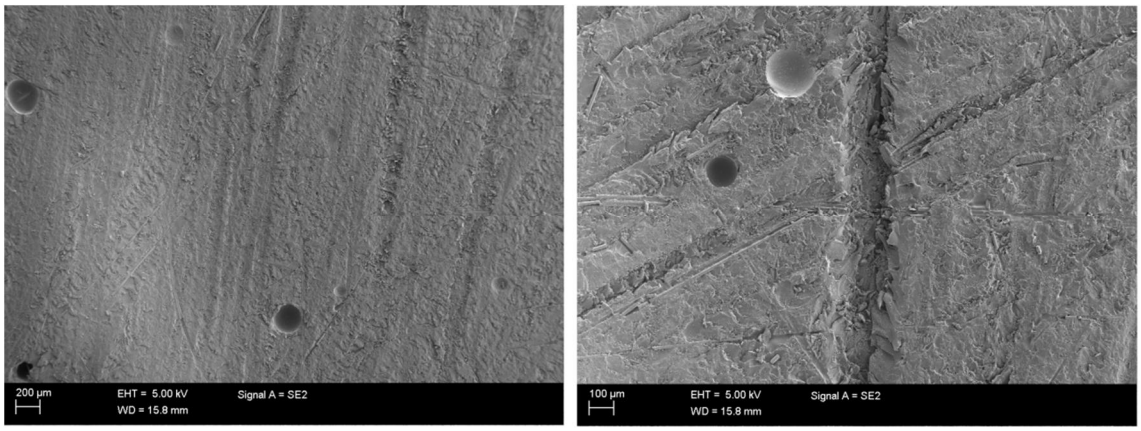

Figure 35. *Scanning electron microscope pictures of laminate A2 (well abraded mould surface).*

Figure 36 and Figure 37 show the SEM images of the surface abraded with a worn wheel. Comparing to the well abraded laminate A, the grooves are narrower and shallower. The grooves are parallel and are not intersecting each other as in the laminate A.

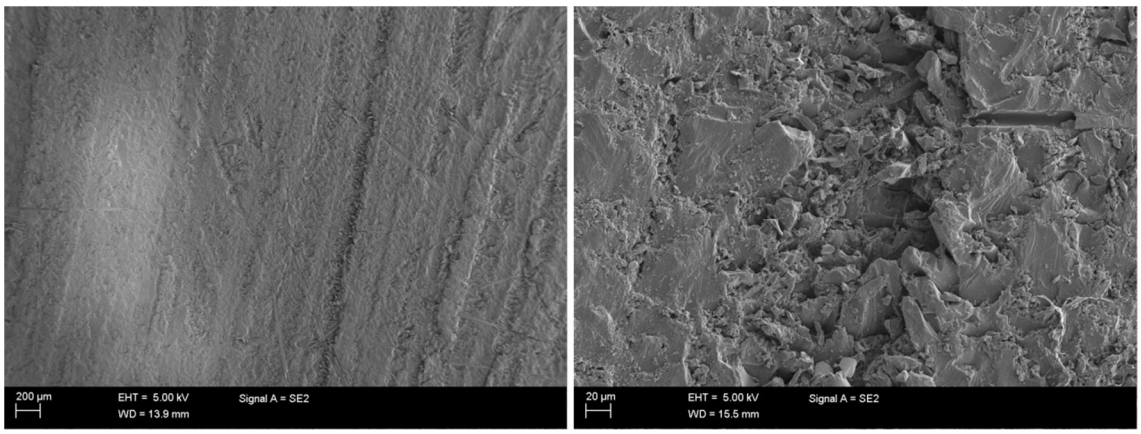

Figure 36. *Scanning electron microscope pictures of laminate B1 (outer surface abraded with a worn wheel).*

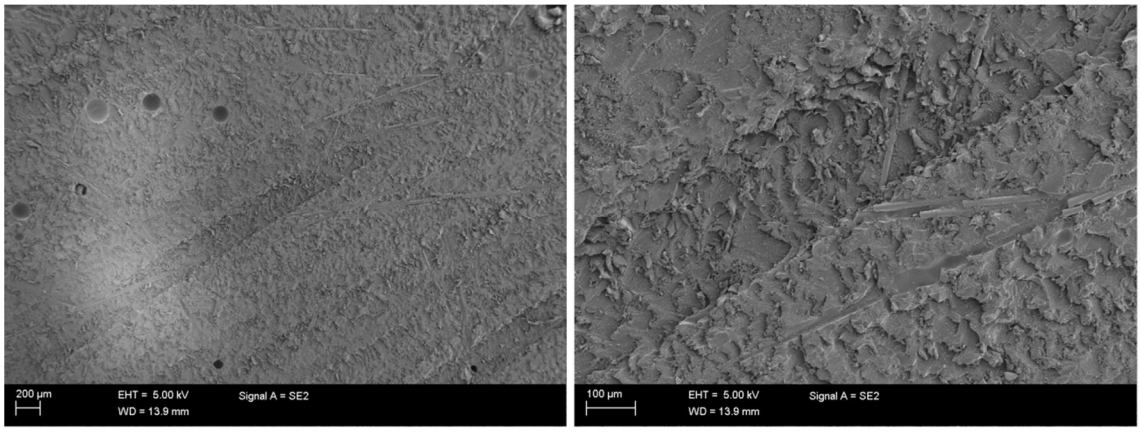

Figure 37. *Scanning electron microscope pictures of laminate B2 (mould surface abraded with a worn wheel).*

The both surfaces of the well sandblasted laminate C are shown in Figure 38 and Figure 39. The images are very different compared to the previous laminates; there are no grooves as the surface is homogenously rough. It is obvious that the surface area is greater than the surface area of laminates A and B. The broken fibers from the chopped strand mat are clearly visible in the outer surface of the laminate.

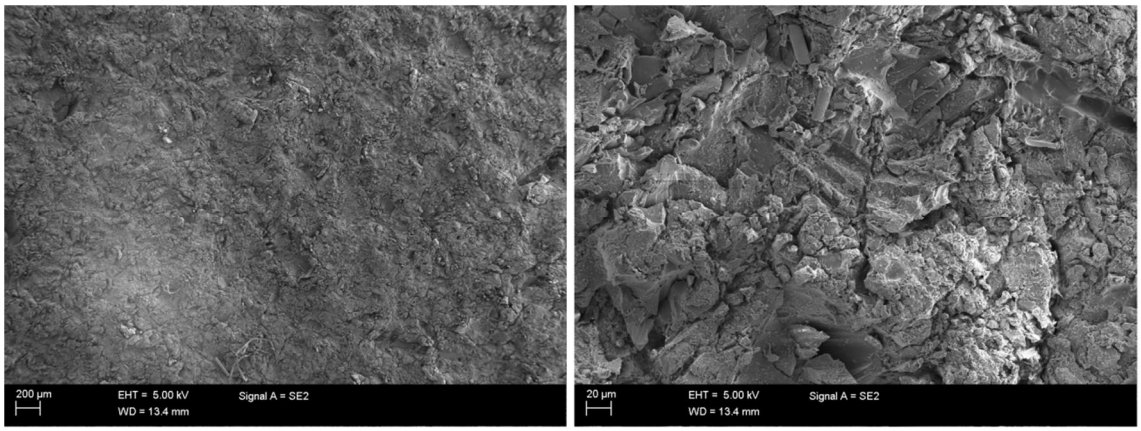

Figure 38. *Scanning electron microscope pictures of laminate C1 (well sandblasted outer surface).*

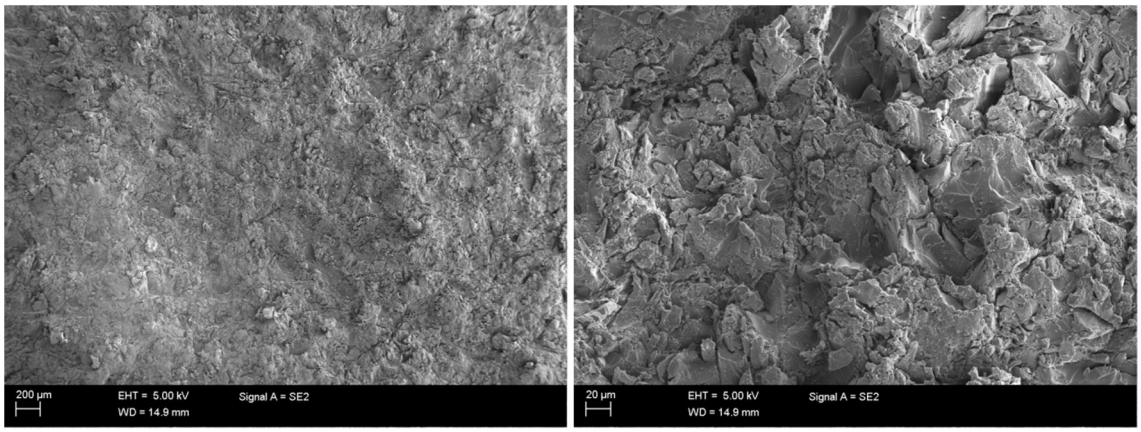

Figure 39. *Scanning electron microscope pictures of laminate C2 (well sandblasted mould surface).*

The difference between well sandblasted surface and negligently sandblasted surface (shown in Figure 40 and Figure 41) is explicit. There are holes that are resulted from the sandblasting, but there are smooth areas in between. It is obvious that the surface area of this sample is smaller than the surface area of well sandblasted sample C.

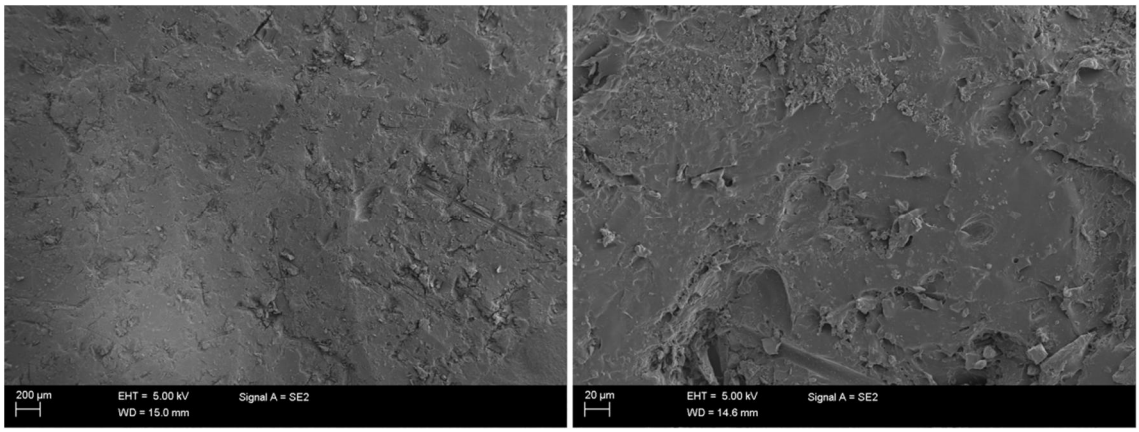

Figure 40. *Scanning electron microscope pictures of laminate D1 (negligently sandblasted outer surface).*

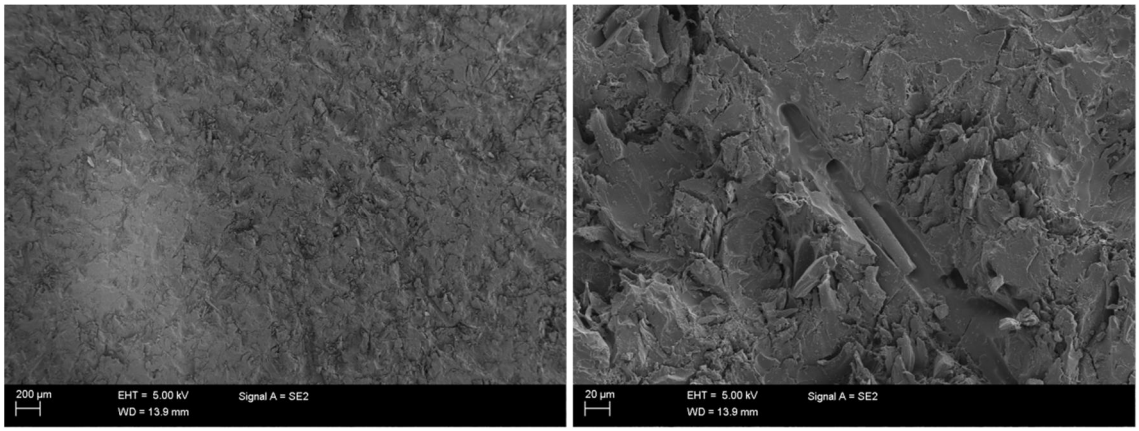

Figure 41. *Scanning electron microscope pictures of sample D2 (negligently sandblasted mould surface).*

Laminate E was sandblasted finely. The SEM images (Figure 42 and Figure 43) show that the surface is almost untouched. On the outer surface in Figure 42 there is clearly resin around the fibers that has cured and left untouched. There are no signs of any kind of tooling or machining. The mould surface resembles the negligently sandblasted laminate D, but there are less holes on the surface, and the smooth areas in between are larger.

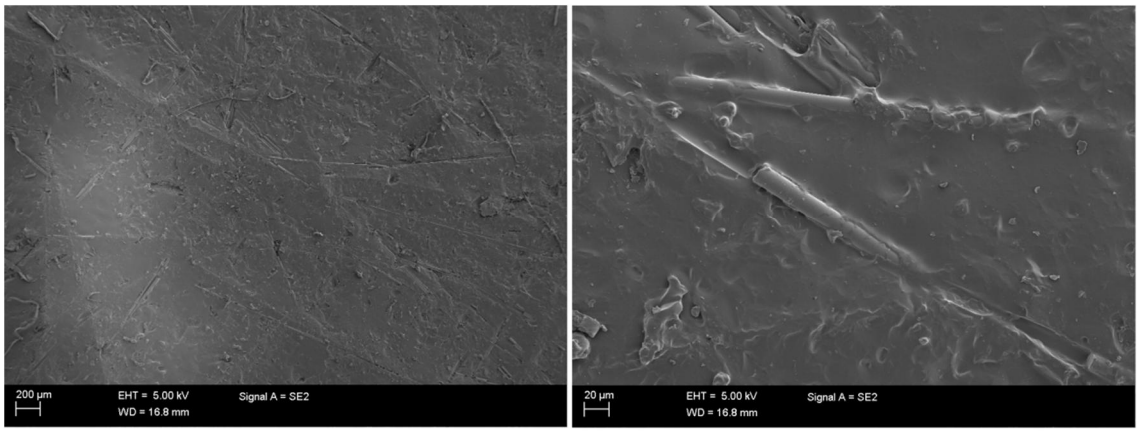

Figure 42. *Scanning electron microscope pictures of laminate E1 (outer surface sand-blasted with too fine sand).*

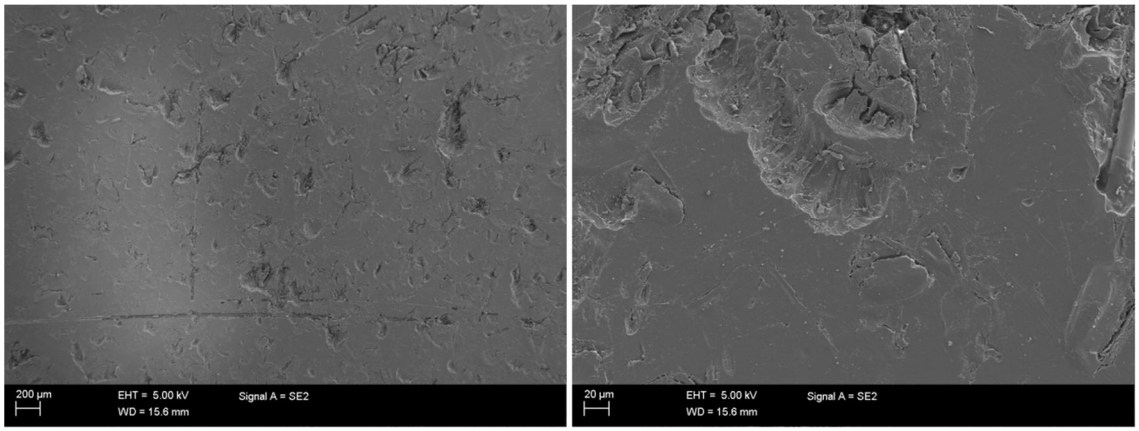

Figure 43. *Scanning electron microscope pictures of laminate E2 (mould surface sand-blasted with too fine sand)*

The images of laminate abraded with a wire brush are presented in Figure 44 and Figure 45. The surfaces are relatively smooth, and in the outer surface there are untouched areas. It seems that the wire brush has only reached the peaks of the surface and the valleys are not abraded at all. The mould surface (Figure 45) has thin, infrequent grooves intersecting each other on the surface. The areas in between the grooves are smooth and they seem untouched.

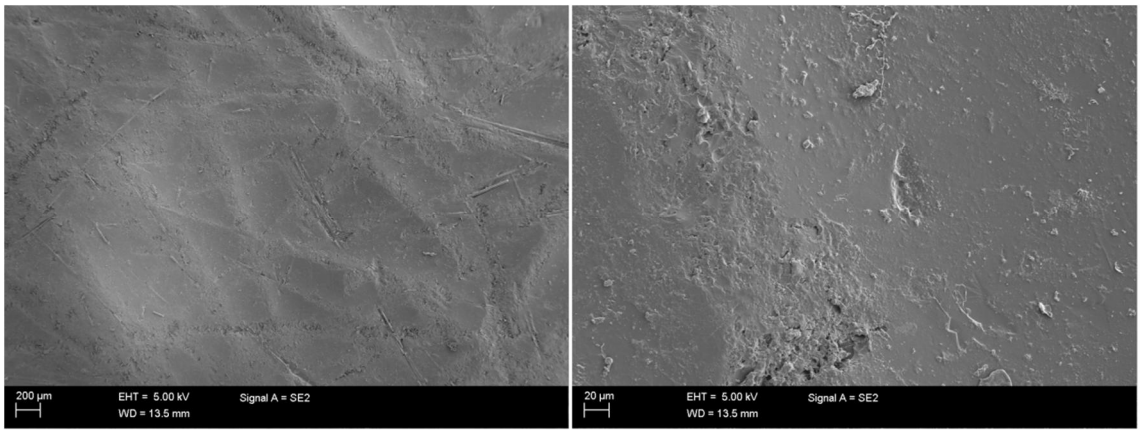

Figure 44. *Scanning electron microscope pictures of sample F1 (outer surface abraded with wire brush)*

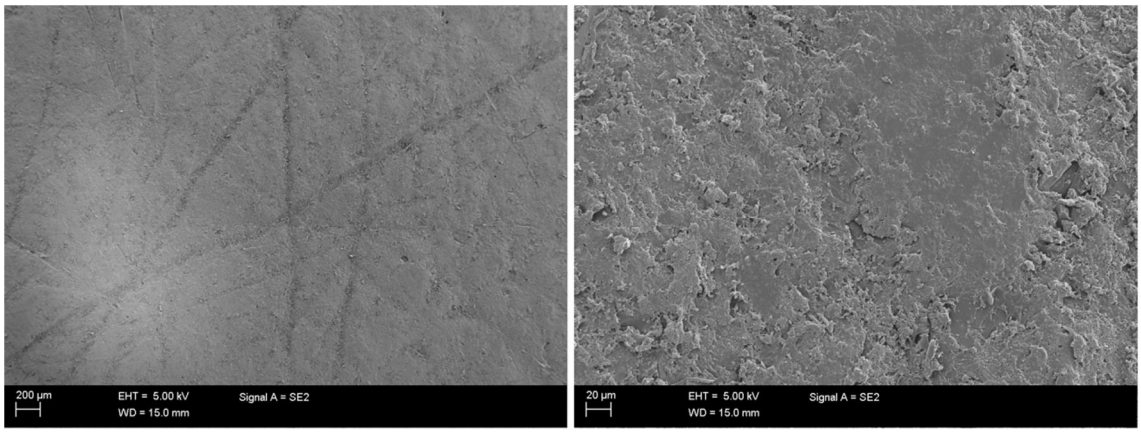

Figure 45. *Scanning electron microscope pictures of laminate F2 (mould surface abraded with wire brush).*

9.5 Pull-off tests

Adhesion between the laminate surface and the resin was measured with pull-off tests, and the results are presented in Figure 46. The results are controversial: it seems that the well abraded surface A, poorly abraded surface B and negligently sandblasted surface D are in the same magnitude. However the deviations of the latter two seem higher. The too finely sandblasted surface E and the surface F abraded with a wire brush needed lower load, as expected. Surprisingly, pulling off the screws adhered to the well sandblasted laminate C required only a low load. This can be explained by the failure mode. In the test laminate C the failure was adhesive between the screw and the adhesive, i.e. the interface between the screw and the adhesive failed before the interface between the laminate and the adhesive. The failures in other laminates were either cohesive failures or adhesive failures between the adhesive and the laminate. The deviation of the measurements is large, and therefore inaccuracies might occur. It must be noted that the actual joints of the reactor vessels are not under pulling load. Shear tests would give more accurate results on the joint strength.

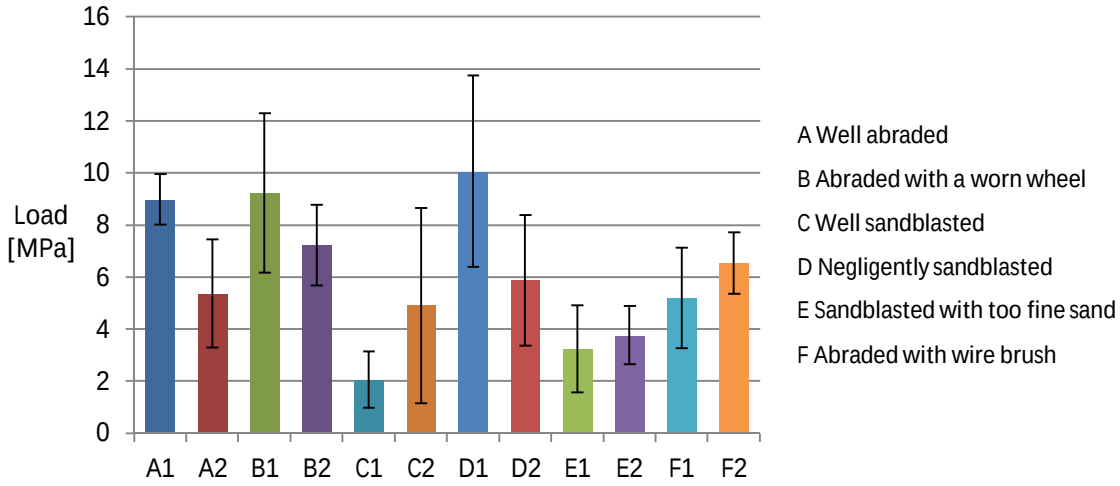

Figure 46. *The load needed to pull off the screw adhered to the laminate.*

10. CONCLUSIONS

In this thesis the surfaces of filament wound laminates and pure resin samples were characterized. First the formation and verification of the removal of the air-inhibited layer was studied. It was confirmed that after curing the composition of the surface layer was different from the rest of the resin. The oxygen inhibits polymerization and there are unreacted double bonds on the surface. Once the air-inhibited layer is removed, e.g. by grinding, it cannot reform as the double bonds in the rest of the resin have already cross-linked with styrene. The air-inhibited layer is thin, as grinding a 3 mm layer removes it. It is likely that any mechanical surface treatment removes the layer, and therefore the layer itself is not an issue in practice.

The effect of acetone wiping on improving the adhesion properties was studied by drop test. The resins that were wiped with acetone showed a slight increase in surface energy, but the increase is not significant. The acetone was laboratory grade, whereas the acetone used on-site most likely has impurities such as oil or traces of resin, and the wiping may contaminate the surface. Contaminants decrease the adhesion, and the possible gain in surface energy is minimal considering the possible disadvantages.

The characterization of surface treatments was conducted as a blind-test; the surface preparation methods were revealed after the characterization and analysis was done. The test results suggest that the most effective way to increase surface roughness and area in a reliable manner is sandblasting. However, it is important to conduct the sandblasting adequately and the end result depends also from the sand grade. If the used sand is too fine, the sufficient surface roughness and area are not achieved. Preparing the surface with a wire brush or sandblasting with too fine sand do not result in the wanted outcome. The risk of these two is that they might even make the surfaces smoother, even though the air-inhibited layer is removed. The difference in surface roughness and area in well and poorly abraded laminates is not significant. Distinguishing the well and poorly abraded surfaces on-site based on the methods used in this study is not possible. However, the visual inspection of the surfaces should not be forgotten, as the visual difference between the laminates is obvious to a trained eye.

A joint between two laminates was simulated with a laminate and the same resin that was used to manufacture the laminate. The adhesion between the surface and the resin was tested by pull-off test. The results are approximate of the joint strength, as the real joints experience shearing forces rather than pulling forces. The difference in the load needed to pull off the screw between the well abraded, the poorly abraded and the negligently sandblasted surfaces was not significant. In the well sandblasted surface the

failure happened between the screw and the resin, and therefore the results are not comparable. However, the change in failure type might mean that the adhesion between the resin and laminate is higher. To continue the study, shear tests, e.g. single lap shear test, should be conducted to verify the results of the mechanical testing to simulate similar mode of loading as in real application..

The best method of the surface characterization that can be used on-site based on this study is a stylus system to determine the surface roughness, at least for the sandblasted surfaces. There are handheld FT-IR devices to verify the removal of the air-inhibited layer. However, the removal of the air-inhibited layer does not guarantee adequate surface preparation. Even the too fine sandblasting and wire brushing removed the layer.

There are many other factors that influence in joint strength, e.g. the choice of adhesive and post-curing cycle. The matter is very complex, because these factors affect each other. Optimization of all the factors requires wider research and testing.

REFERENCES

[1] S.K. Mazumdar, Joining of Composite Materials, in: Composites Manufacturing: Materials, Product, and Process Engineering, CRC Press, 2001.

[2] M. Davis, D. Bond, Principles and practices of adhesive bonded structural joints and repairs, International Journal of Adhesion and Adhesives, Vol. 19, No. 2–3, 1999, pp. 91-105.

[3] S. Nassar, X. Yang, Fastening and Joining of Composite Materials, in: E. Patterson, D. Backman, G. Cloud (ed.), Springer New York, 2013, pp. 5-23.

[4] W. Sandra Polesky, Thermal Effects on the Bearing Behavior of Composite Joints, NASA Langley Technical Report Server, 2001, 127 p.

[5] J.J. Tierney, J.W. Gillespie Jr, P.-. Bourban, 2.31 - Joining of Composites, in: A.K. Zweben (ed.), Comprehensive Composite Materials, Pergamon, Oxford, 2000, pp. 1029-1047.

[6] A.A. Taib, R. Boukhili, S. Achiou, S. Gordon, H. Boukehili, Bonded joints with composite adherends. Part I. Effect of specimen configuration, adhesive thickness, spew fillet and adherend stiffness on fracture, International Journal of Adhesion and Adhesives, Vol. 26, No. 4, 2006, pp. 226-236.

[7] R.P. Brill, G.R. Palmese, An investigation of vinyl-ester–styrene bulk copolymerization cure kinetics using Fourier transform infrared spectroscopy, Journal of Applied Polymer Science, Vol. 76, No. 10, 2000, pp. 1572-1582.

[8] T.J. Tulig, M. Tirrell, Molecular theory of the Trommsdorff effect, Macromolecules, Vol. 14, No. 5, 1981, pp. 1501-1511.

[9] T.F. Scott, W.D. Cook, J.S. Forsythe, Kinetics and network structure of thermally cured vinyl ester resins, European Polymer Journal, Vol. 38, No. 4, 2002, pp. 705-716.

[10] T.F. Scott, W.D. Cook, J.S. Forsythe, Photo-DSC cure kinetics of vinyl ester resins. I. Influence of temperature, Polymer, Vol. 43, No. 22, 2002, pp. 5839-5845.

[11] T.F. Scott, W.D. Cook, J.S. Forsythe, Effect of the degree of cure on the viscoelastic properties of vinyl ester resins, European Polymer Journal, Vol. 44, No. 10, 2008, pp. 3200-3212.

[12] F.A. Rueggeberg, D.H. Margeson, The effect of oxygen inhibition on an unfilled/filled composite system, Journal of dental research, Vol. 69, No. 10, 1990, pp. 1652-1658.

[13] J. Bijelic-Donova, S. Garoushi, L.V.J. Lassila, P.K. Vallittu, Oxygen inhibition layer of composite resins: effects of layer thickness and surface layer treatment on the

interlayer bond strength, European journal of oral sciences, Vol. 123, No. 1, 2015, pp. 53-60.

[14] E. Velazquez, J. Vaidyanathan, T.K. Vaidyanathan, M. Houpt, Z. Shey, S. Von Hagen, Effect of primer solvent and curing mode on dentin shear bond strength and interface morphology, Quintessence international (Berlin, Germany : 1985), Vol. 34, No. 7, 2003, pp. 548-555.

[15] D. Truffier-Boutry, E. Place, J. Devaux, G. Leloup, Interfacial layer characterization in dental composite, Journal of oral rehabilitation, Vol. 30, No. 1, 2003, pp. 74-77.

[16] J. LI, Effects of surface properties on bond strength between layers of newly cured dental composites, Journal of oral rehabilitation, Vol. 24, No. 5, 1997, pp. 358-360.

[17] K.A. Kupiec, W.W. Barkmeier, Laboratory evaluation of surface treatments for composite repair, Operative dentistry, Vol. 21, No. 2, 1996, pp. 59-62.

[18] W.J. Finger, K. Lee, W. Podszun, Monomers with low oxygen inhibition as enamel/dentin adhesives, Dental Materials, Vol. 12, No. 4, 1996, pp. 256-261.

[19] D.E. Packham, Surface energy, surface topography and adhesion, International Journal of Adhesion and Adhesives, Vol. 23, No. 6, 2003, pp. 437-448.

[20] G. Barnes, I. Gentle, Interfacial science: an introduction, Oxford University Press Inc., New York, 2005, 247 p.

[21] K.S. Birdi, Solid Surfaces, in: Surface Chemistry Essentials, CRC Press, 2013, pp. 137-163.

[22] S. Wu, Polar and nonpolar interactions in adhesion, The Journal of Adhesion, Vol. 5, No. 1, 1973, pp. 39-55.

[23] M. Banea, L.F. da Silva, Adhesively bonded joints in composite materials: an overview, Proceedings of the Institution of Mechanical Engineers, Part L: Journal of Materials Design and Applications, Vol. 223, No. 1, 2009, pp. 1-18.

[24] L.F.M. da Silva, N.M.A.J. Ferreira, V. Richter-Trummer, E.A.S. Marques, Effect of grooves on the strength of adhesively bonded joints, International Journal of Adhesion and Adhesives, Vol. 30, No. 8, 2010, pp. 735-743.

[25] S. Ebnesajjad, 8 - Surface Preparation of Thermoplastics, Thermosets, and Elastomers, in: S. Ebnesajjad (ed.), Surface Treatment of Materials for Adhesion Bonding, William Andrew Publishing, Norwich, NY, 2006, pp. 197-250.

[26] J. Ahmad, Machining of Polymer Composites, 2009.

[27] Q. Bénard, M. Fois, M. Grisel, Peel ply surface treatment for composite assemblies: chemistry and morphology effects, Composites Part A: Applied Science and Manufacturing, Vol. 36, No. 11, 2005, pp. 1562-1568.

[28] Q. Bénard, M. Fois, M. Grisel, P. Laurens, Surface treatment of carbon/epoxy and glass/epoxy composites with an excimer laser beam, International Journal of Adhesion and Adhesives, Vol. 26, No. 7, 2006, pp. 543-549.

[29] K.L. Mittal, T. Bahners, Adhesion and Adhesives: Fundamental and Applied Aspects: Laser Surface Modification and Adhesion, Wiley, Somerset, NJ, USA, 2014, 441 p.

[30] D. Basting, G. Marowsky, Excimer Laser Technology, Springer, Berlin Heidelberg, 2005, 433 p.

[31] Dumitras, D.C. (ed.). 2012. Nd YAG Laser. Croatia, InTech. 318 p.

[32] N.V. Raghavendra, L. Krishnamurthy, 9. Metrology of Surface Finish, in: Engineering Metrology and Measurements, Oxford University Press, Mysore, India, 2013, pp. 219-230.

[33] R. Leach, Introduction to Surface Texture Measurement, in: R. Leach (ed.), Optical Measurement of Surface Topography, Springer Berlin Heidelberg, 2011, pp. 1-14.

[34] S.G. Kazarian, K.L.A. Chan, Sampling Approaches in Fourier Transform Infrared Imaging Applied to Polymers, in: K. Grundke, M. Stamm, H. Adler (ed.), Characterization of Polymer Surfaces and Thin Films, Springer, Berlin Heidelberg, 2006, pp. 1-6.

[35] B.C. Smith, How an FTIR Works, in: Fundamentals of Fourier Transform Infrared Spectroscopy, 2nd ed., CRC Press, Boca Raton, Florida, 2011, pp. 19-53.

[36] G. Häusler, S. Ettl, Limitations of Optical 3D Sensors, in: R. Leach (ed.), Optical Measurement of Surface Topography, Springer Berlin Heidelberg, 2011, pp. 23-48.

[37] R. Danzl, F. Helmli, S. Scherer, Focus variation–a robust technology for high resolution optical 3D surface metrology, Strojniški vestnik-Journal of mechanical engineering, Vol. 57, No. 3, 2011, pp. 245-256.

[38] X.E. Gros, NDT Data Fusion, Butterworth-Heinemann, Oxford, 1996, 211 p.

[39] V.M. Karbhari, L.S. Lee, 7. Non-Destructive Testing and Evaluation (NDT/NDE) of Civil Structures Rehabilitated Using Fiber Reinforced Polymer (FRP) Composites, in: V.M. Karbhari, L.S. Lee (ed.), Service Life Estimation and Extension of Civil Engineering Structures, Woodhead Publishing, Cambridge, 2011, pp. 193-222.

[40] R. Zoughi, Microwave Non-Destructive Testing and Evaluation Principles, Springer Science & Business Media, Dordrecht, 2000, 263 p.

[41] T.W. Liao, Y. Li, An automated radiographic NDT system for weld inspection: Part II—Flaw detection, NDT & E International, Vol. 31, No. 3, 1998, pp. 183-192.

[42] W. Sachse, Review of Progress in Quantitative Nondestructive Evaluation, Springer, 1991, 1575-1582 p.

[43] Ultrasonic Weld Testing : Ultrasonic Non Destructive Testing : Offshore Pipeline Inspections, Global X-Ray & Testing Corporation, web page. Available (accessed 29.12.2015): http://www.globalxray.com/ultrasonic-weld-testing.

[44] U.B. Halabe, A. Vasudevan, H.V.S. GangaRao, P. Klinkhachorn, G. Lonkar, Subsurface Defect Detection in FRP Composites Using Infrared Thermography, AIP Conference Proceedings, Vol. 760, No. 1, 2005, pp. 1477-1484.

[45] A. Hammami, N. Al-Ghuilani, Durability and environmental degradation of glass-vinylester composites, Polymer composites, Vol. 25, No. 6, 2004, pp. 609-616.

[46] I.A. Ashcroft, D.J. Hughes, S.J. Shaw, Adhesive bonding of fibre reinforced polymer composite materials, Assembly Automation, Vol. 20, No. 2, 2000, pp. 150-161.

[47] M. Bowditch, The durability of adhesive joints in the presence of water, International Journal of Adhesion and Adhesives, Vol. 16, No. 2, 1996, pp. 73-79.

[48] K. Armstrong, Effect of absorbed water in CFRP composites on adhesive bonding, International Journal of Adhesion and Adhesives, Vol. 16, No. 1, 1996, pp. 21-28.

[49] V. Karbhari, S. Zhang, E-glass/vinylester composites in aqueous environments–I: experimental results, Applied Composite Materials, Vol. 10, No. 1, 2003, pp. 19-48.

[50] Y. Zhang, A.P. Vassilopoulos, T. Keller, Effects of low and high temperatures on tensile behavior of adhesively-bonded GFRP joints, Composite Structures, Vol. 92, No. 7, 2010, pp. 1631-1639.

[51] M. Banna, J. Shirokoff, J. Molgaard, Effects of two aqueous acidic solutions on polyester and bisphenol A epoxy vinyl ester resins, Materials Science and Engineering: A, Vol. 528, No. 4, 2011, pp. 2137-2142.

[52] A. Kootsookos, P. Burchill, The effect of the degree of cure on the corrosion resistance of vinyl ester/glass fibre composites, Composites Part A: Applied Science and Manufacturing, Vol. 35, No. 4, 2004, pp. 501-508.

[53] M. Grujicic, Y. Sun, K. Koudela, The effect of covalent functionalization of carbon nanotube reinforcements on the atomic-level mechanical properties of poly-vinyl-ester-epoxy, Applied Surface Science, Vol. 253, No. 6, 2007, pp. 3009-3021.

[54] S.H. Goodman, Handbook of Thermoset Plastics (2nd Edition), William Andrew Publishing/Noyes, Westwood, New Jersey, 1998, 582 p.

[55] P. Cook, Vinyl Ester Resins, Van Nostrand's Encyclopedia of Chemistry, 2005, .

[56] F.T. Wallenberger, J.C. Watson, H. Li, 4. Glass Fibers, in: D.B. Miracle, S.L. Donaldson (ed.), ASM Handbook, Volume 21 - Composites, ASM International, Ohio, 2001, pp. 27-34.

[57] F.R. Jones, 6. Glass Fibres, in: J.W.S. Hearle (ed.), High Performance Fibres, Woodhead Publishing, Cambridge, 2001, pp. 191-238.

[58] ASTM D 578-98, SI units and recommendations for the use of their multiples and of certain other units, ASTM International, West Conshohocken, Pennsylvania, 2001, 51 p.

[59] Surface profile 3D measuring systems, Department of Materials Science, Tampere University of Technology, web page. Available (accessed 27.12.2015): http://www.tut.fi/en/about-tut/departments/materials-science/research/research-equipment/surface-analysis/surface-profile-measuring-system/index.htm.

[60] Scanning electron microscopy, The Department of Materials ScienceTampere University of Technology, web page. Available (accessed 7.1.2016): http://www.tut.fi/en/about-tut/departments/materials-science/research/research-equipment/microscopy/sem/index.htm.

[61] TMA-0187 Issue 06, Elcometer 110 P.A.T.T.I.® Pneumatic Adhesion Tester, Elcometer Limited, 2008, 20 p.

APPENDIX A: THE FT-IR SPECTRA OF THE RESIN SAMPLES AND LAMINATES

RESIN 1

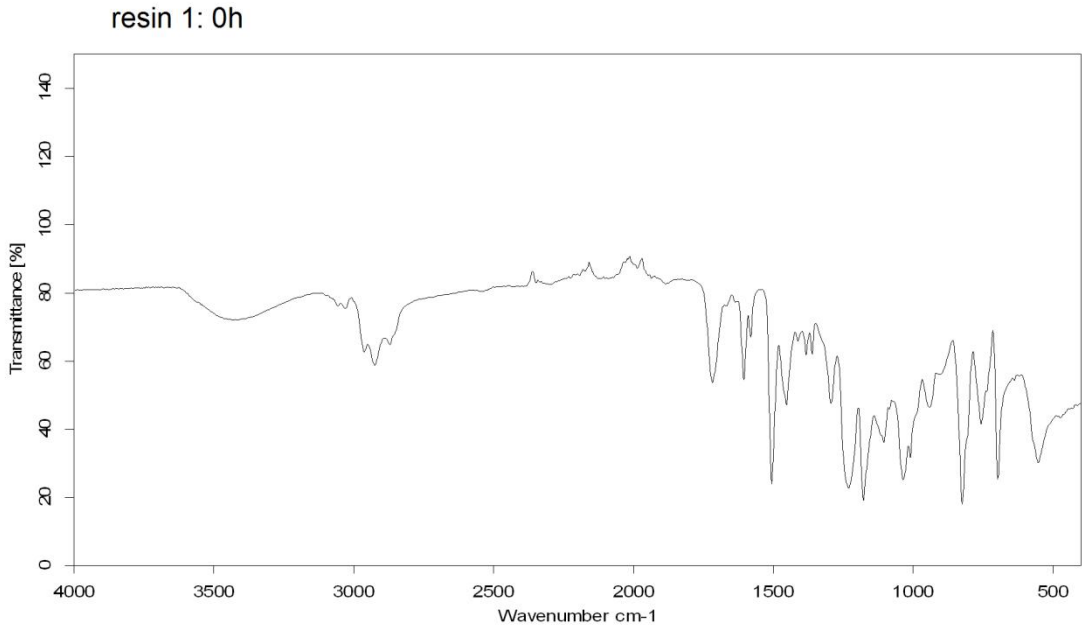

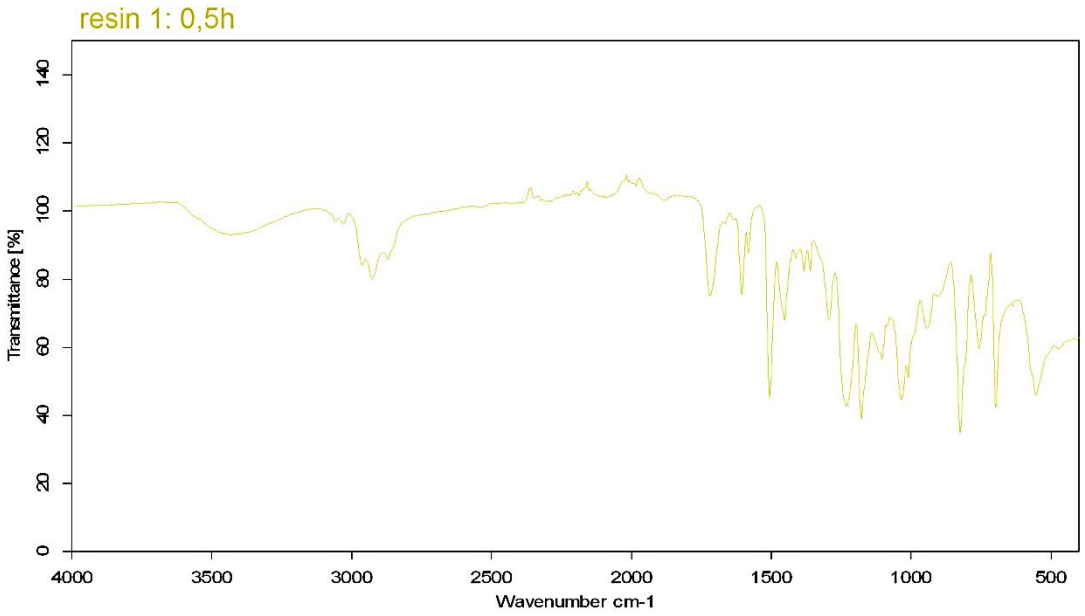

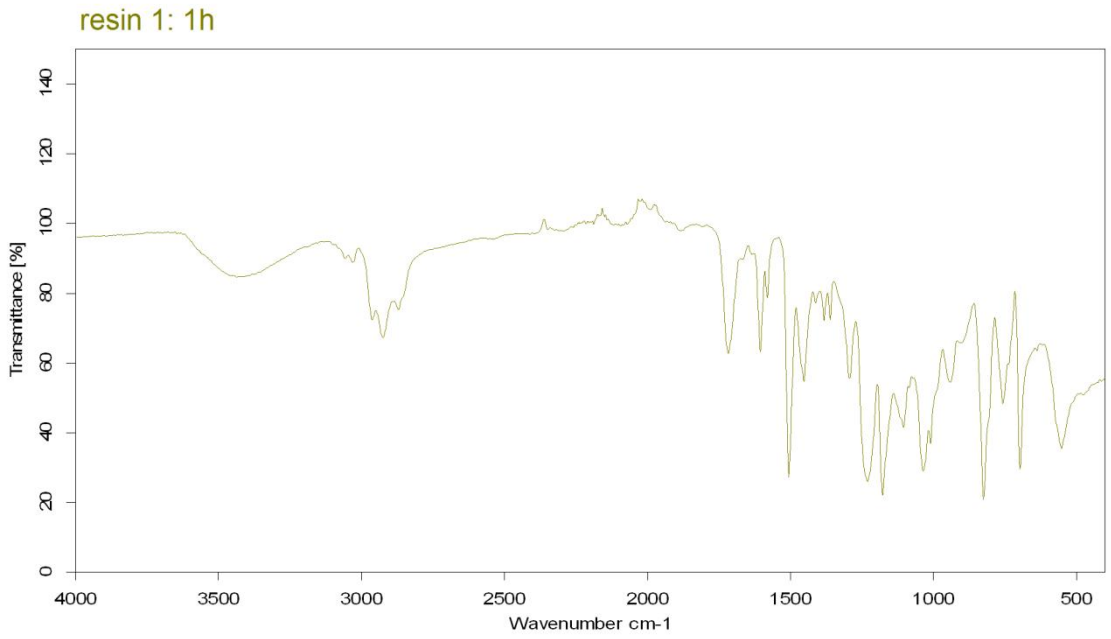
resin 1: 1h
Transmittance [%]
0
20
40
60
80
100
120
140
4000
3500
3000
2500
2000
1500
1000
500
Wavenumber cm-1

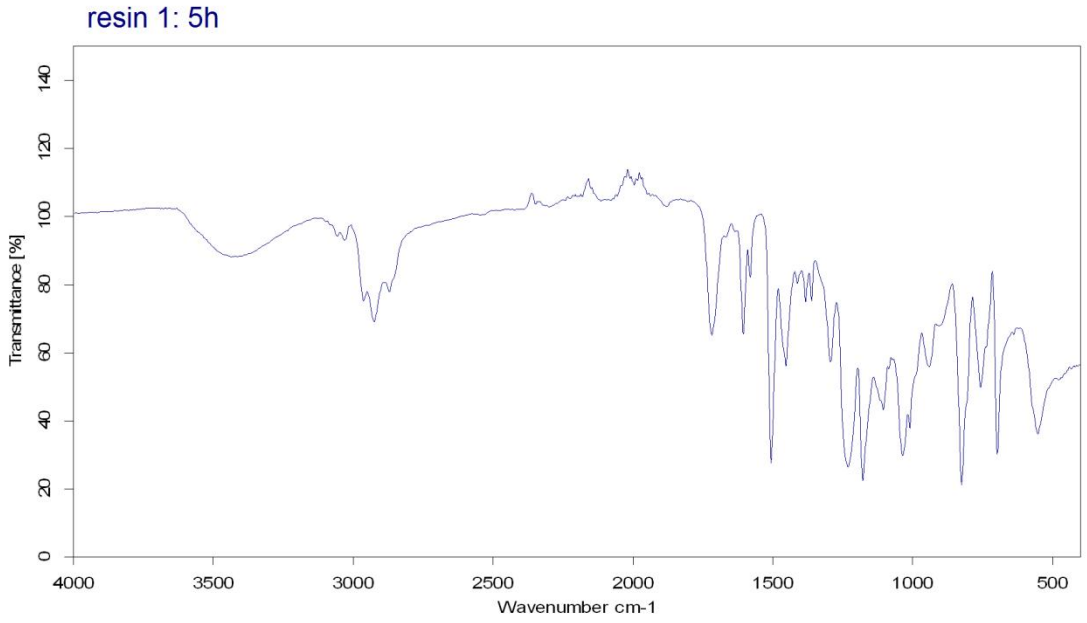
resin 1: 5h
Transmittance [%]
0
20
40
60
80
100
120
140
4000
3500
3000
2500
2000
1500
1000
500
Wavenumber cm-1

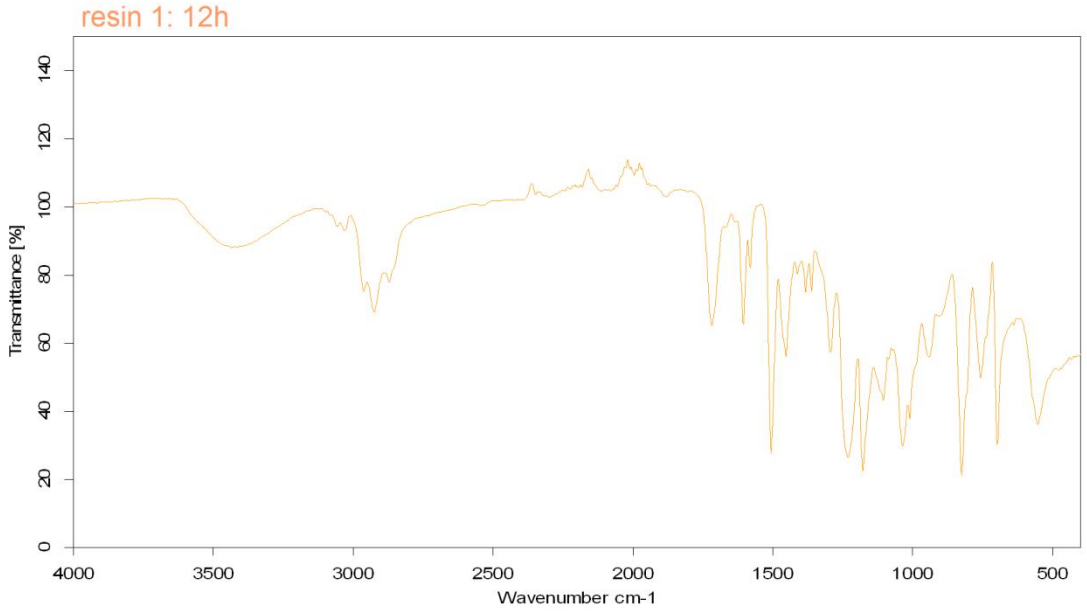
resin 1: 12h
Transmittance [%]
0
20
40
60
80
100
120
140
4000
3500
3000
2500
2000
1500
1000
500
Wavenumber cm-1

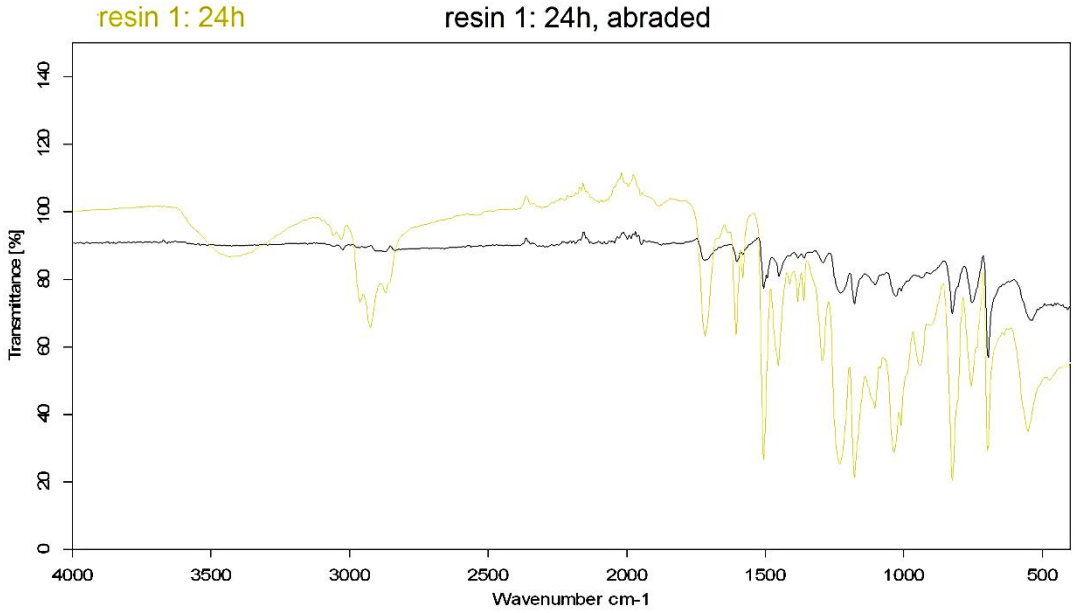
resin 1: 24h
resin 1: 24h, abraded
Transmittance [%]
0
20
40
60
80
100
120
140
4000
3500
3000
2500
2000
1500
1000
500
Wavenumber cm-1

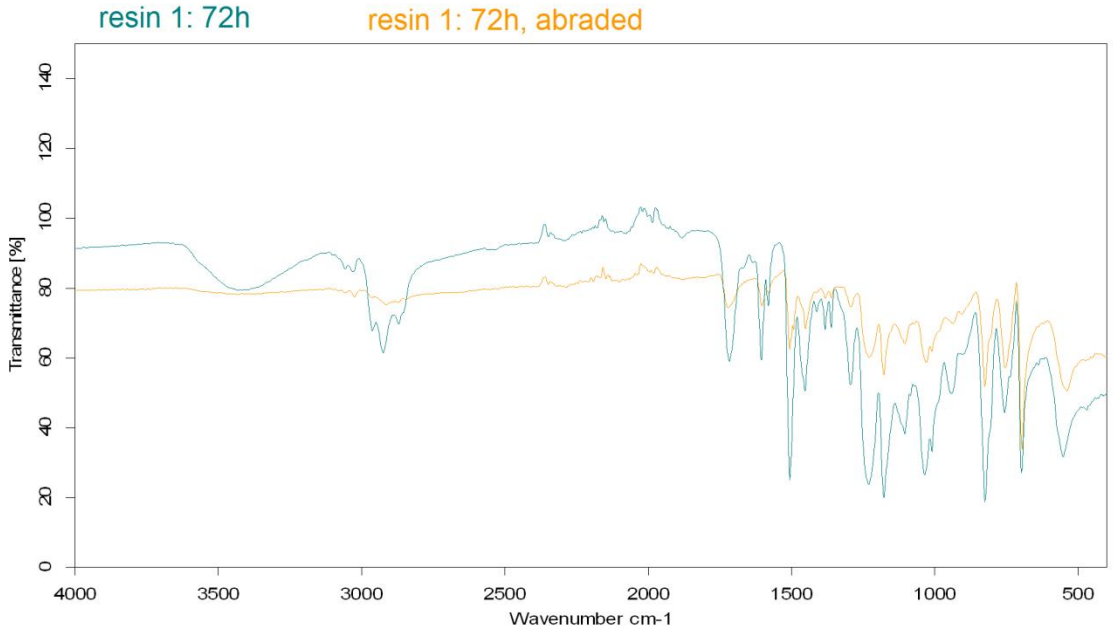
resin 1: 72h
resin 1: 72h, abraded
Transmittance [%]
0
20
40
60
80
100
120
140
4000
3500
3000
2500
2000
1500
1000
500
Wavenumber cm-1

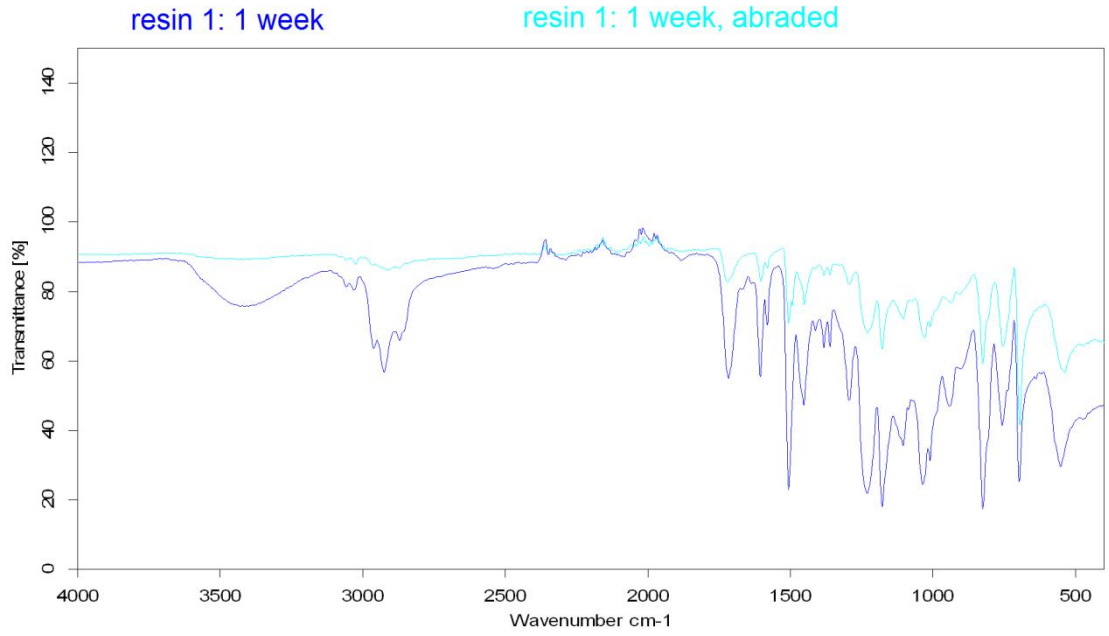
resin 1: 1 week
resin 1: 1 week, abraded
Transmittance [%]
0
20
40
60
80
100
120
140
4000
3500
3000
2500
2000
1500
1000
500
Wavenumber cm-1

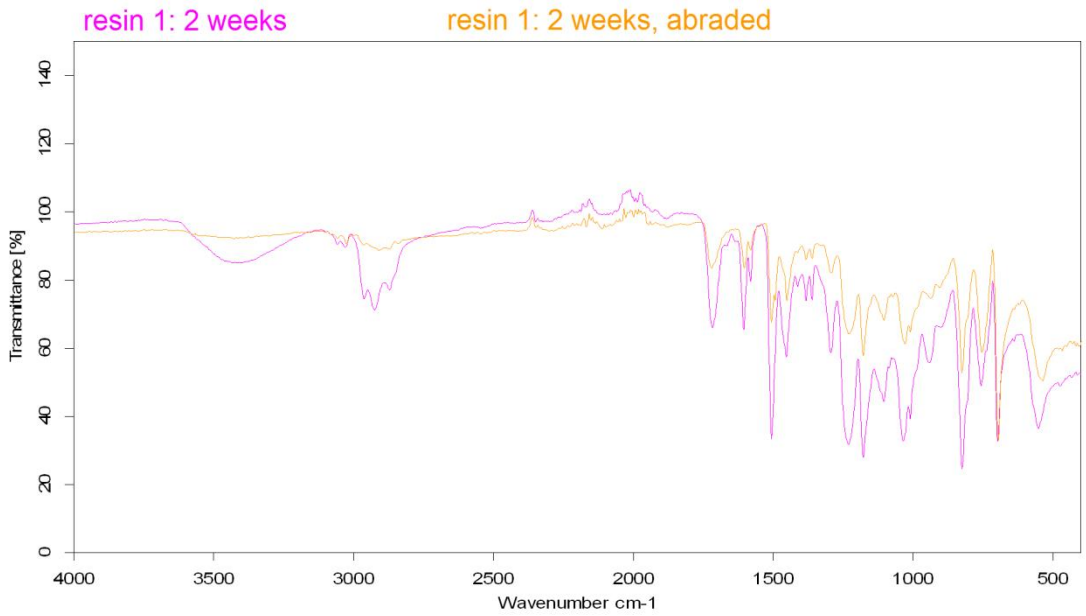
resin 1: 2 weeks
resin 1: 2 weeks, abraded
Transmittance [%]
0
20
40
60
80
100
120
140
4000
3500
3000
2500
2000
1500
1000
500
Wavenumber cm-1

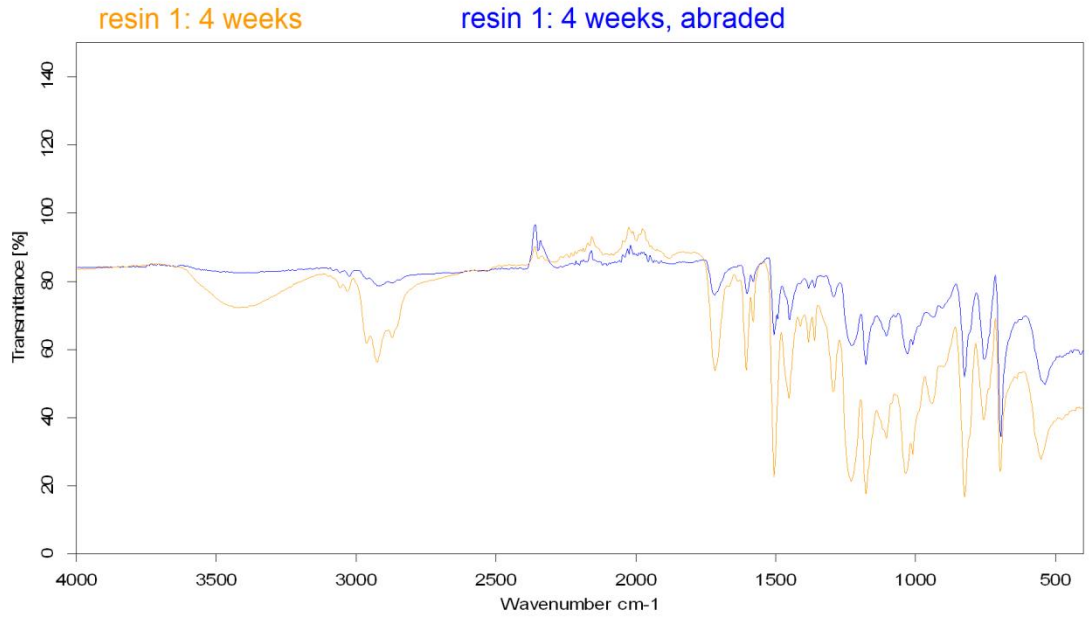
resin 1: 4 weeks
resin 1: 4 weeks, abraded
Transmittance [%]
0
20
40
60
80
100
120
140
4000
3500
3000
2500
2000
1500
1000
500
Wavenumber cm-1

RESIN 2

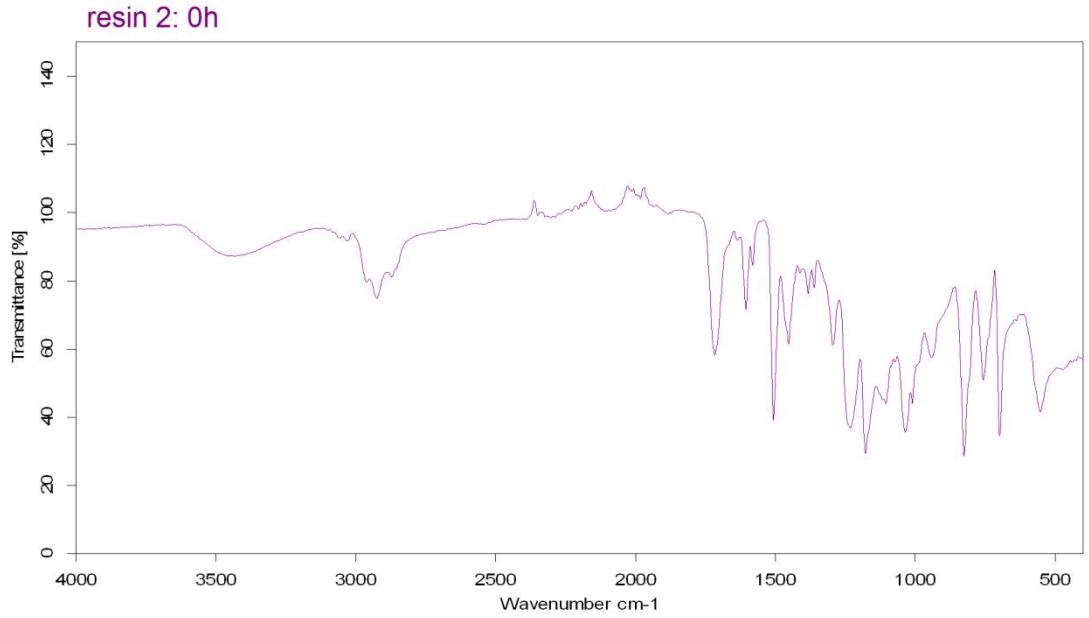
resin 2: 0h
Transmittance [%]
0
20
40
60
80
100
120
140
4000
3500
3000
2500
2000
1500
1000
500
Wavenumber cm-1

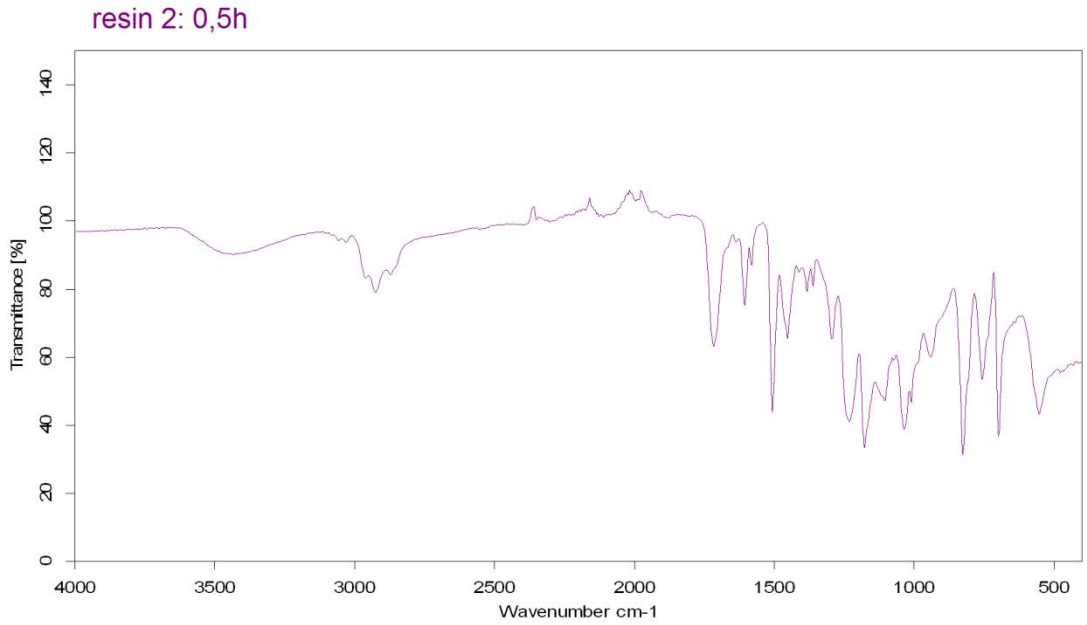
resin 2: 0,5h
Transmittance [%]
0
20
40
60
80
100
120
140
4000
3500
3000
2500
2000
1500
1000
500
Wavenumber cm-1

resin 2: 1h

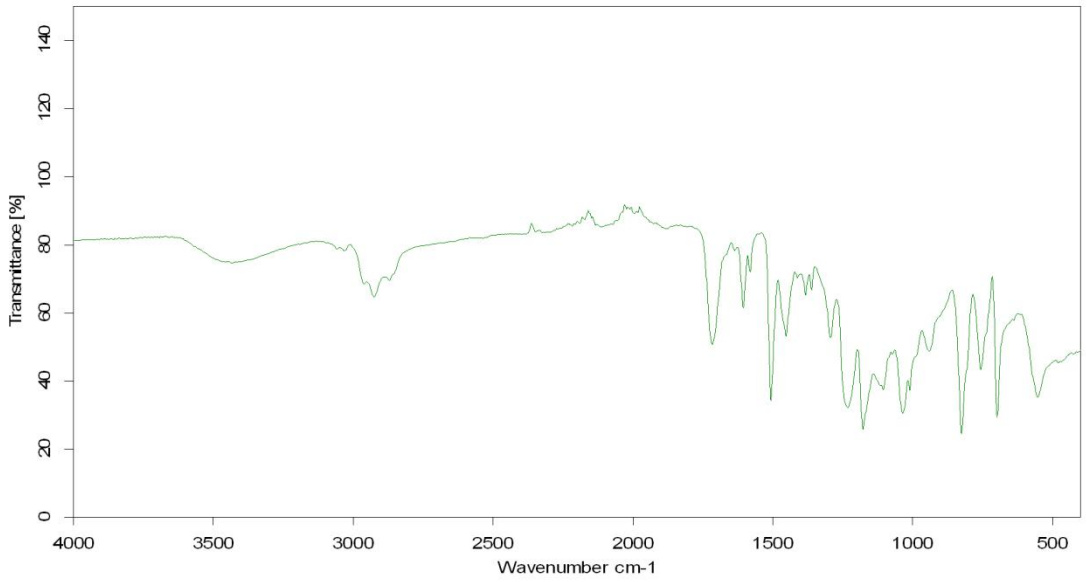

resin 2: 5h

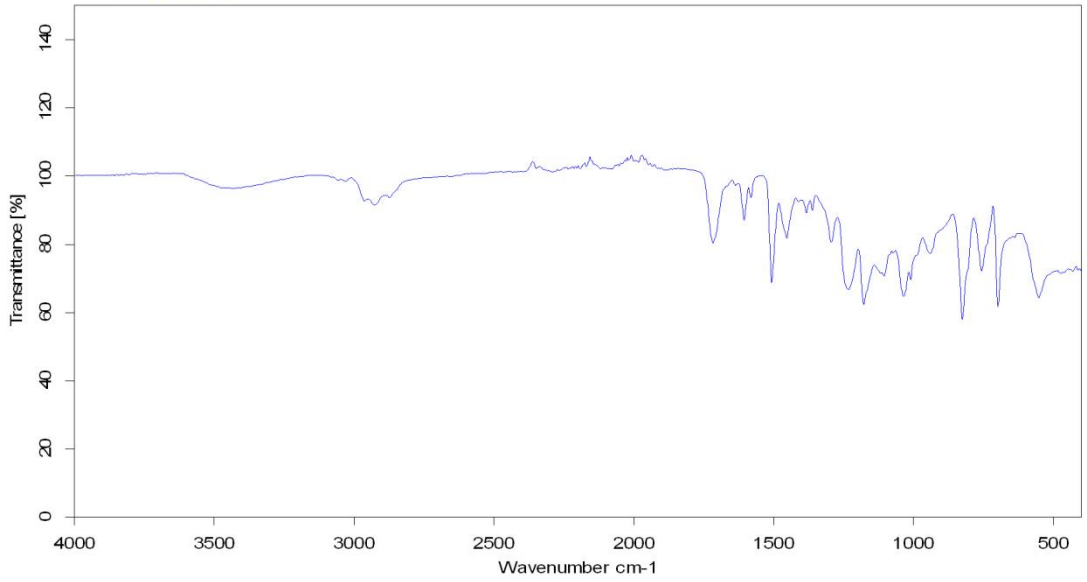

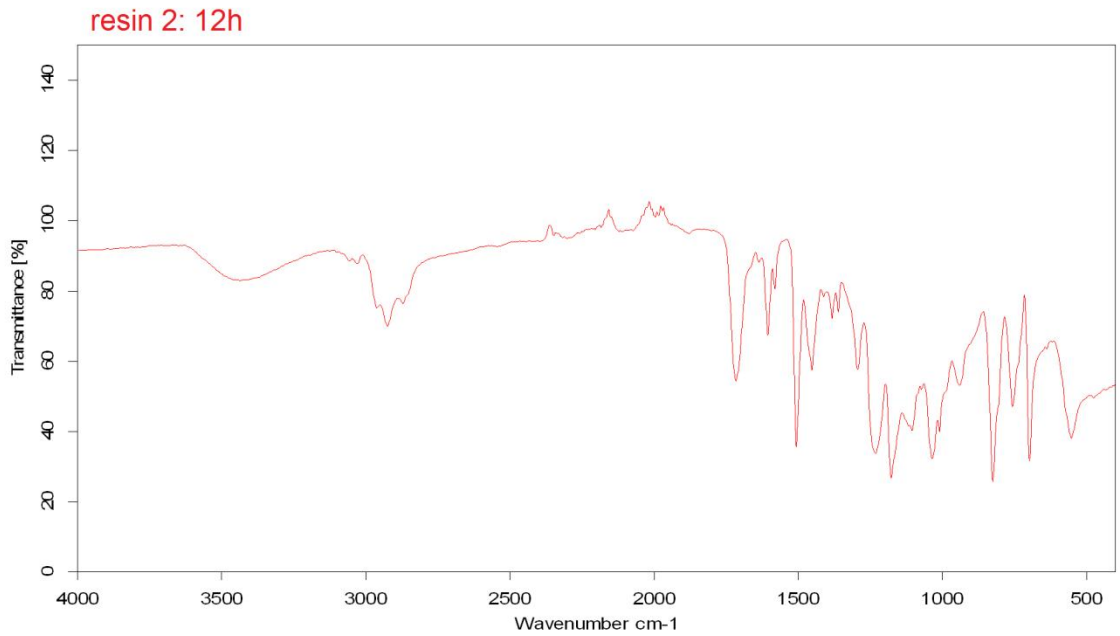
resin 2: 12h
Transmittance [%]
0
20
40
60
80
100
120
140
4000
3500
3000
2500
2000
1500
1000
500
Wavenumber cm-1

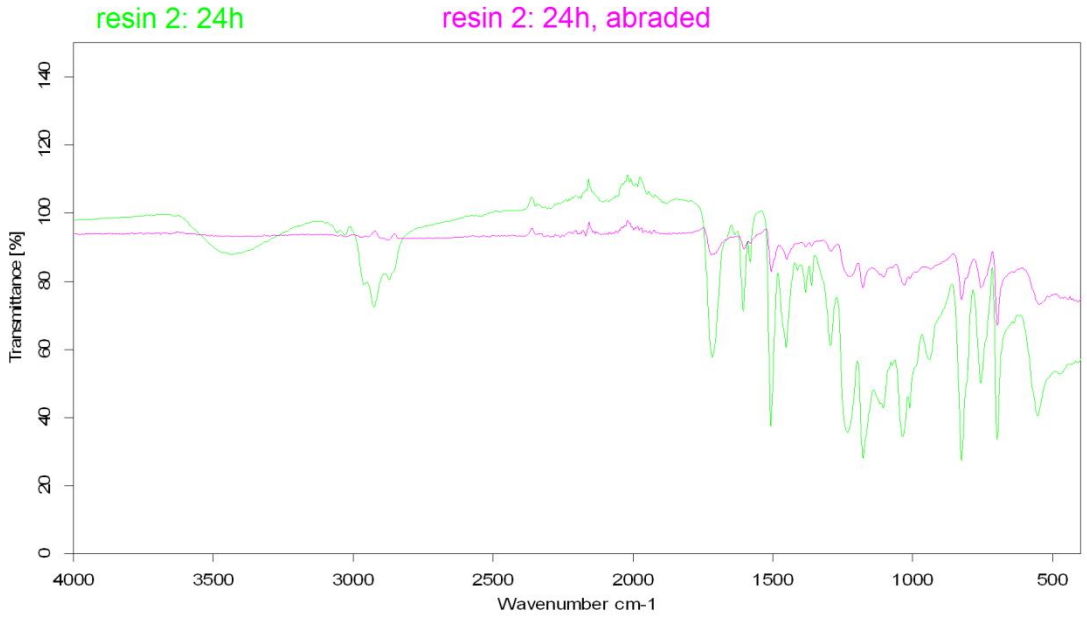
resin 2: 24h
resin 2: 24h, abraded
Transmittance [%]
0
20
40
60
80
100
120
140
4000
3500
3000
2500
2000
1500
1000
500
Wavenumber cm-1

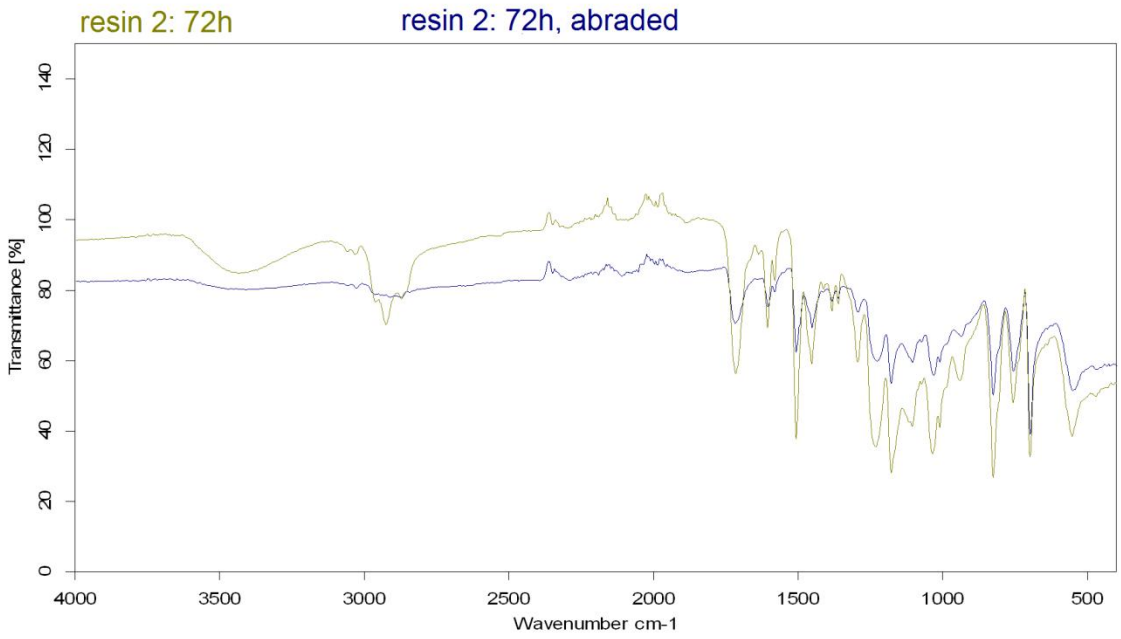
resin 2: 72h
resin 2: 72h, abraded
Transmittance [%]
0
20
40
60
80
100
120
140
4000
3500
3000
2500
2000
1500
1000
500
Wavenumber cm-1

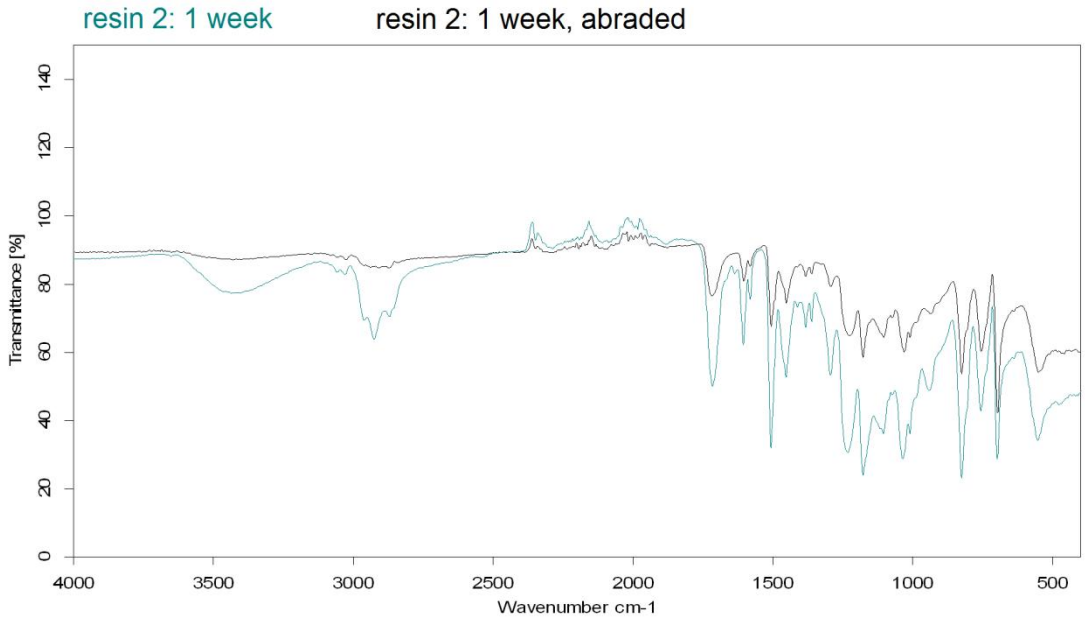
resin 2: 1 week
resin 2: 1 week, abraded
Transmittance [%]
0
20
40
60
80
100
120
140
4000
3500
3000
2500
2000
1500
1000
500
Wavenumber cm-1

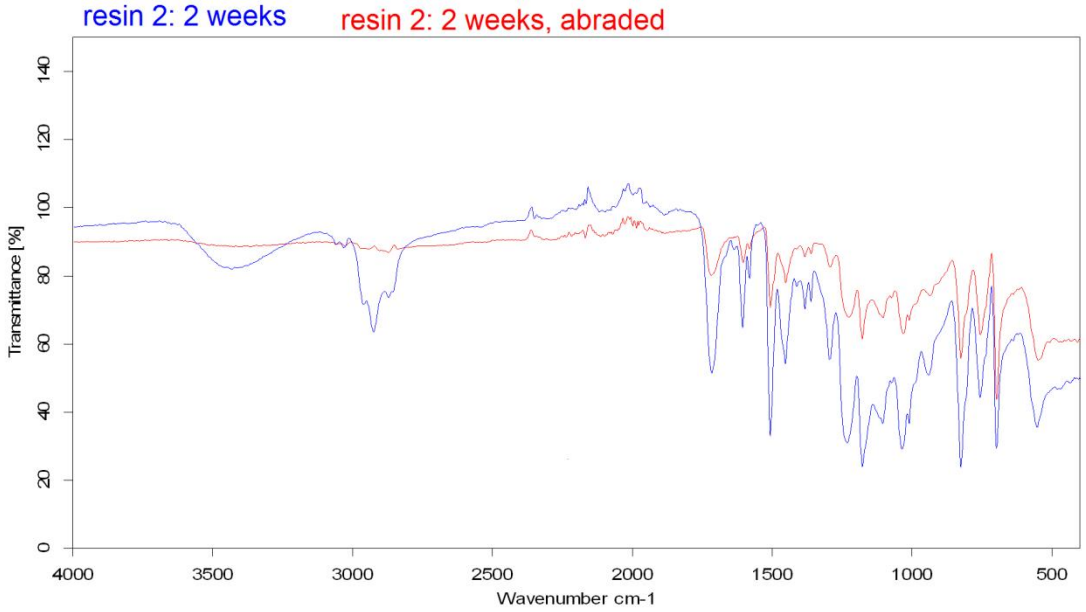
resin 2: 2 weeks
resin 2: 2 weeks, abraded
Transmittance [%]
0
20
40
60
80
100
120
140
4000
3500
3000
2500
2000
1500
1000
500
Wavenumber cm-1

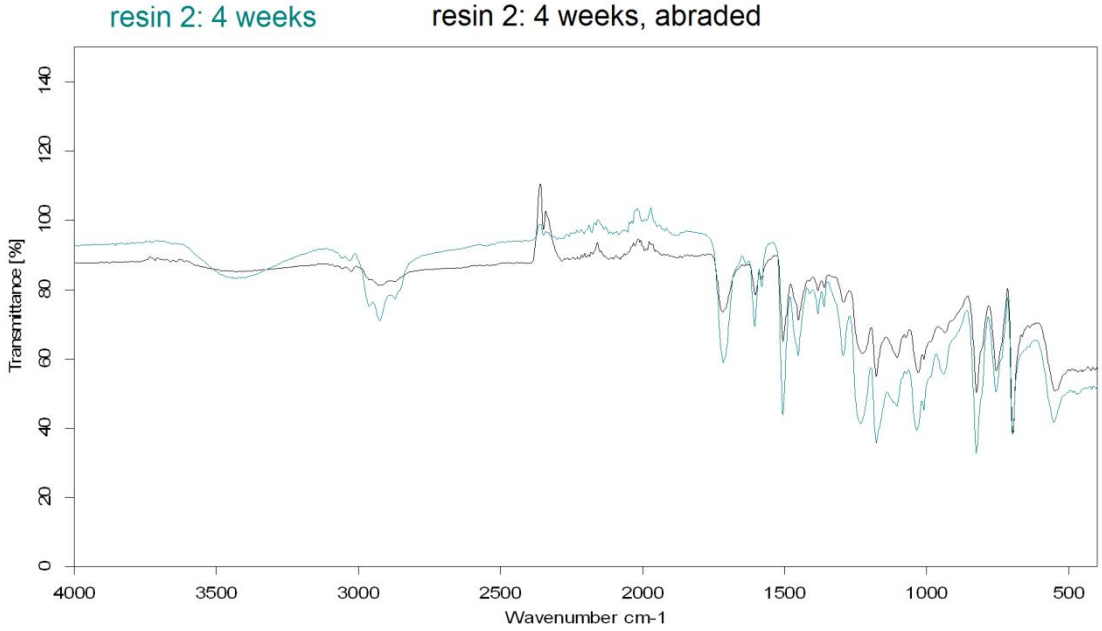
resin 2: 4 weeks
resin 2: 4 weeks, abraded
Transmittance [%]
0
20
40
60
80
100
120
140
4000
3500
3000
2500
2000
1500
1000
500
Wavenumber cm-1

RESIN 3

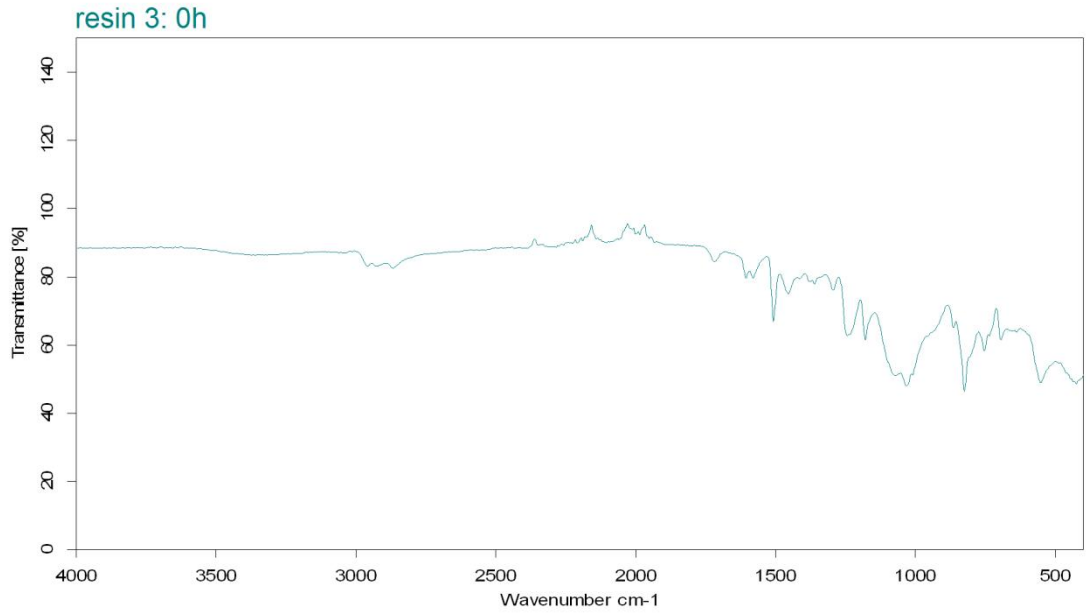
resin 3: 0h
Transmittance [%]
0
20
40
60
80
100
120
140
4000
3500
3000
2500
2000
1500
1000
500
Wavenumber cm-1

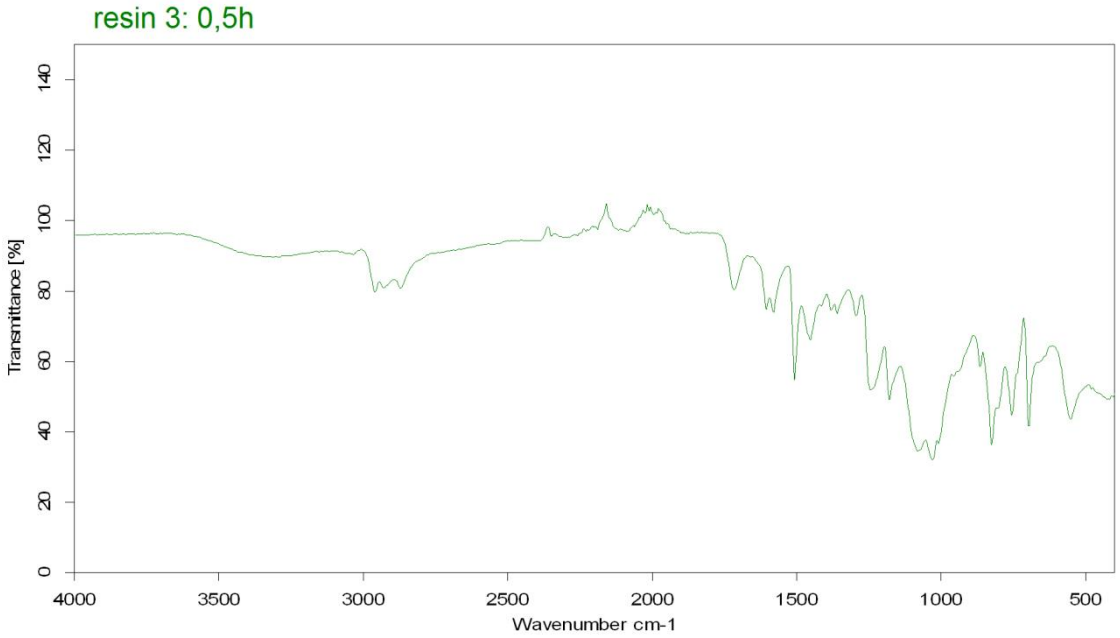
resin 3: 0,5h
Transmittance [%]
0
20
40
60
80
100
120
140
4000
3500
3000
2500
2000
1500
1000
500
Wavenumber cm-1

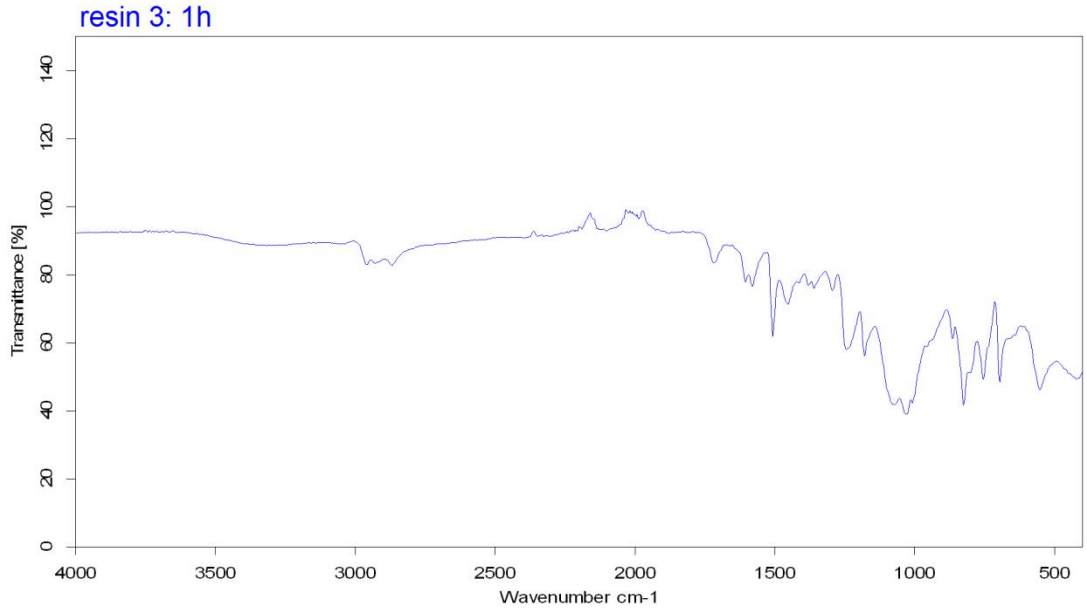
resin 3: 1h
Transmittance [%]
0
20
40
60
80
100
120
140
4000
3500
3000
2500
2000
1500
1000
500
Wavenumber cm-1

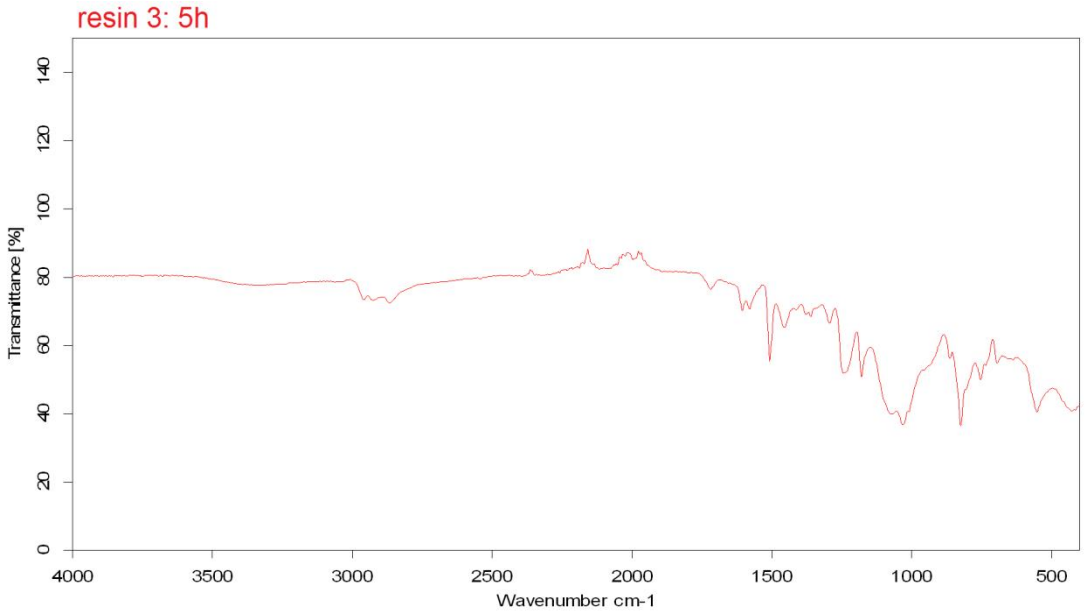
resin 3: 5h
Transmittance [%]
0
20
40
60
80
100
120
140
4000
3500
3000
2500
2000
1500
1000
500
Wavenumber cm-1

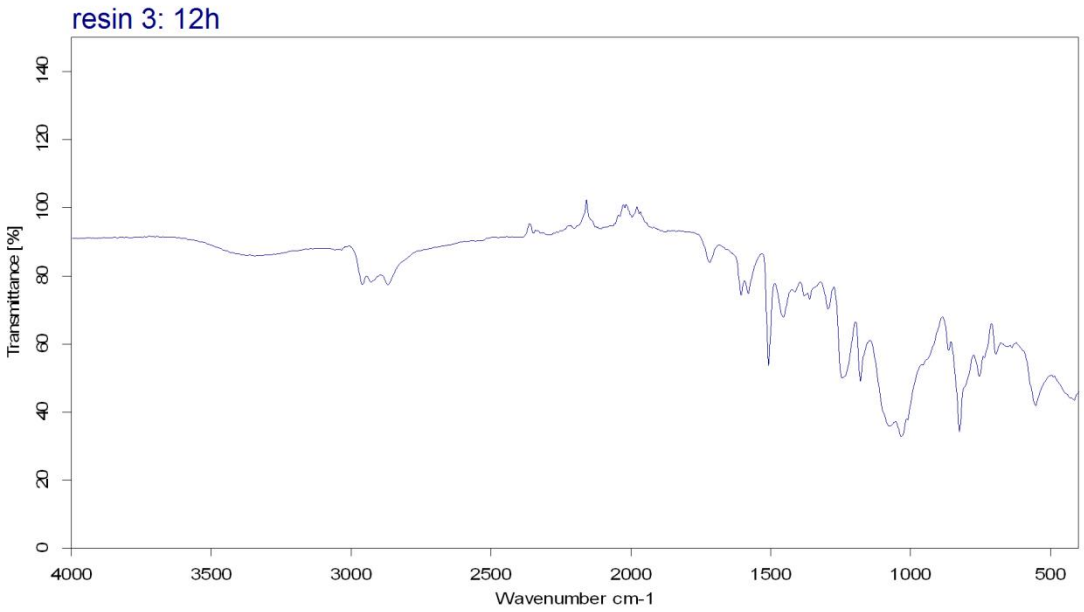
resin 3: 12h
Transmittance [%]
0
20
40
60
80
100
120
140
4000
3500
3000
2500
2000
1500
1000
500
Wavenumber cm-1


resin 3: 24h
resin 3: 24h, abraded
Transmittance [%]
0
20
40
60
80
100
120
140
4000
3500
3000
2500
2000
1500
1000
500
Wavenumber cm-1


resin 3: 72h
resin 3: 72h, abraded
Transmittance [%]
0
20
40
60
80
100
120
140
4000
3500
3000
2500
2000
1500
1000
500
Wavenumber cm-1

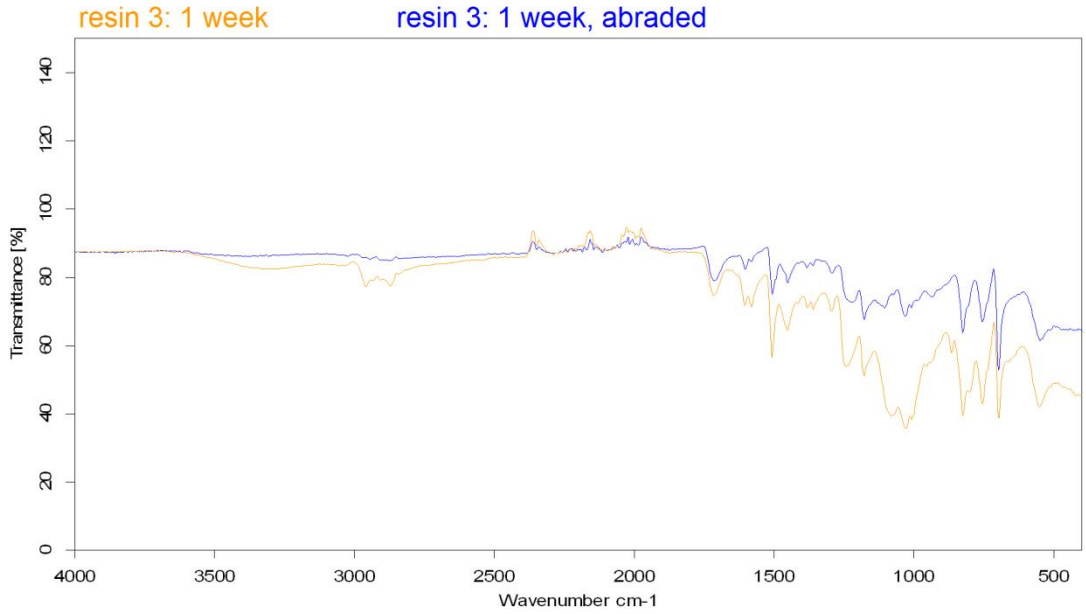
resin 3: 1 week
resin 3: 1 week, abraded
Transmittance [%]
0
20
40
60
80
100
120
140
4000
3500
3000
2500
2000
1500
1000
500
Wavenumber cm-1

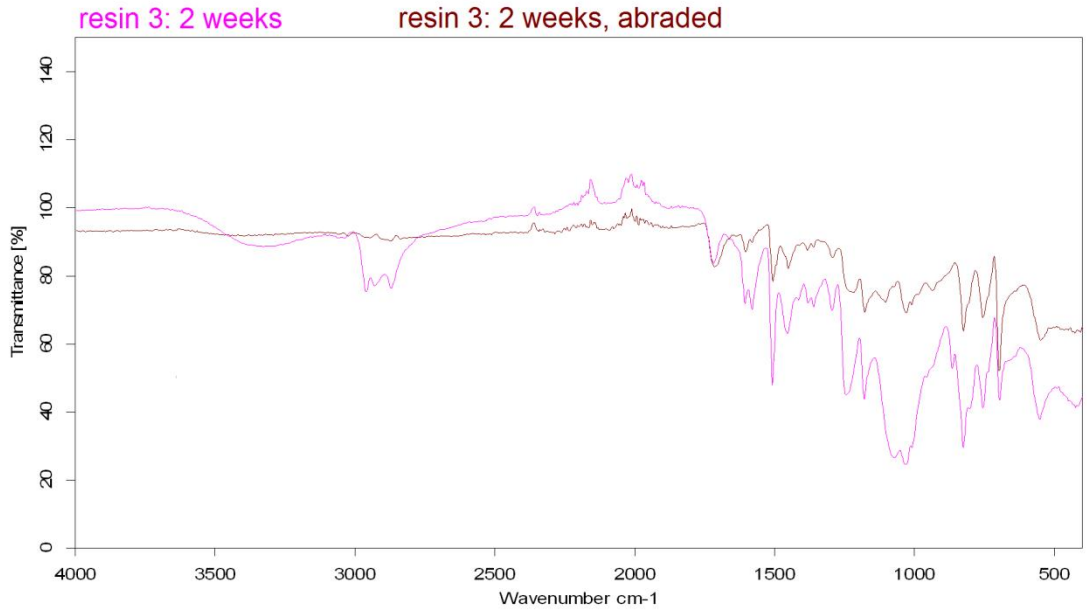
resin 3: 2 weeks
resin 3: 2 weeks, abraded
Transmittance [%]
0
20
40
60
80
100
120
140
4000
3500
3000
2500
2000
1500
1000
500
Wavenumber cm-1

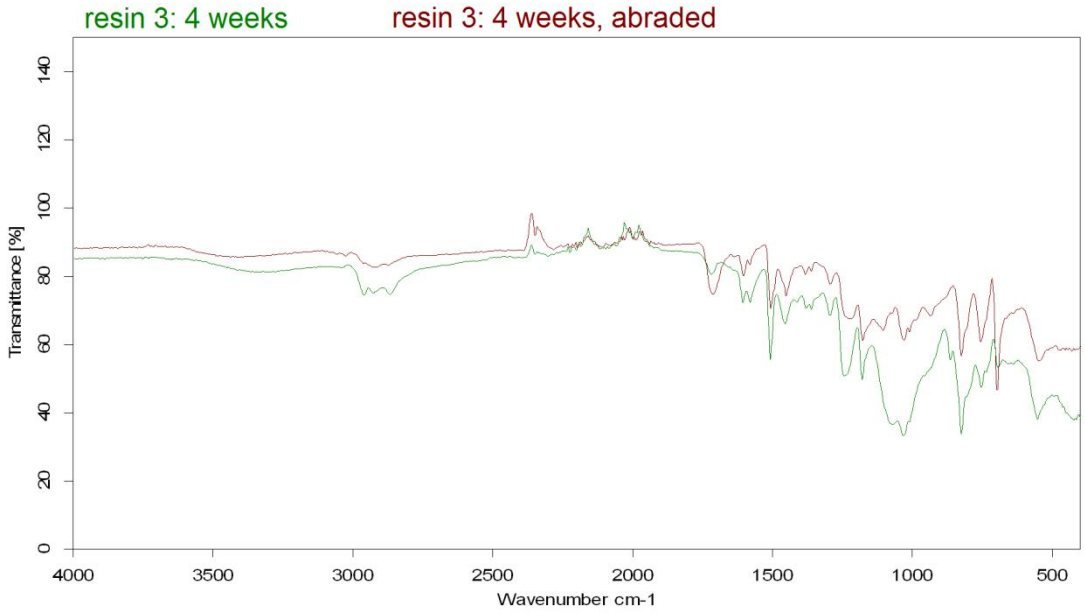
resin 3: 4 weeks
resin 3: 4 weeks, abraded
Transmittance [%]
0
20
40
60
80
100
120
140
4000
3500
3000
2500
2000
1500
1000
500
Wavenumber cm-1

RESIN 4

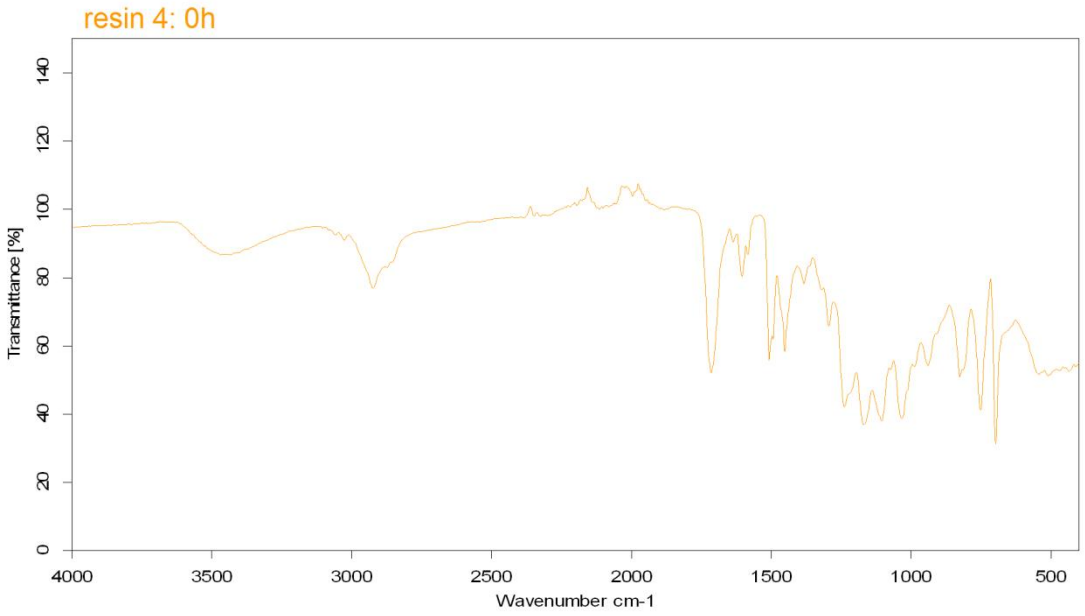
resin 4: 0h
Transmittance [%]
0
20
40
60
80
100
120
140
4000
3500
3000
2500
2000
1500
1000
500
Wavenumber cm-1

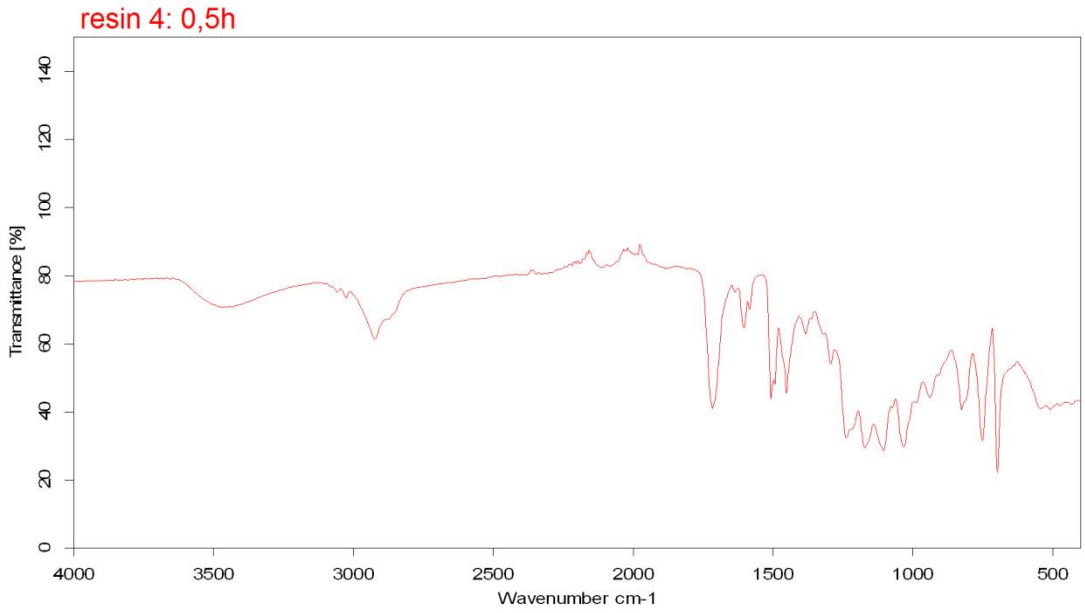
resin 4: 0,5h
Transmittance [%]
0
20
40
60
80
100
120
140
4000
3500
3000
2500
2000
1500
1000
500
Wavenumber cm-1

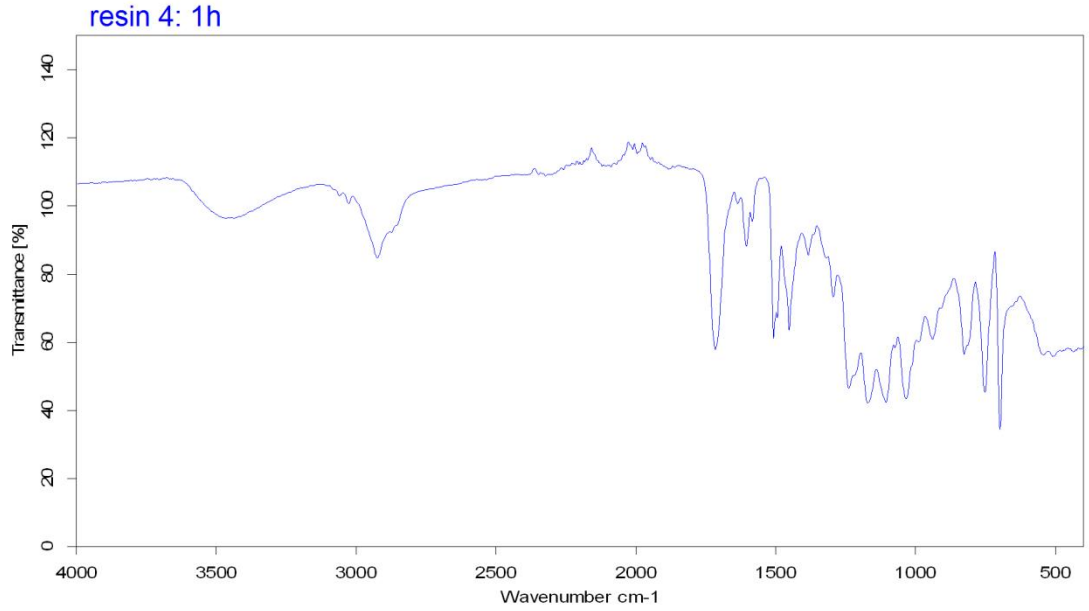
resin 4: 1h
Transmittance [%]
0
20
40
60
80
100
120
140
4000
3500
3000
2500
2000
1500
1000
500
Wavenumber cm-1

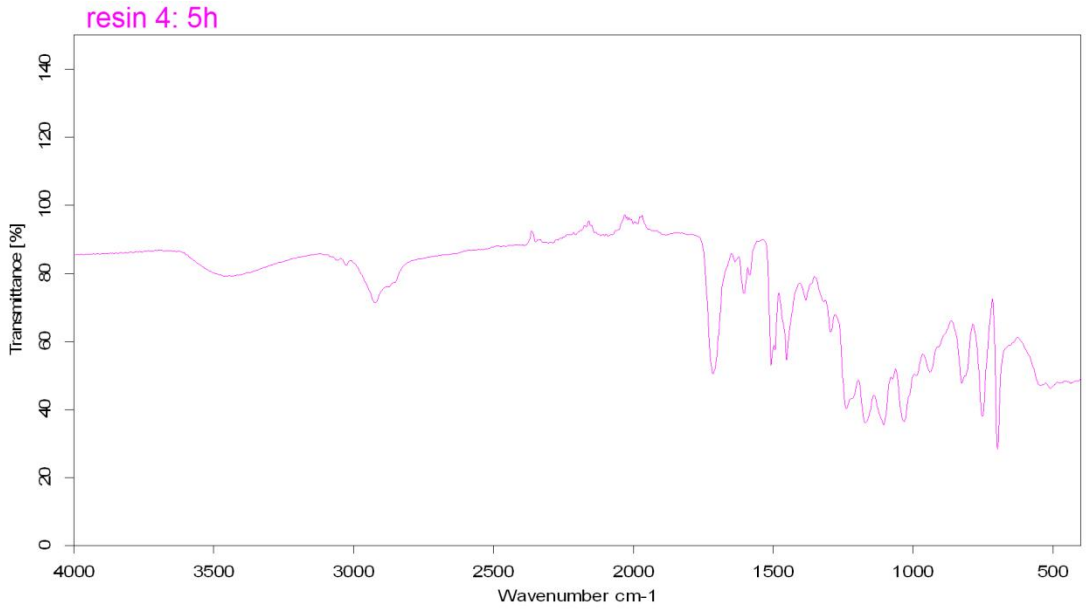
resin 4: 5h
Transmittance [%]
0
20
40
60
80
100
120
140
4000
3500
3000
2500
2000
1500
1000
500
Wavenumber cm-1

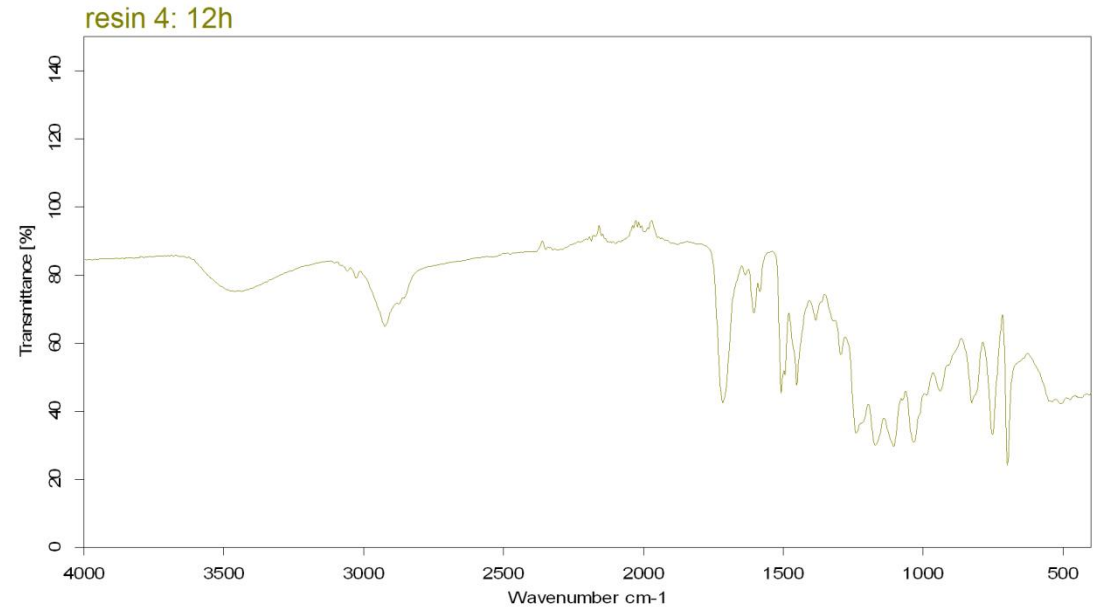
resin 4: 12h
Transmittance [%]
0
20
40
60
80
100
120
140
4000
3500
3000
2500
2000
1500
1000
500
Wavenumber cm-1

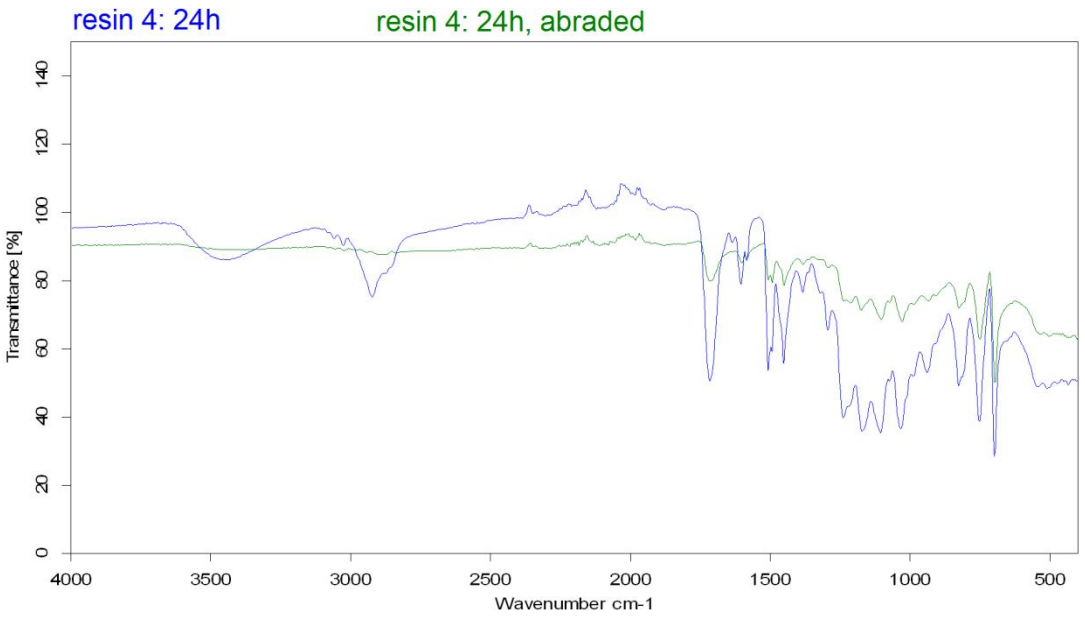
resin 4: 24h
resin 4: 24h, abraded
Transmittance [%]
0
20
40
60
80
100
120
140
4000
3500
3000
2500
2000
1500
1000
500
Wavenumber cm-1

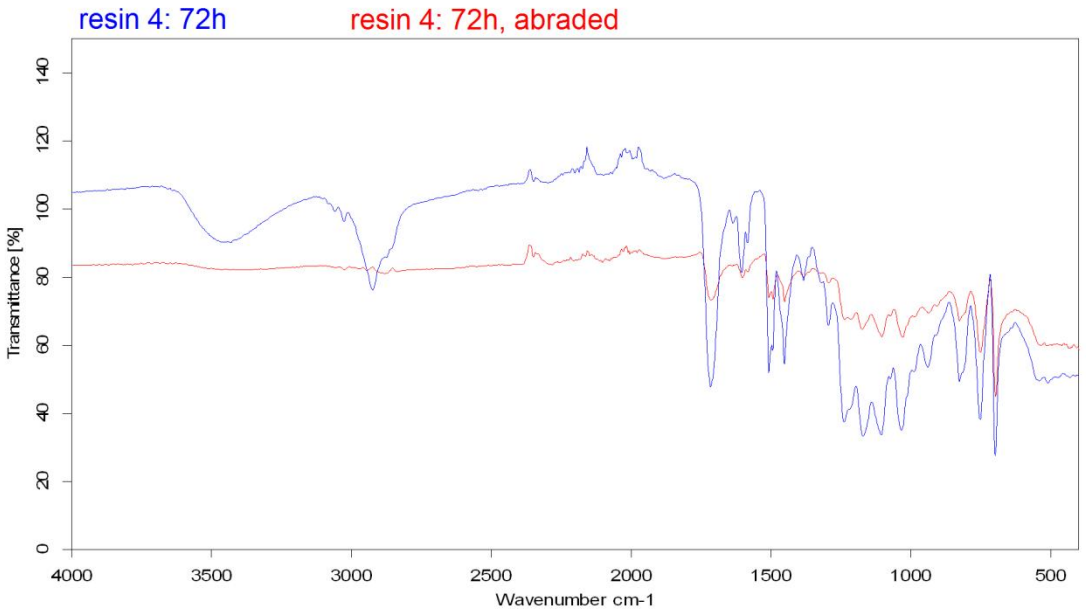
resin 4: 72h
resin 4: 72h, abraded
Transmittance [%]
0
20
40
60
80
100
120
140
4000
3500
3000
2500
2000
1500
1000
500
Wavenumber cm-1

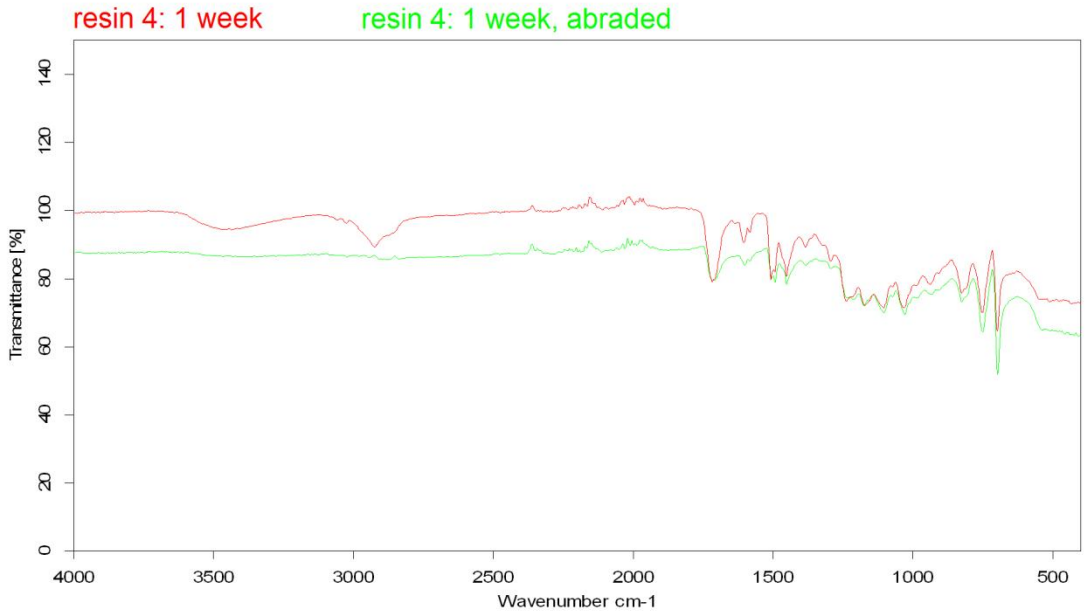
resin 4: 1 week
resin 4: 1 week, abraded
Transmittance [%]
0
20
40
60
80
100
120
140
4000
3500
3000
2500
2000
1500
1000
500
Wavenumber cm-1

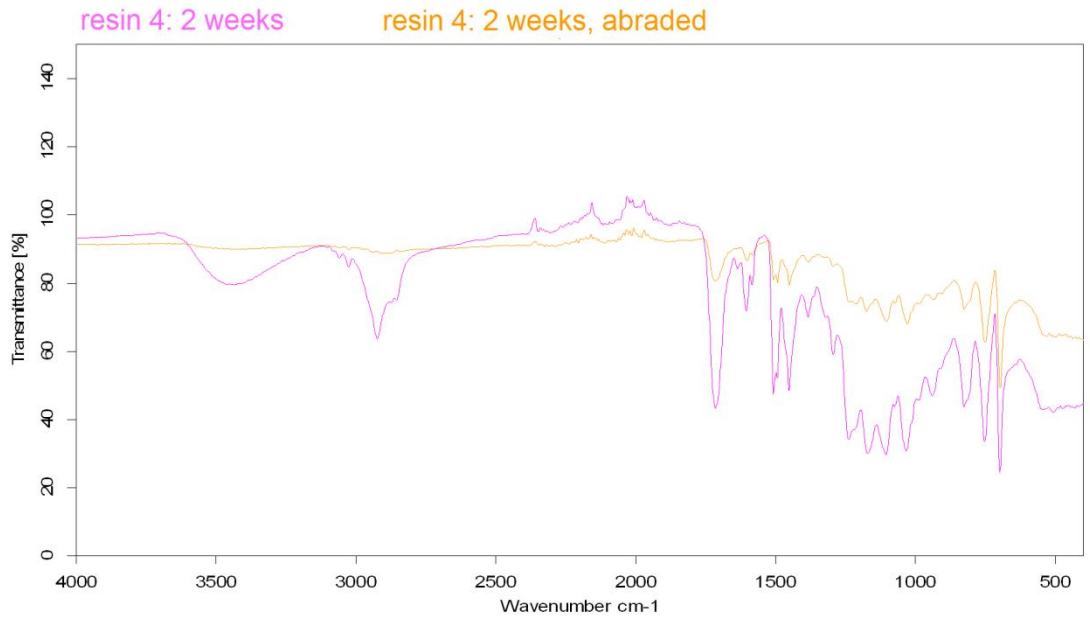
resin 4: 2 weeks
resin 4: 2 weeks, abraded
Transmittance [%]
0
20
40
60
80
100
120
140
4000
3500
3000
2500
2000
1500
1000
500
Wavenumber cm-1

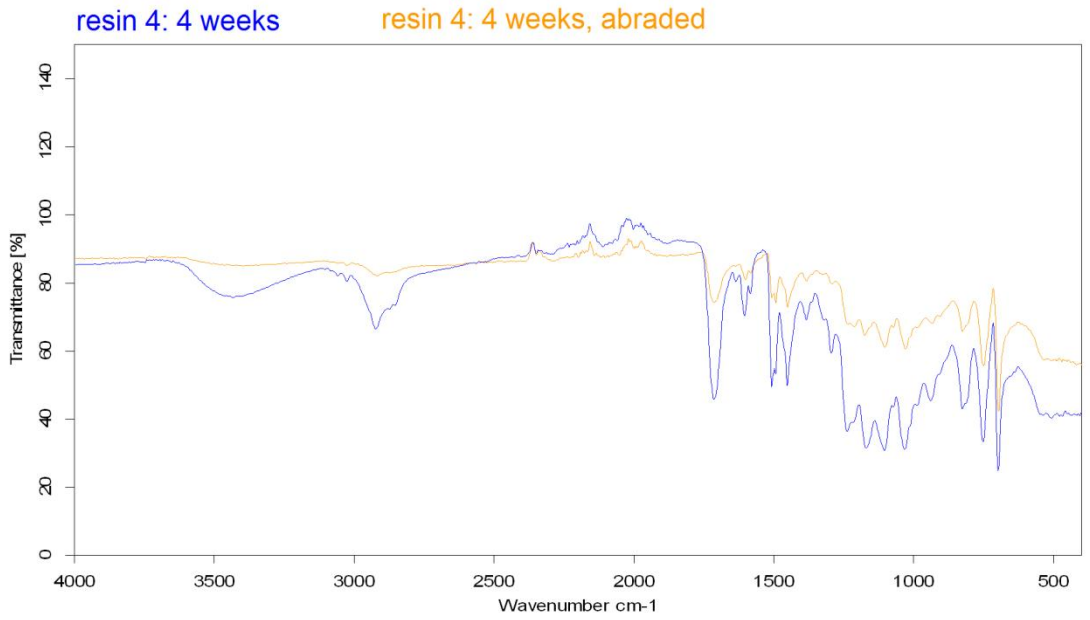
resin 4: 4 weeks
resin 4: 4 weeks, abraded
Transmittance [%]
0
20
40
60
80
100
120
140
4000
3500
3000
2500
2000
1500
1000
500
Wavenumber cm-1

LAMINATE A: WELL ABRADED

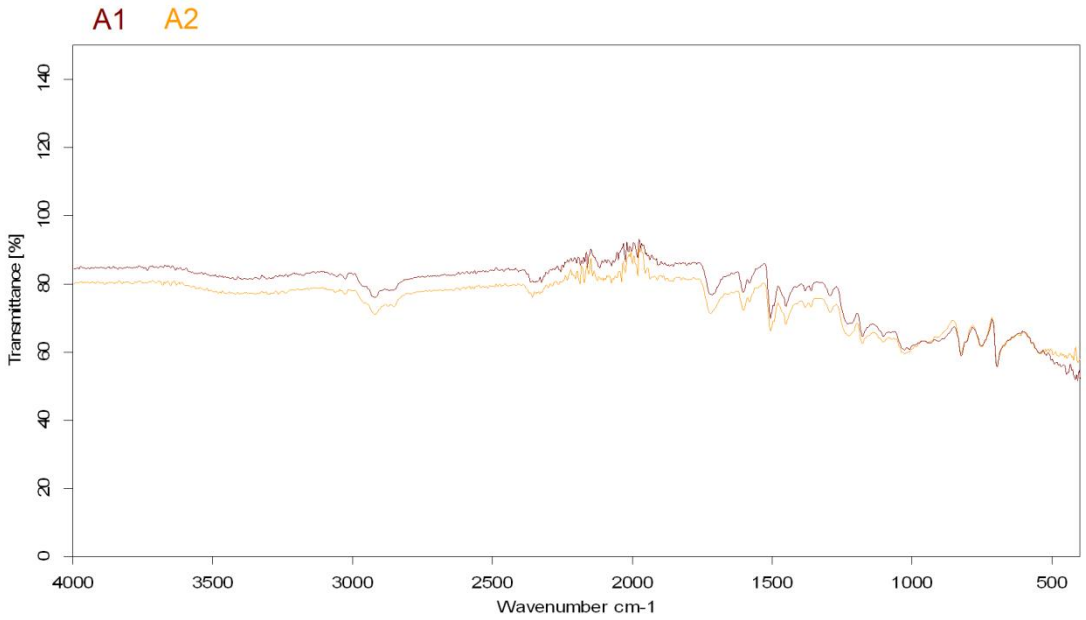

LAMINATE B: POORLY ABRADED

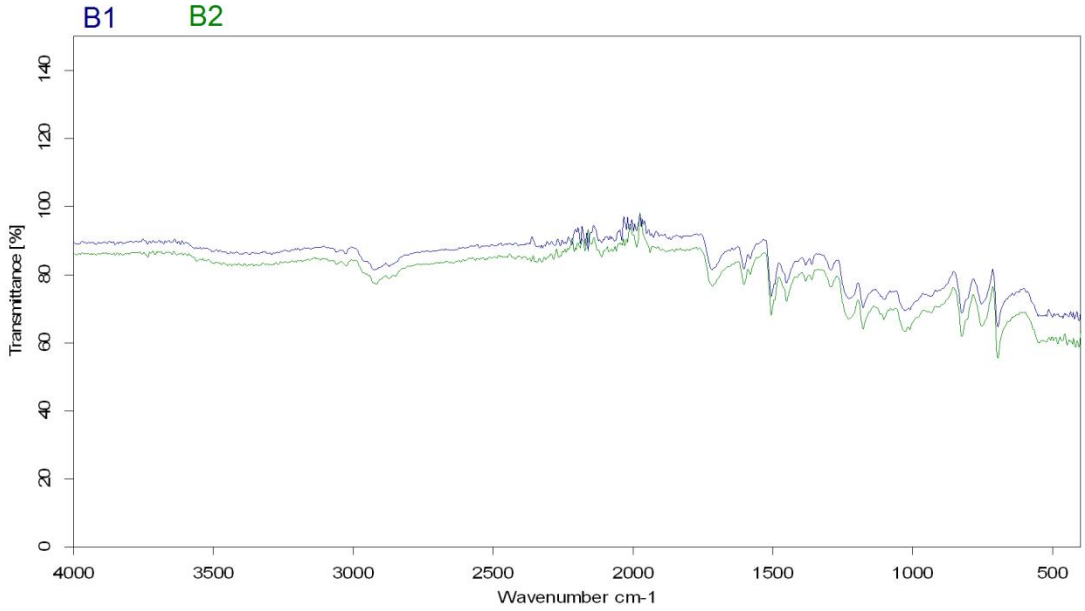

LAMINATE C: WELL SANDBLASTED

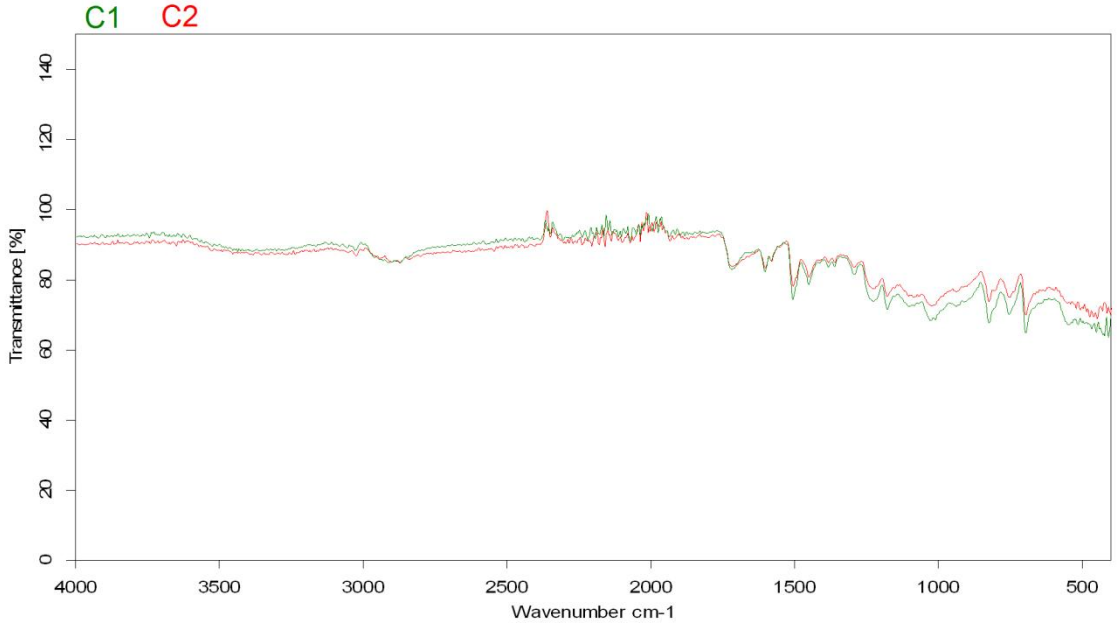

LAMINATE D: NEGLIGENTLY SANDBLASTED

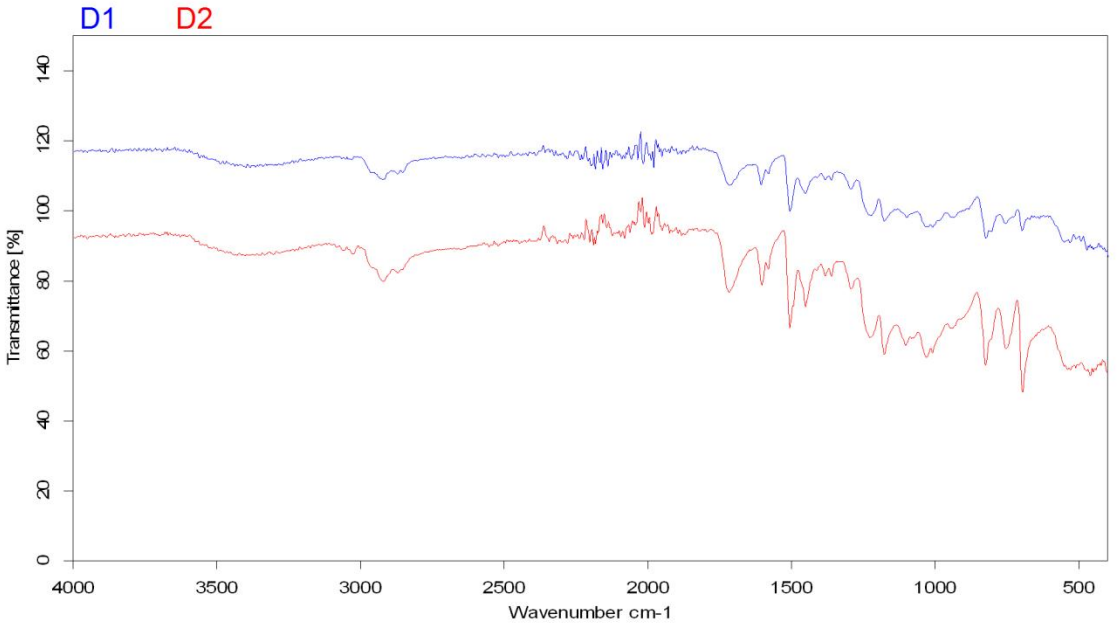

LAMINATE E: SANDBLASTED WITH TOO FINE SAND

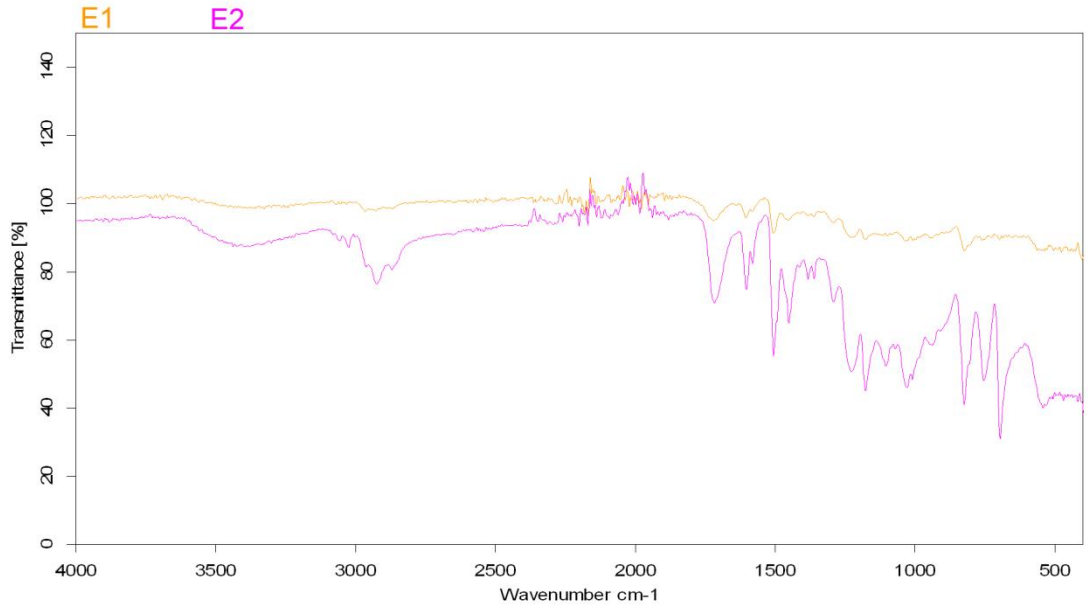

LAMINATE F: ABRADED WITH A WIRE BRUSH

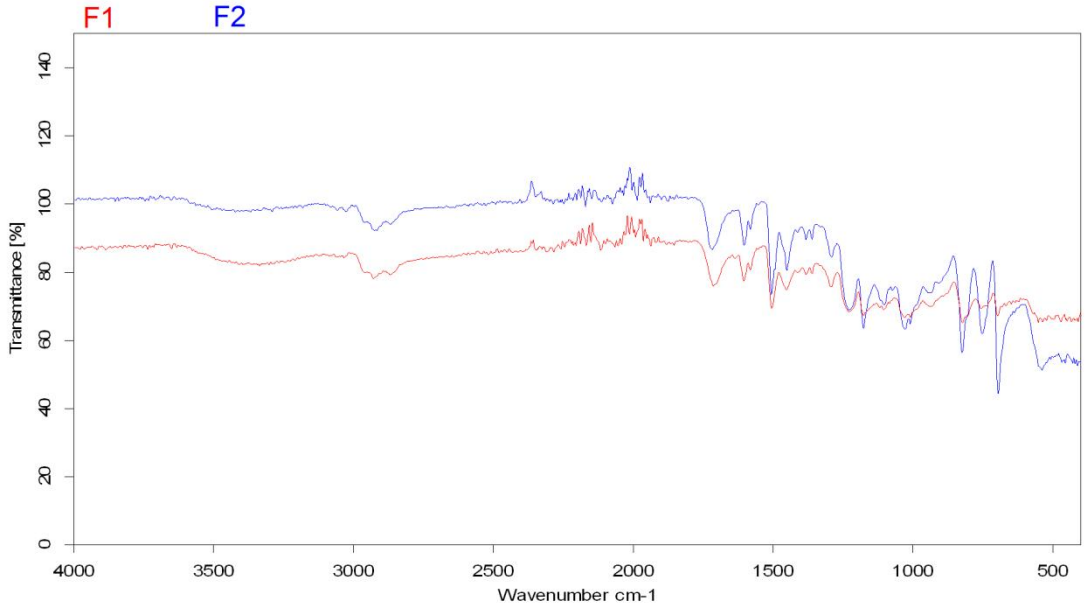

APPENDIX B: THE SCANNING ELECTON MICROSCOPE IMAGES OF THE LAMINATES

LAMINATE A1: WELL ABRADED OUTER SURFACE

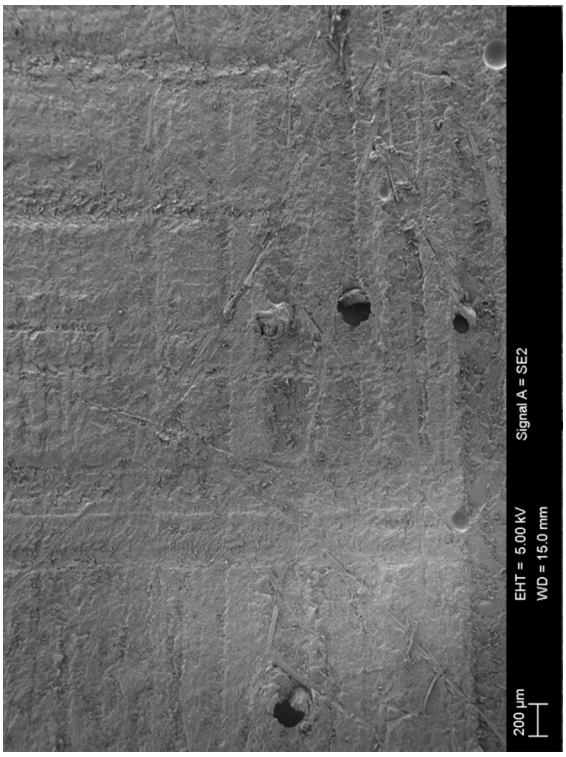

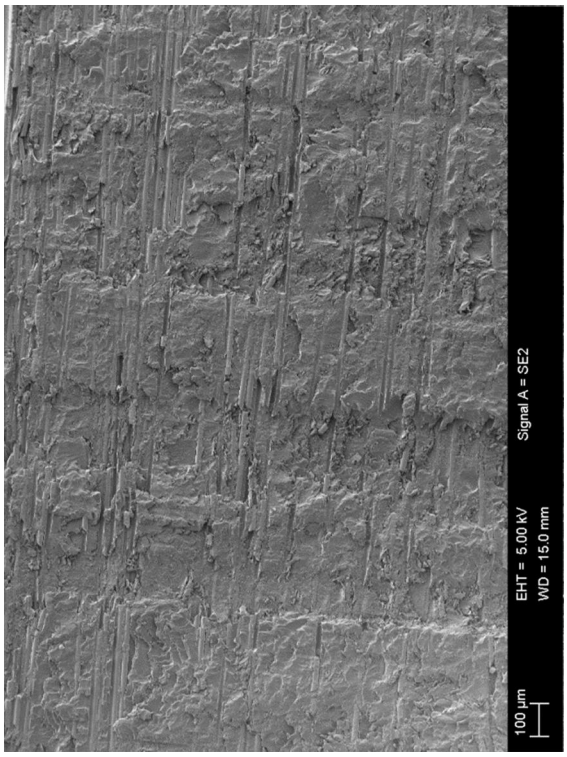

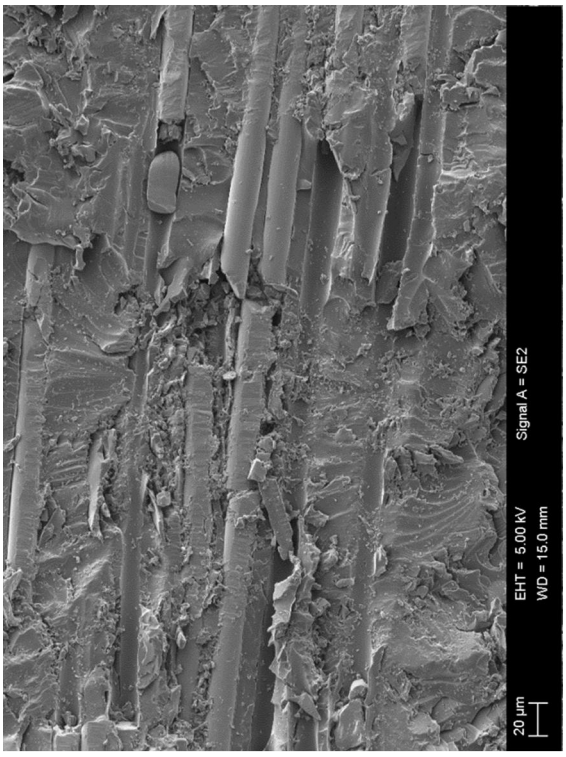

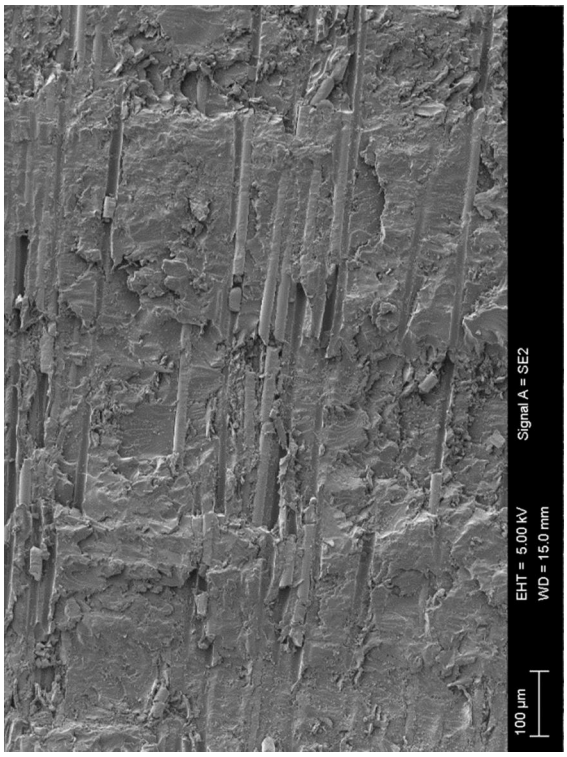

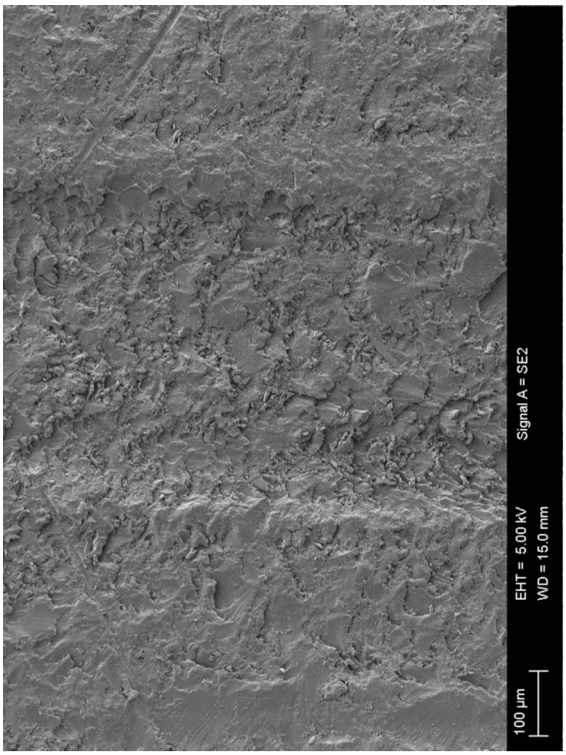
100 µm
EHT = 5.00 kV
WD = 15.0 mm
Signal A = SE2

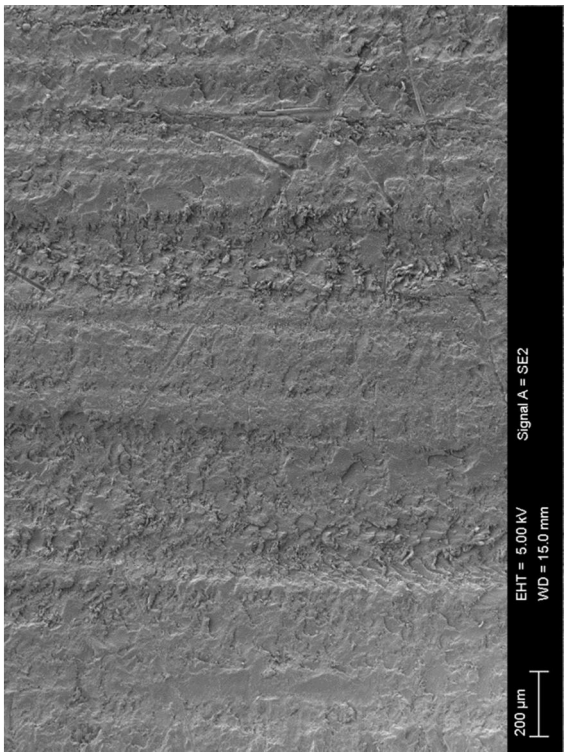
200 µm
EHT = 5.00 kV
WD = 15.0 mm
Signal A = SE2

LAMINATE A2: WELL ABRADED MOULD SURFACE

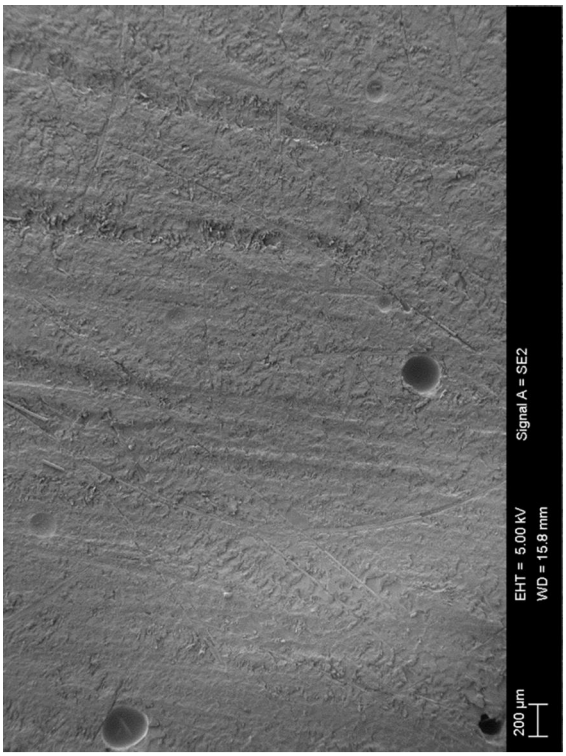

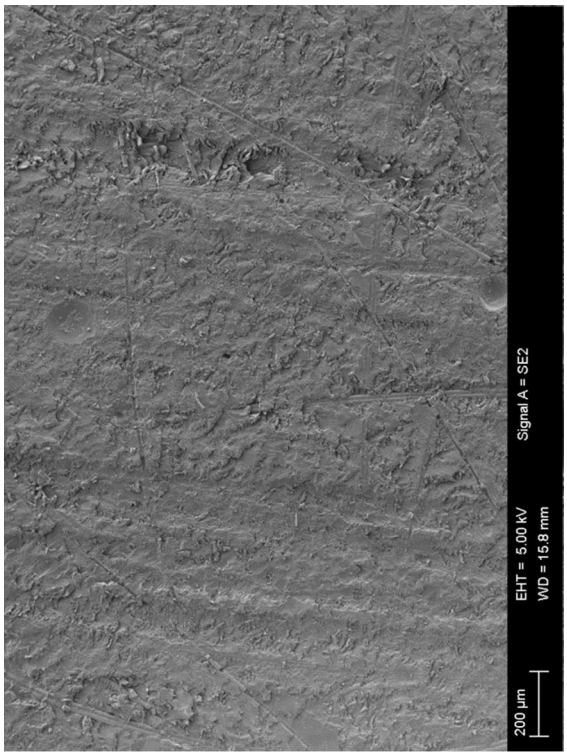

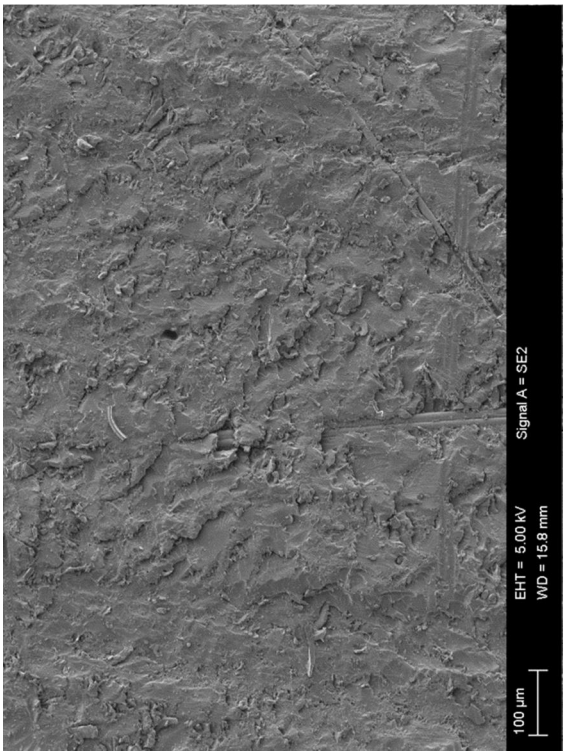

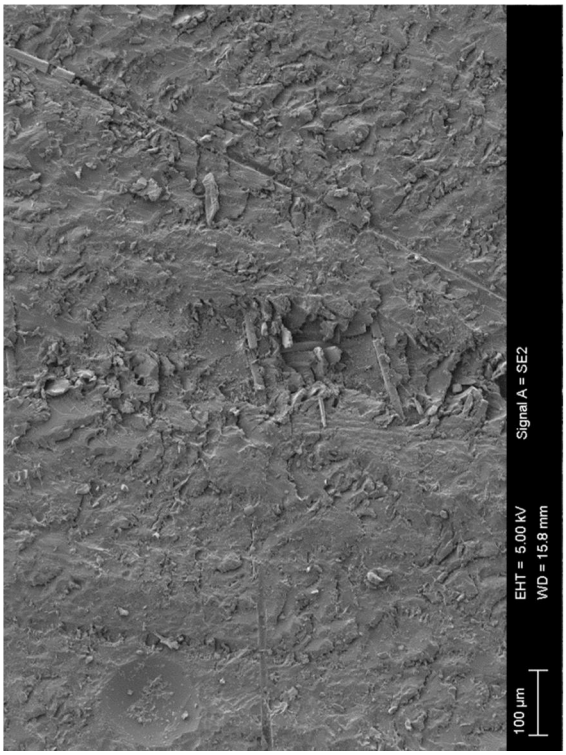

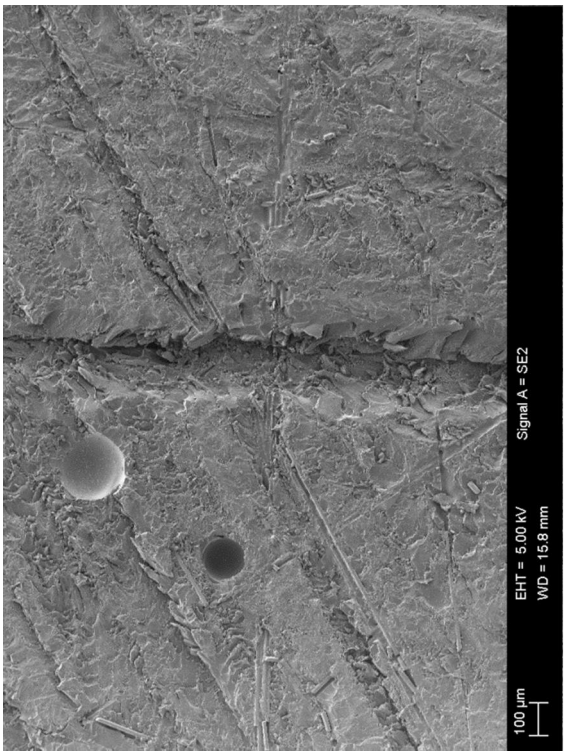
100 µm
EHT = 5.00 kV
WD = 15.8 mm
Signal A = SE2

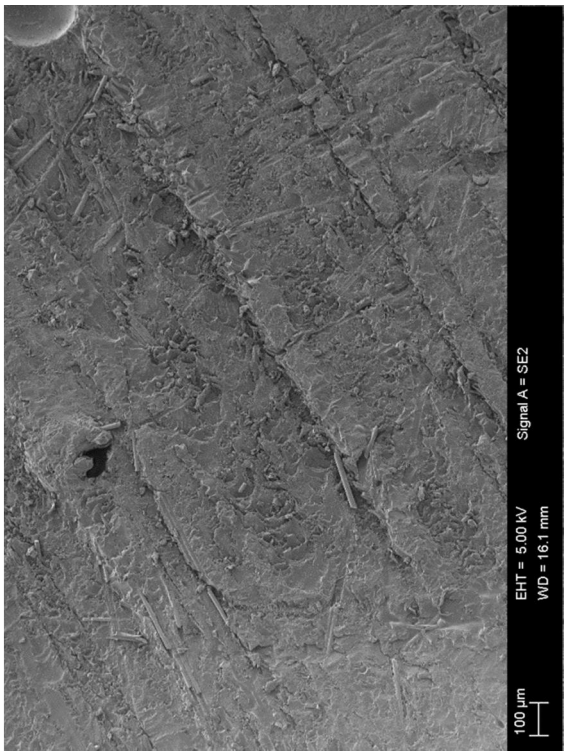
100 µm
EHT = 5.00 kV
WD = 16.1 mm
Signal A = SE2

LAMINATE B1: POORLY ABRADED OUTER SURFACE

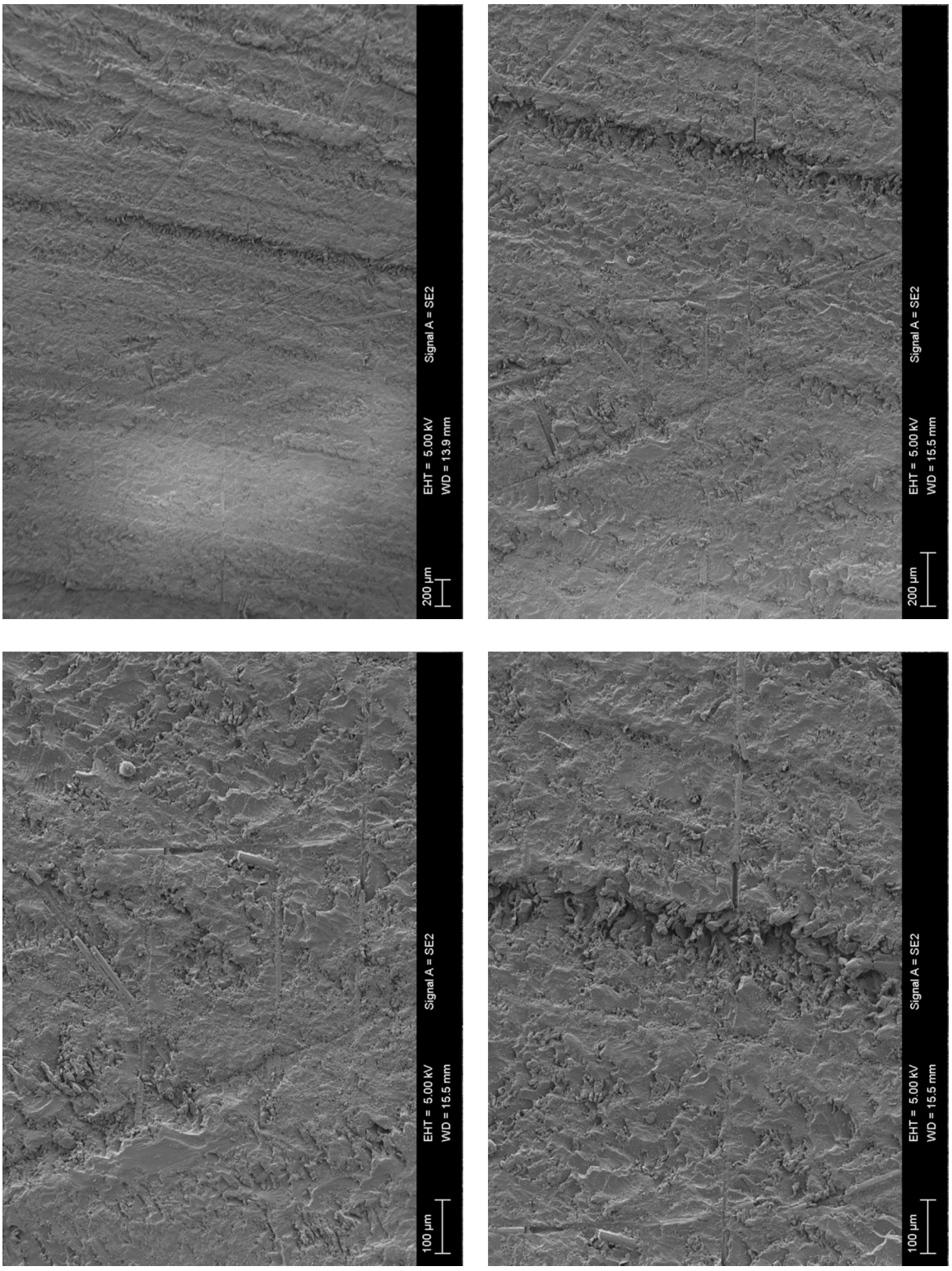

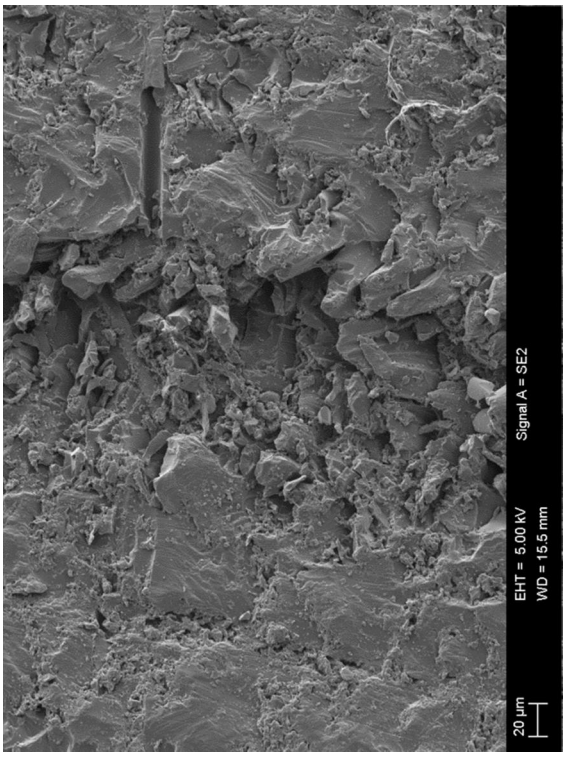
20 µm
EHT = 5.00 kV
WD = 15.5 mm
Signal A = SE2

LAMINATE B2: POORLY ABRADED MOULD SURFACE

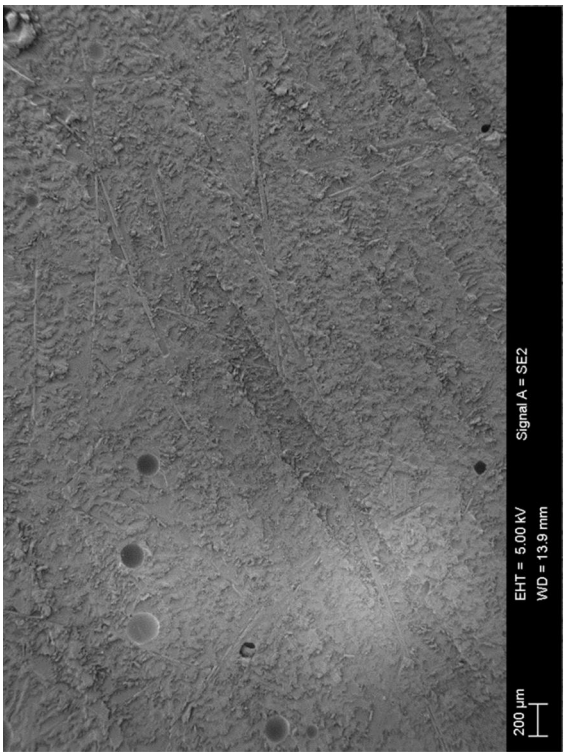

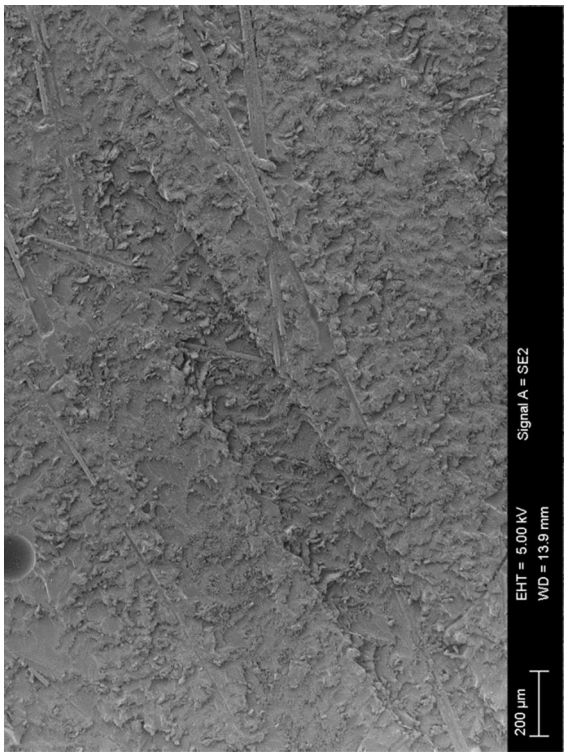

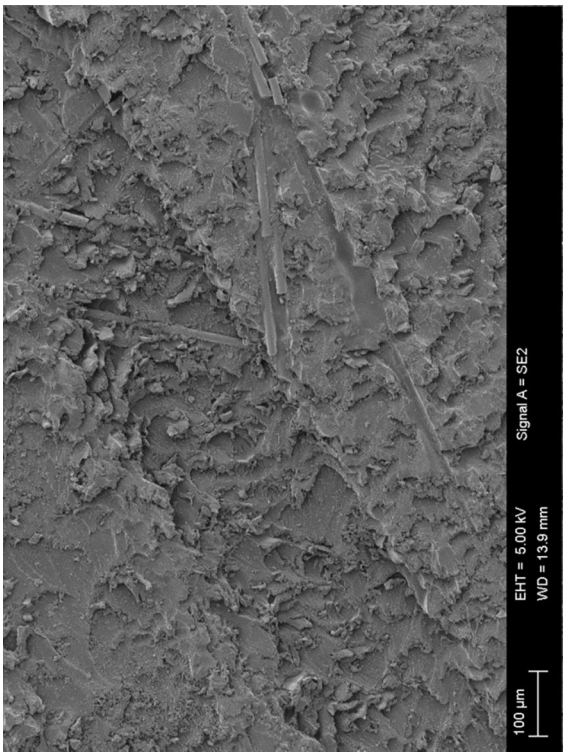

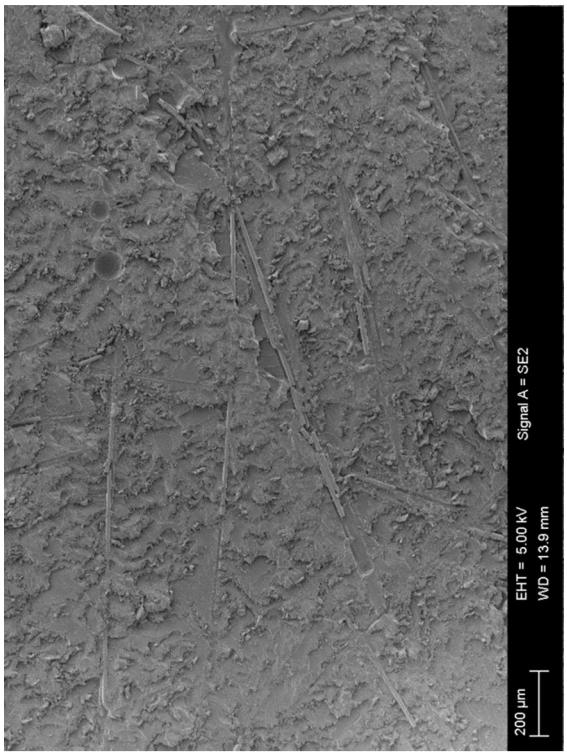

LAMINATE C1: WELL SANDBLASTED OUTER SURFACE

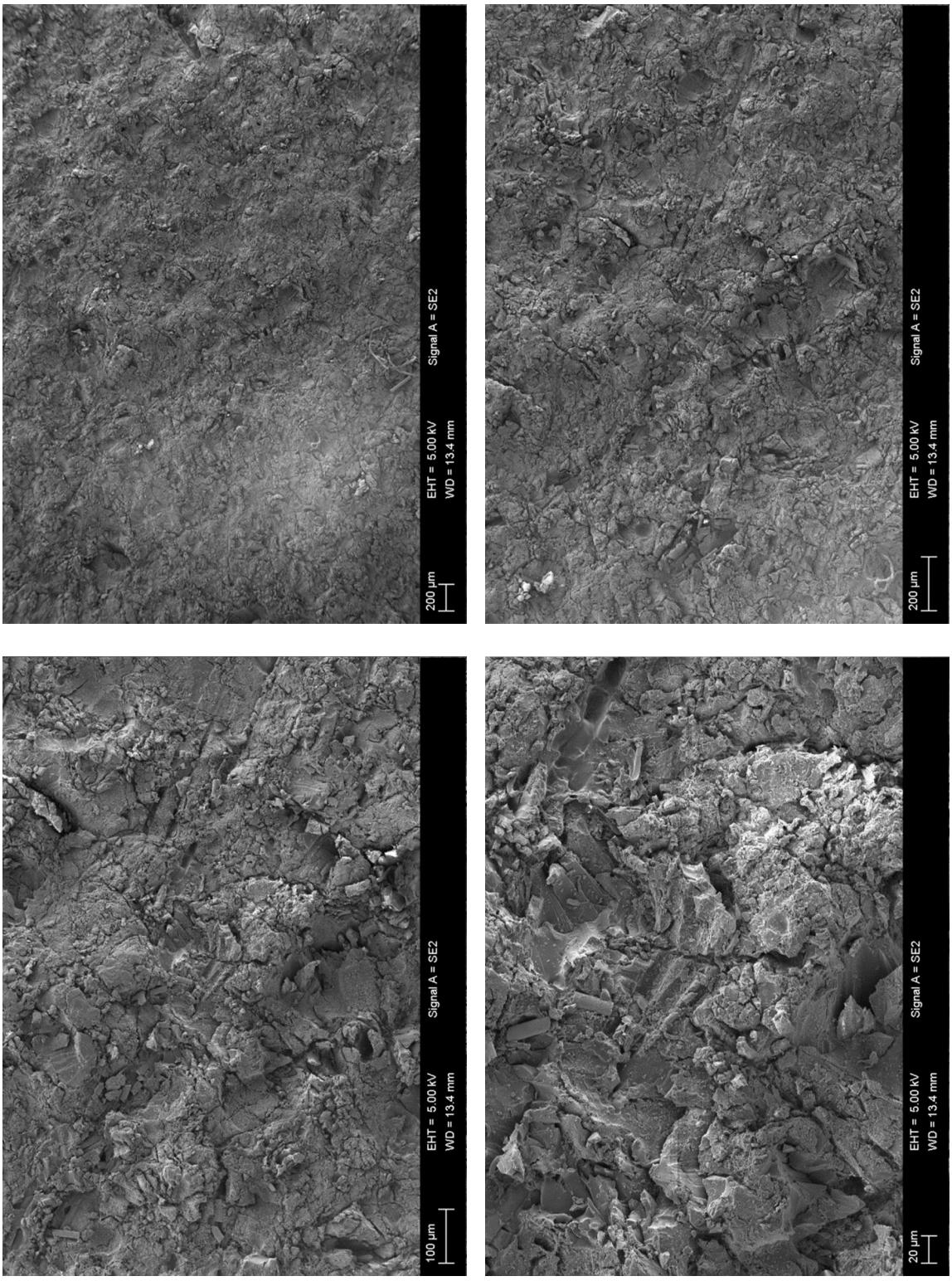

LAMINATE C2: WELL SANDBLASTED MOULD SURFACE

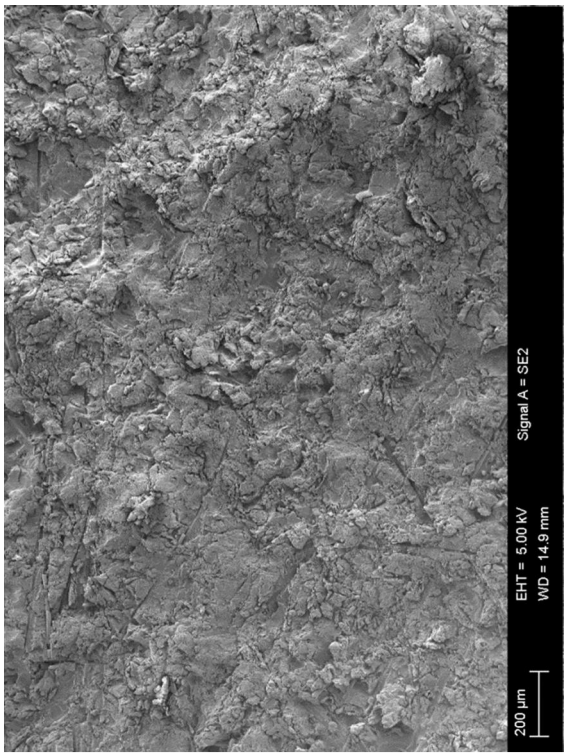

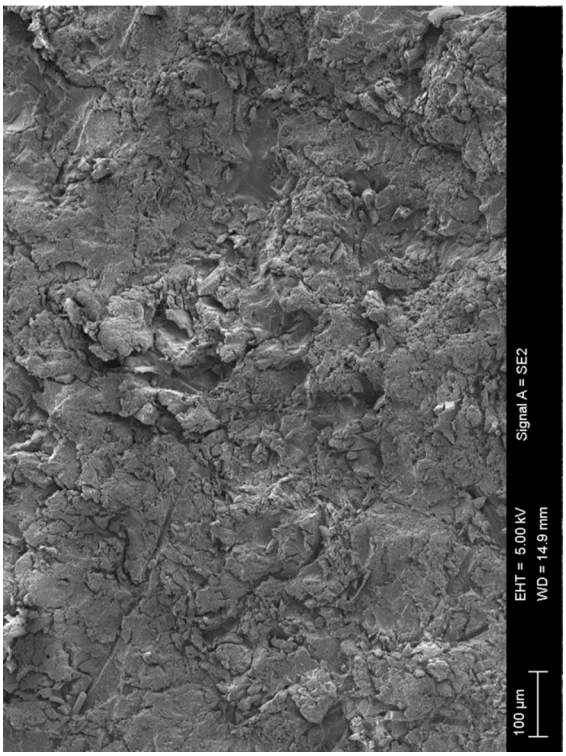

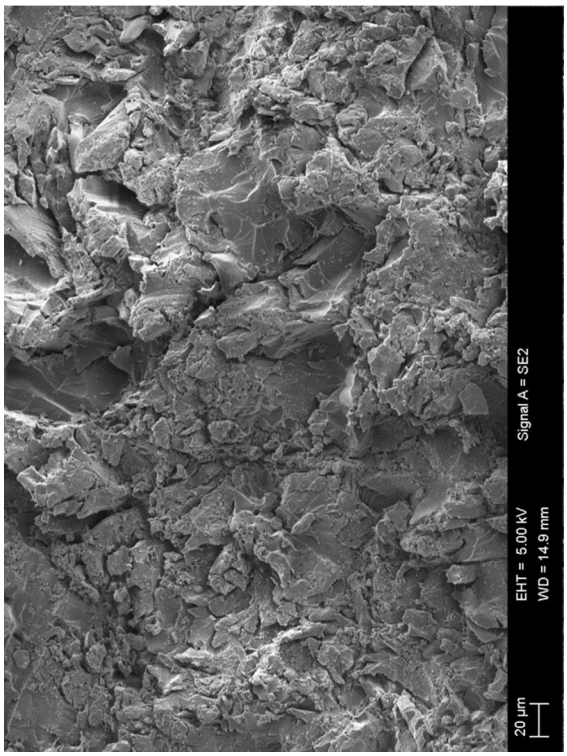

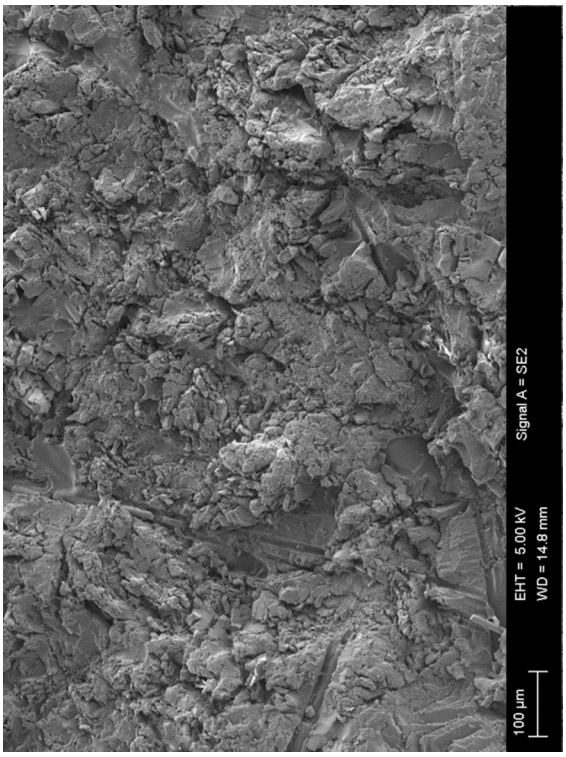
100 µm
EHT = 5.00 kV
WD = 14.8 mm
Signal A = SE2

LAMINATE D1: NEGLIGENTLY SANDBLASTED OUTER SURFACE

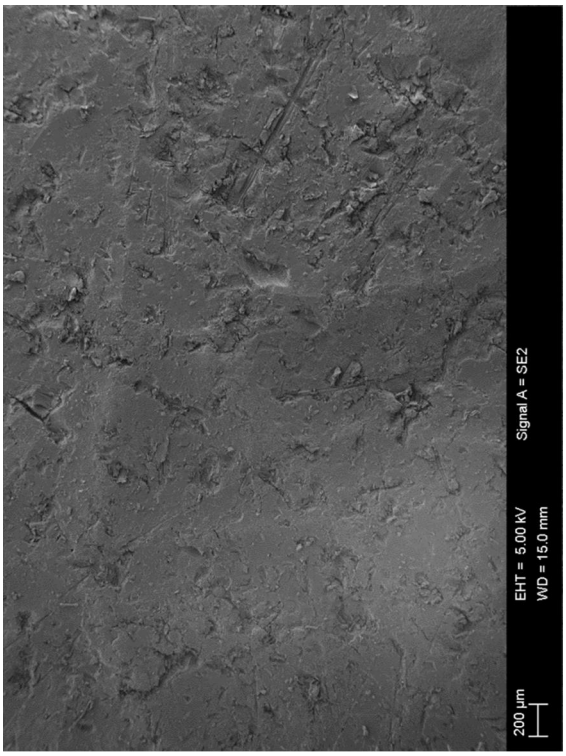

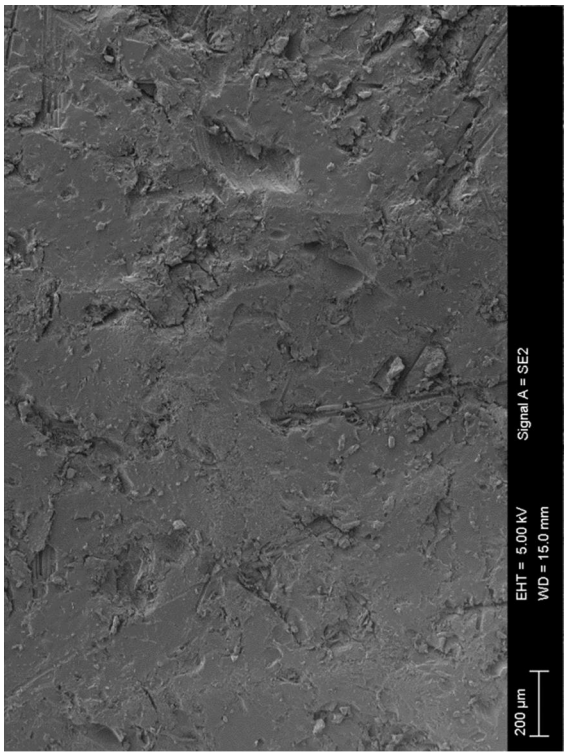

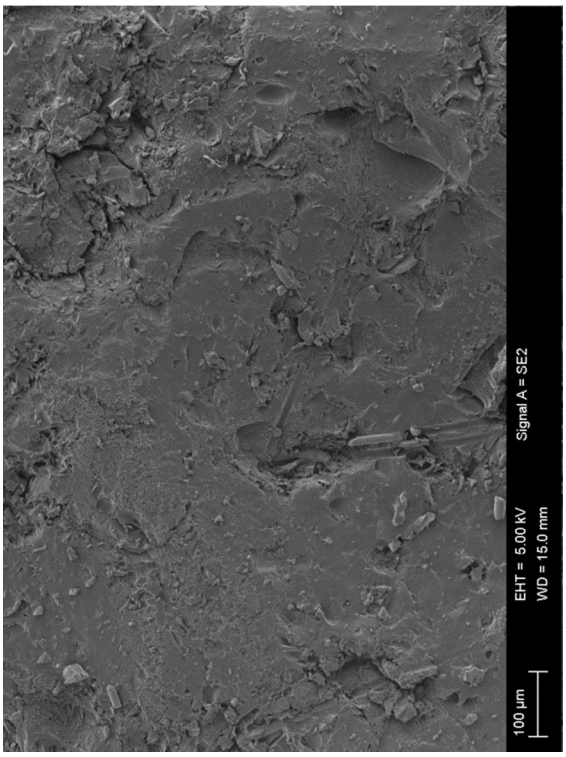

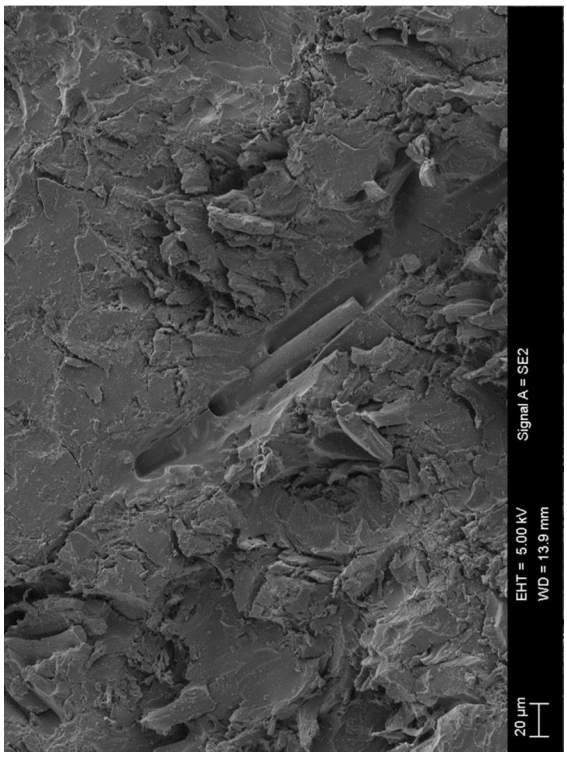

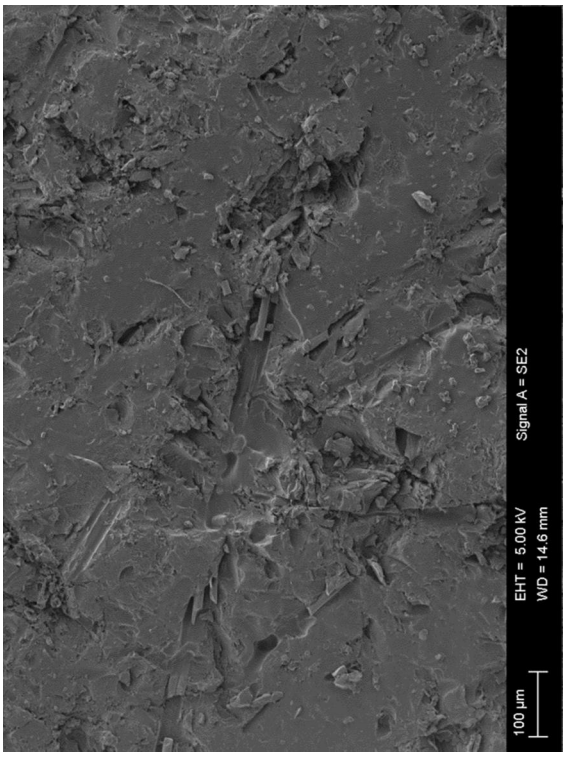
100 µm
EHT = 5.00 kV
WD = 14.6 mm
Signal A = SE2

LAMINATE D2: NEGLIGENTLY SANDBLASTED MOULD SURFACE

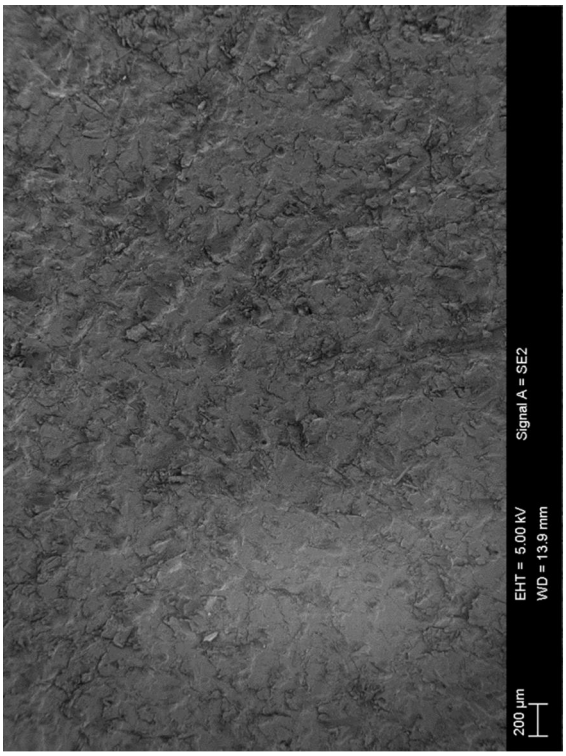

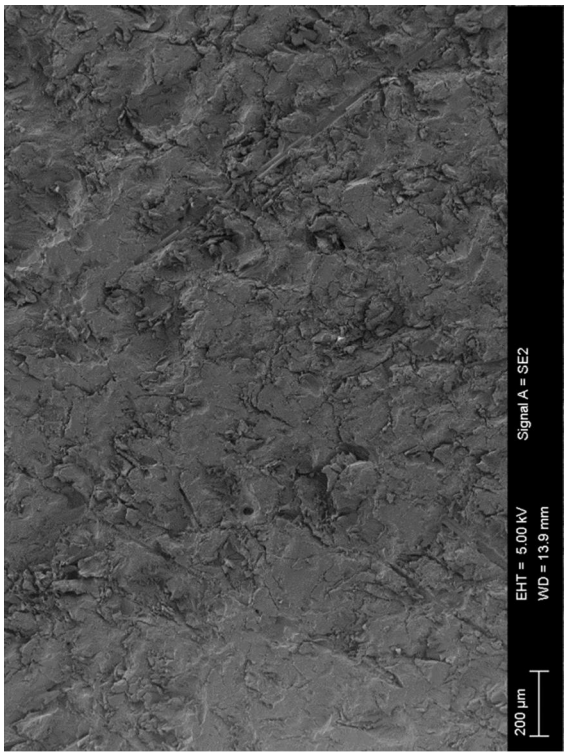

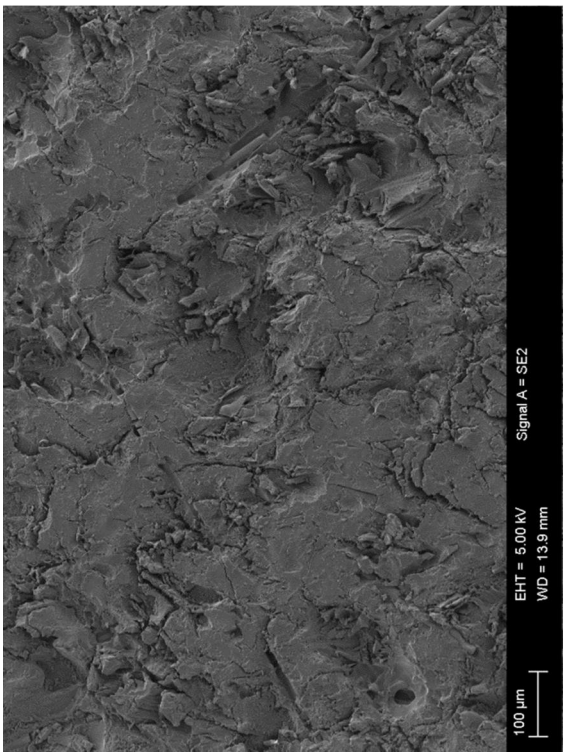

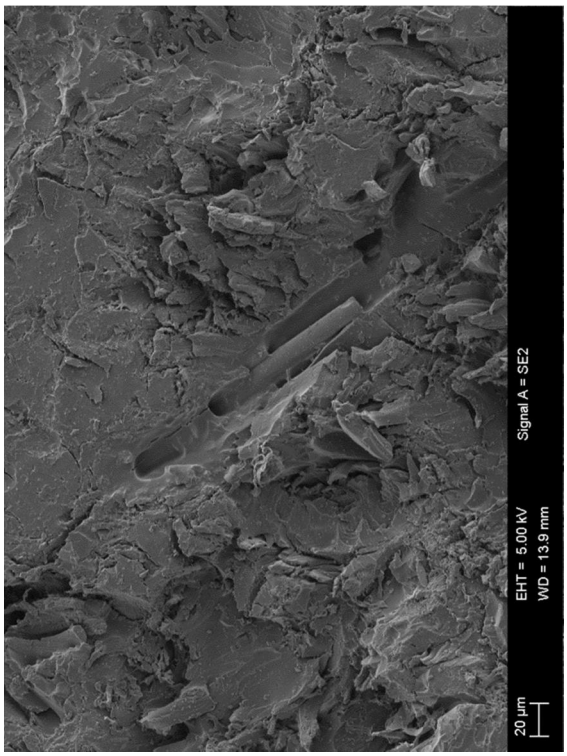

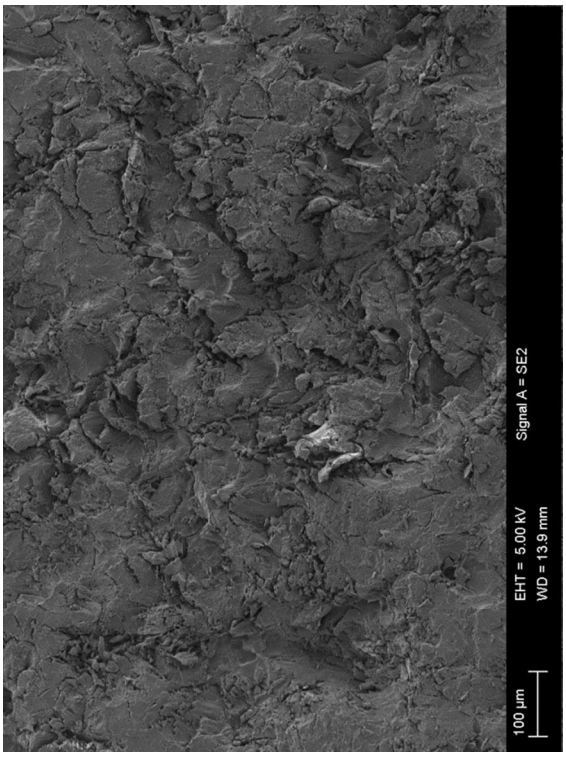
100 µm
EHT = 5.00 kV
WD = 13.9 mm
Signal A = SE2

LAMINATE E1: TOO FINELY SANDBLASTED OUTER SURFACE

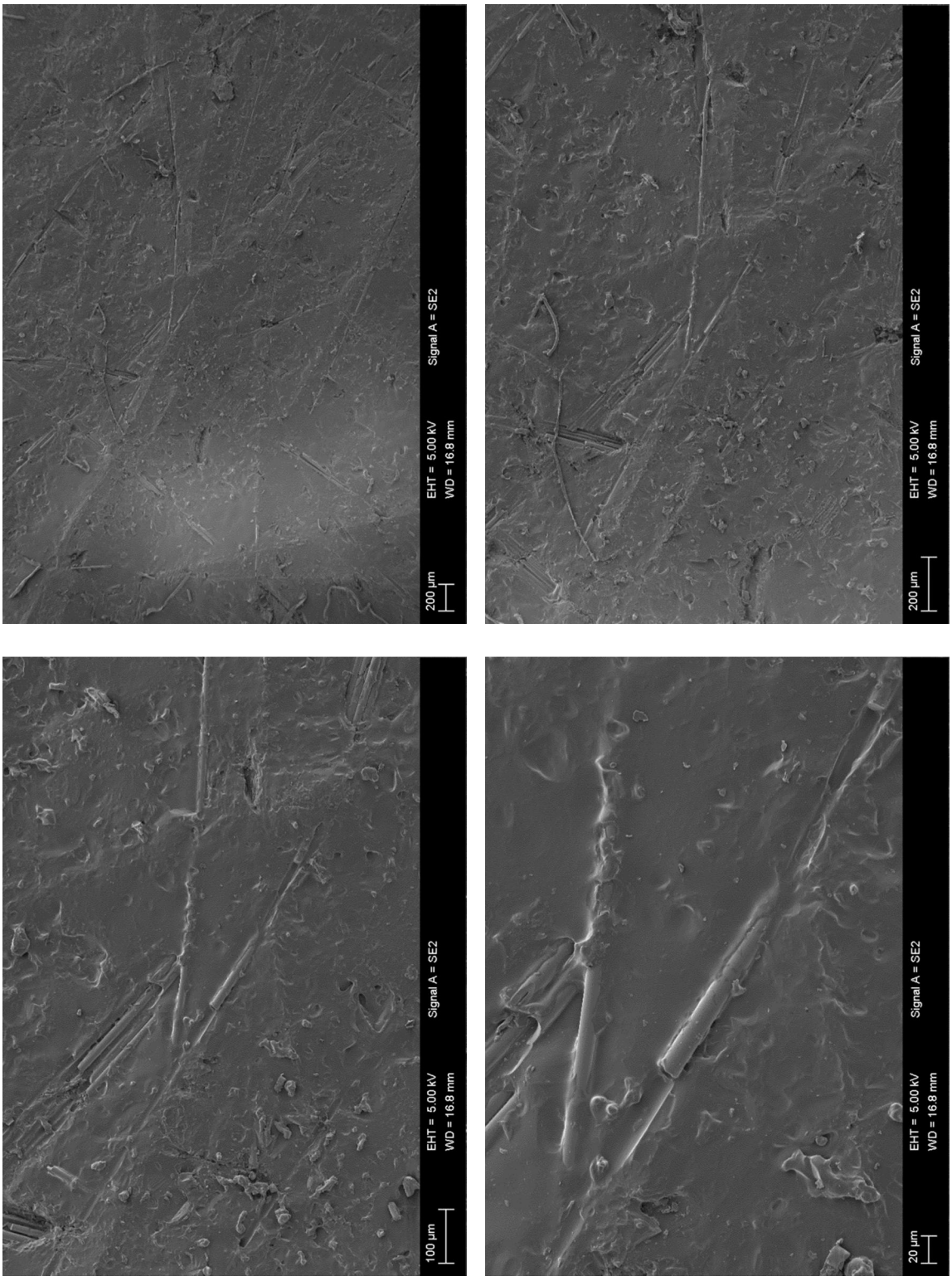

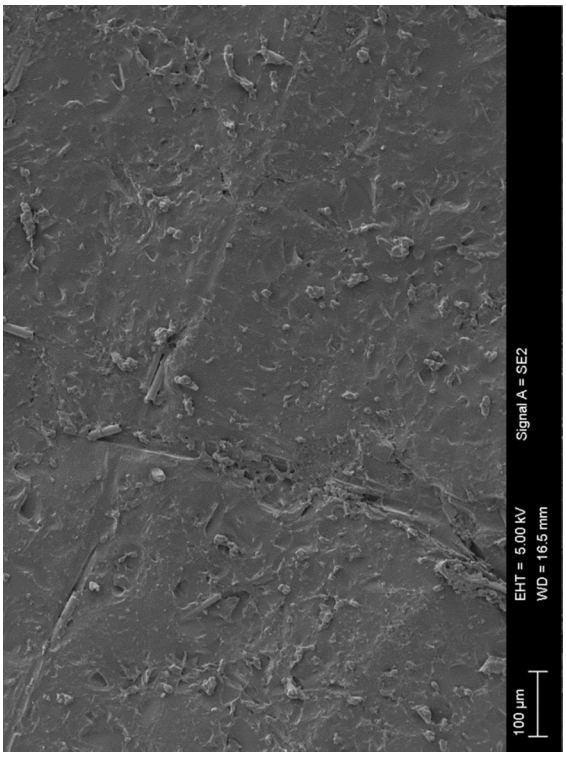
100 µm
EHT = 5.00 kV
WD = 16.5 mm
Signal A = SE2

LAMINATE E2: TOO FINELY SANDBLASTED MOULD SURFACE

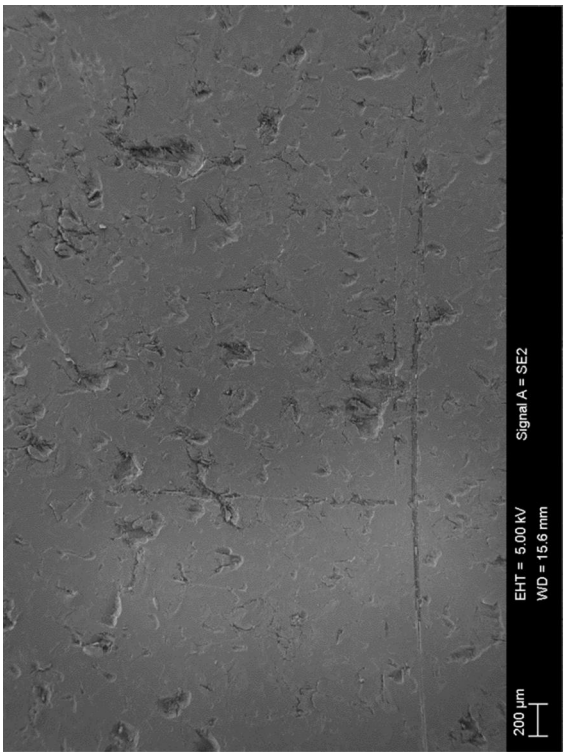

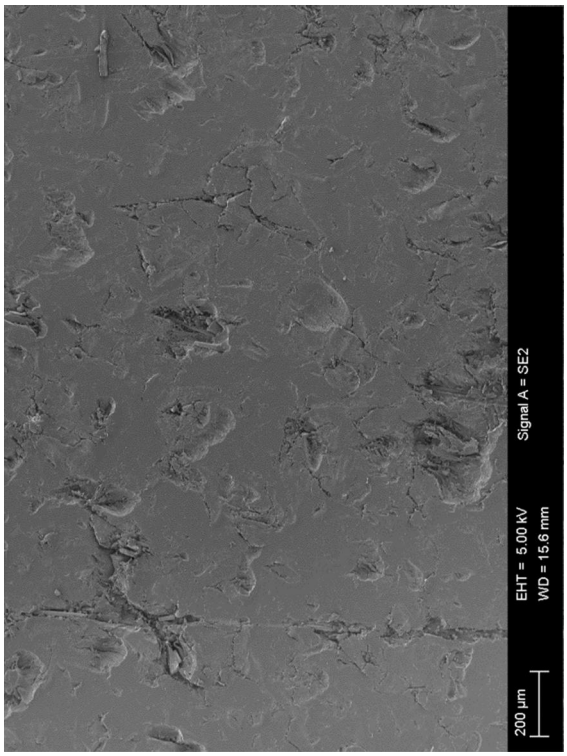

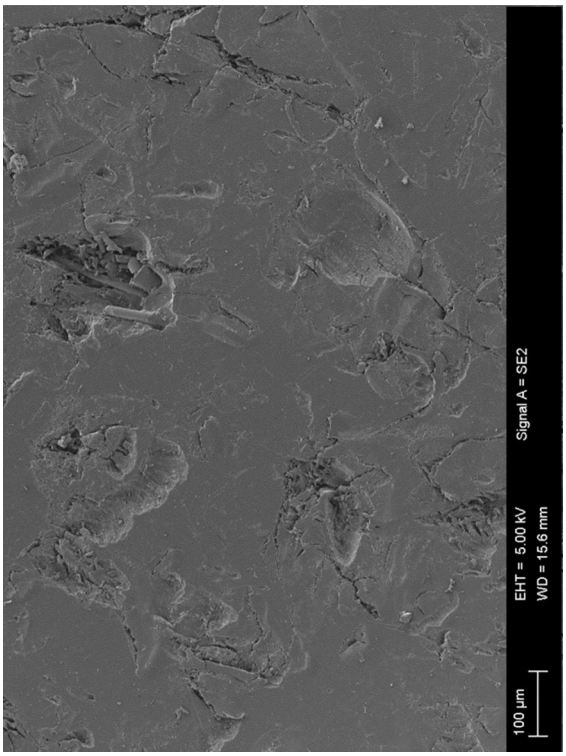

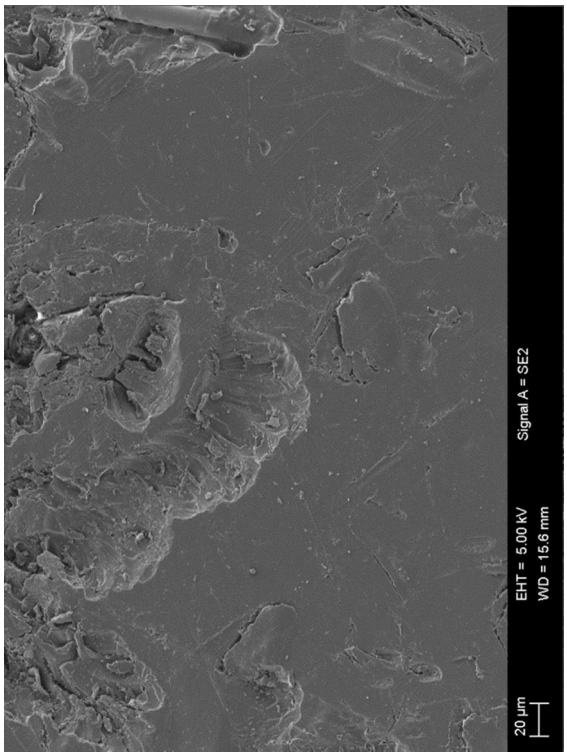

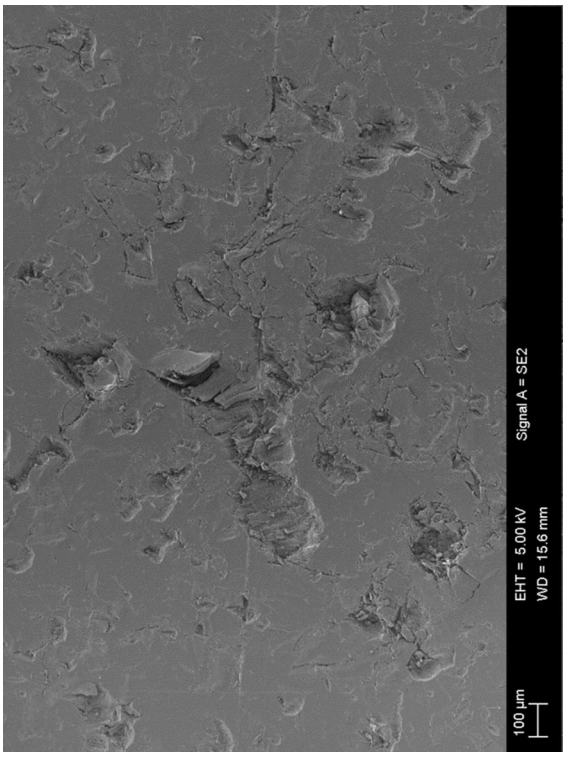
100 µm
EHT = 5.00 kV
WD = 15.6 mm
Signal A = SE2

LAMINATE F1: WIRE BRUSHED OUTER SURFACE

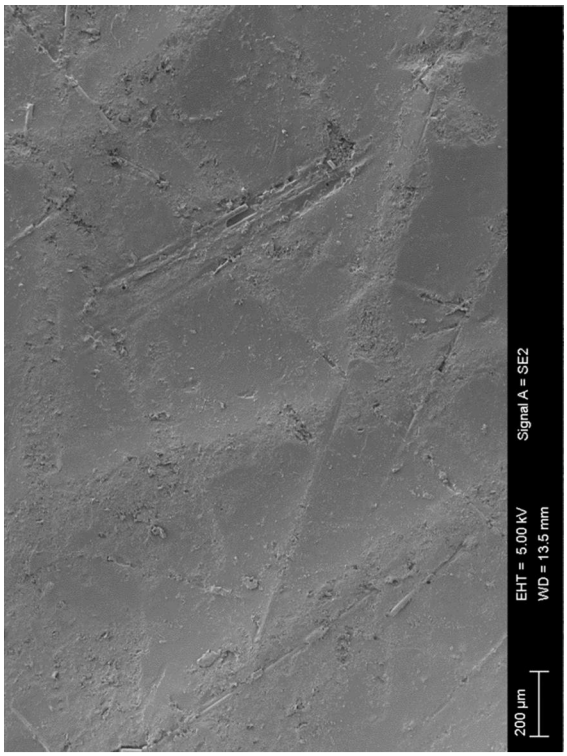

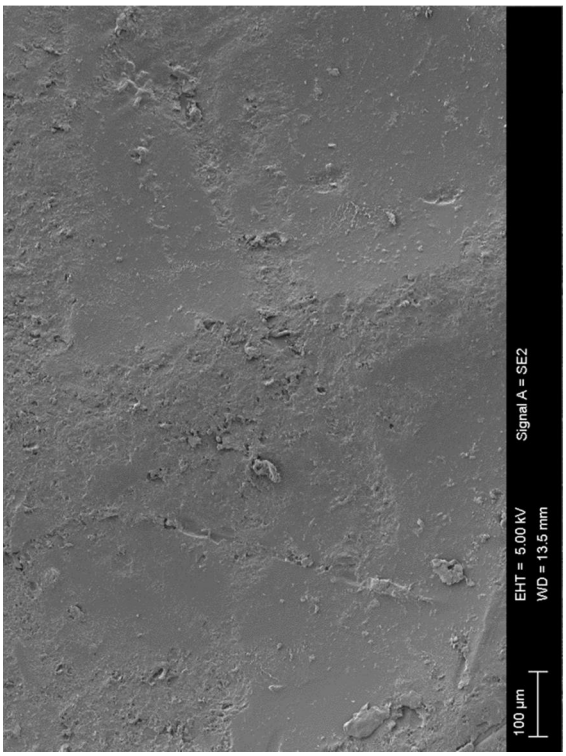

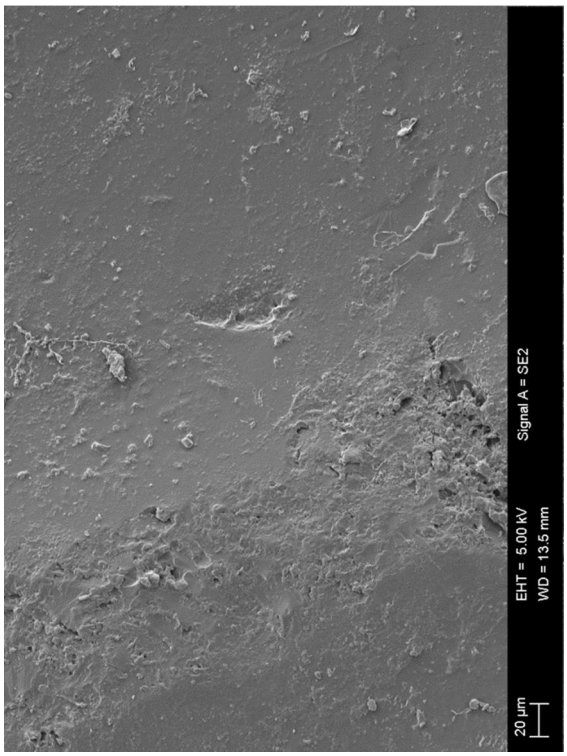

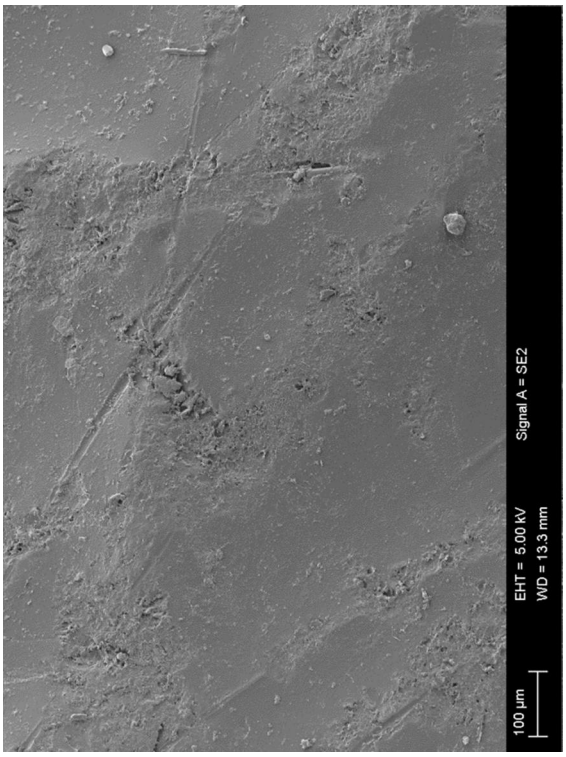
100 µm
EHT = 5.00 kV
WD = 13.3 mm
Signal A = SE2

LAMINATE F2: WIRE BRUSHED MOULD SURFACE

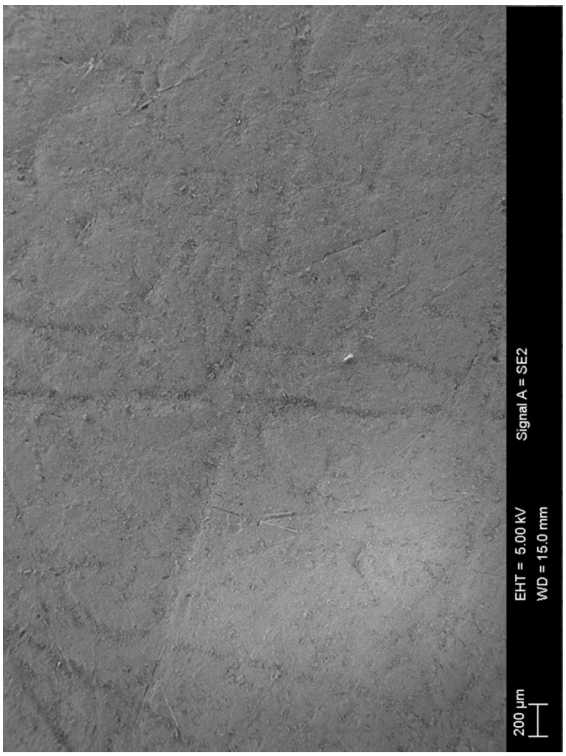

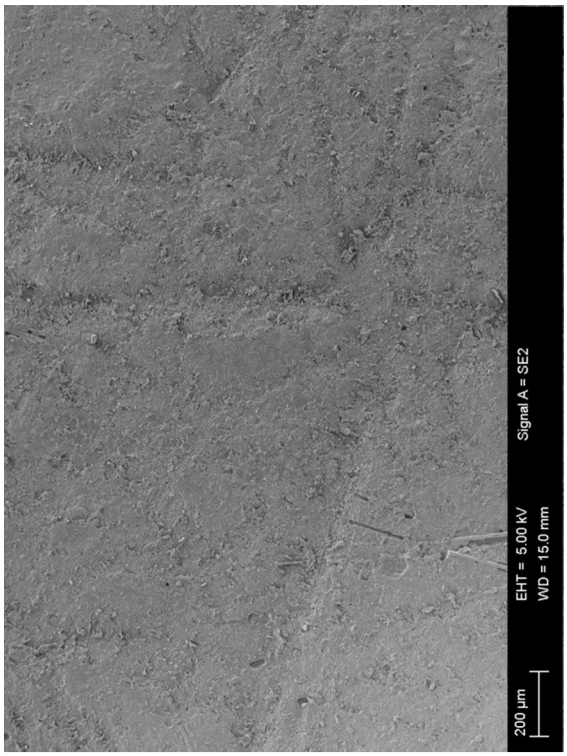

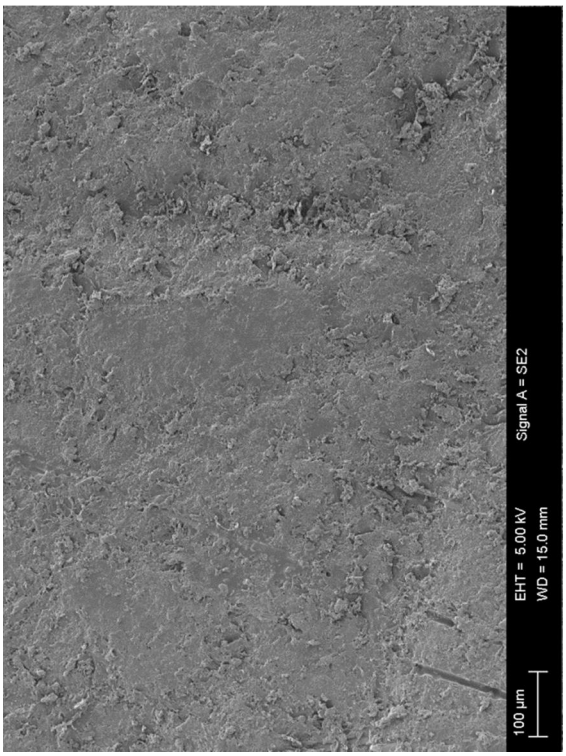

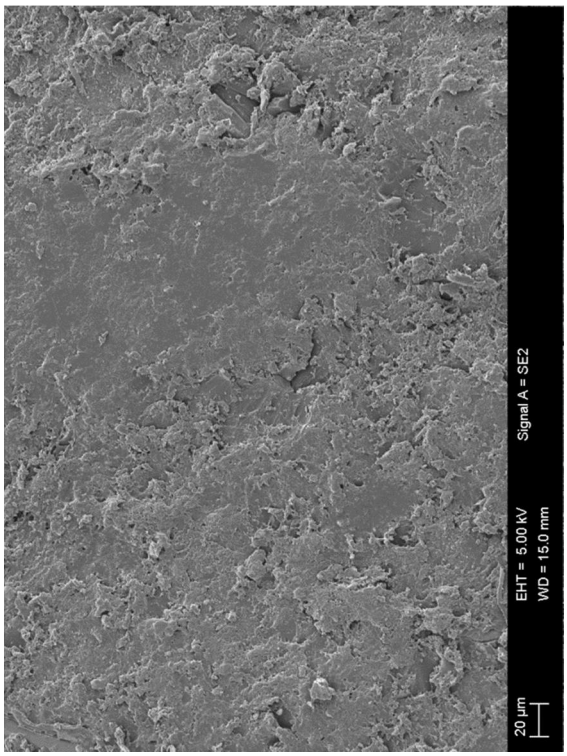

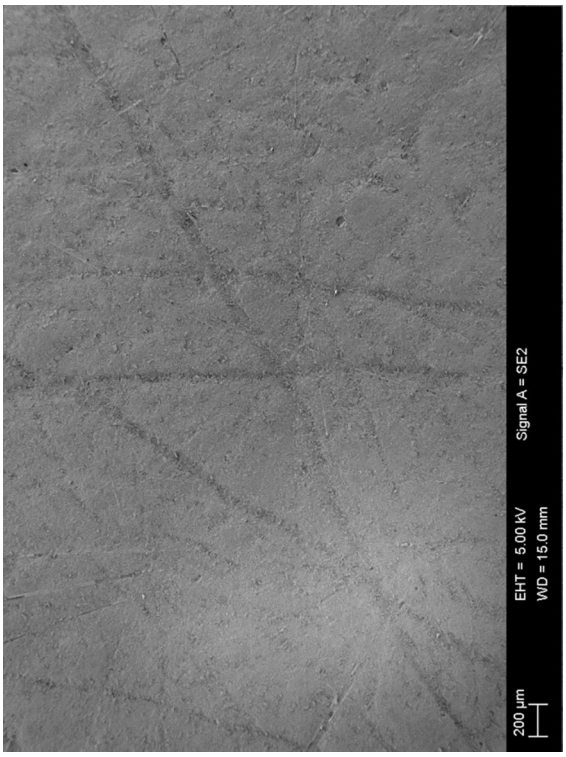
200 µm
EHT = 5.00 kV
WD = 15.0 mm
Signal A = SE2

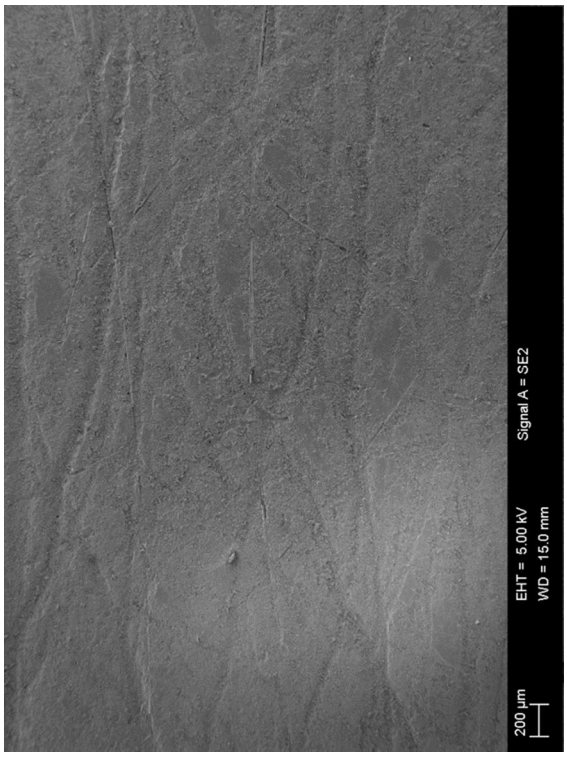
200 µm
EHT = 5.00 kV
WD = 15.0 mm
Signal A = SE2